

**This dissertation has been
microfilmed exactly as received**

69-18,332

**BLACKLOCK, James Richard, 1936-
PLANE STRESS FINITE ELEMENTS FOR NONLINEAR
ANALYSIS.**

**University of Arizona, Ph.D., 1969
Engineering, civil**

University Microfilms, Inc., Ann Arbor, Michigan

PLANE STRESS FINITE ELEMENTS FOR
NONLINEAR ANALYSIS

by

James Richard Blacklock

A Dissertation Submitted to the Faculty of the

DEPARTMENT OF CIVIL ENGINEERING

In Partial Fulfillment of the Requirements

For the Degree of

DOCTOR OF PHILOSOPHY

In the Graduate College

THE UNIVERSITY OF ARIZONA

1969

THE UNIVERSITY OF ARIZONA
GRADUATE COLLEGE

I hereby recommend that this dissertation prepared under my
direction by James Richard Blacklock
entitled Plane Stress Finite Elements for Nonlinear Analysis

be accepted as fulfilling the dissertation requirement of the
degree of Doctor of Philosophy

Ralph M. Richard
Dissertation Director

April 7, 1969
Date

After inspection of the final copy of the dissertation, the
following members of the Final Examination Committee concur in
its approval and recommend its acceptance:*

Ralph M. Richard

April 7, 1969

Allan J. Melvick

April 7, 1969

Harren A. Mihlofsky

April 7, 1969

James W. Kuegh

April 7, 1969

Roger A. Andersson

April 7, 1969

*This approval and acceptance is contingent on the candidate's
adequate performance and defense of this dissertation at the
final oral examination. The inclusion of this sheet bound into
the library copy of the dissertation is evidence of satisfactory
performance at the final examination.

STATEMENT BY AUTHOR

This dissertation has been submitted in partial fulfillment of requirements for an advanced degree at The University of Arizona and is deposited in the University Library to be made available to borrowers under rules of the Library.

Brief quotations from this dissertation are allowable without special permission, provided that accurate acknowledgment of source is made. Requests for permission for extended quotation from or reproduction of this manuscript in whole or in part may be granted by the head of the major department or the Dean of the Graduate College when in his judgment the proposed use of the material is in the interests of scholarship. In all other instances, however, permission must be obtained from the author.

SIGNED: James L. Blacklock

ACKNOWLEDGMENTS

The author wishes to express his sincere appreciation to Professor R. M. Richard and the Civil Engineering Department faculty for their guidance, encouragement and continued friendship during the course of this study.

Special thanks is given to those at General Dynamics and at the Air Force Materials Laboratory who gave their support to this research program.

Above all others, the author wishes to express his deep gratitude to his wife--Anne--and to his children--Russell, Pamela and Melanie--for their unending inspiration and understanding.

TABLE OF CONTENTS

<u>Chapter</u>	<u>Page</u>
LIST OF ILLUSTRATIONS	vi
ABSTRACT	xi
1. INTRODUCTION	1
2. NONLINEAR STRESS ANALYSIS METHODS	4
2.1 Basis of Nonlinear Methods	4
2.2 Initial Strain Methods	5
2.3 Incremental Methods	6
2.4 Differential Methods	7
3. BASIC NONLINEAR FINITE ELEMENTS	9
3.1 Bar Element Number 1	10
3.2 Triangular Plate Element Number 2	10
3.3 Rectangular Plate Element Number 3	13
4. NONLINEAR FINITE ELEMENT DEVELOPMENT	15
4.1 Quadrilateral Plate Element Number 4.	16
4.2 Quadrilateral Plate Element Number 5.	22
5. THE SHEAR-LAG PROBLEM	28
5.1 Problem Definition	28
5.2 Fine Grid Solution	32
5.3 Coarse Grid Solution	35
5.4 Final Remarks on the Shear-Lag Problem.	40
6. THE CANTILEVER PROBLEM	43
6.1 Problem Definition	45
6.2 Problem Simulation	48
6.3 The Cantilever Plate Analysis	55

TABLE OF CONTENTS (Continued)

<u>Chapter</u>		<u>Page</u>
	6.3.1 Deflection Analysis	55
	6.3.2 Special Deflection Problem. . .	63
	6.3.3 Plate Stress Analysis	65
6.4	The Cantilever Beam Analysis.	70
	6.4.1 Deflection Analysis	70
	6.4.2 Stress Analysis	72
6.5	The Tapered Cantilever Beam Analysis. .	78
6.6	Final Remarks on the Cantilever Problem	82
7.	DISCUSSION	86
	7.1 Significance of the Method	87
	7.2 Implications for Solution of Other Problems	88
	7.3 Recommendations	89
	APPENDIX I RQ1 FORTRAN LISTING	91
	LIST OF REFERENCES	119

LIST OF ILLUSTRATIONS

<u>Figure</u>	<u>Title</u>	<u>Page</u>
1	Bar Element Number 1	11
2	Triangular Plate Element Number 2	12
3	Rectangular Plate Element Number 3	14
4	Quadrilateral Plate Element Number 4	17
5	Quadrilateral Plate Local Stress Con- ventions	20
6	Quadrilateral Study Problem	21
7	Quadrilateral Plate Stresses, Average Deflection - Average Stress	23
8	Quadrilateral Plate Stresses, Actual Deflection-Average Stress	24
9	Quadrilateral Plate Element Number 5	26
10	Shear-Lag Specimen	30
11	Stress Strain Plot of Test Data	31
12	Fine Grid Simulation	33
13	Center Strain vs Applied Load (Fine Grid) .	34
14	Strain (ϵ_y) Distribution Along the Line $y = 0.0$	36
15	Strain (ϵ_x) Distribution	36
16	Coarse Grid Simulation	38

LIST OF ILLUSTRATIONS (Continued)

<u>Figure</u>	<u>Title</u>	<u>Page</u>
17	Nonlinear Deflected Shape	39
18	Average Center Stress vs Load	41
19	Stress (σ_y) Along Line $y = 0.0$	41
20	Cantilever Plate Problem, Models I Through IV	46
21	Cantilever Beam Problem, Models IA Through IVA	46
22	Tapered Cantilever Beam Problem. Models IB Through IVB	47
23	Nonlinear Stress-Strain Curve	47
24	Model I Simulation, 5-Grid Plate	49
25	Model IA Simulation, Plain Beam	49
26	Model IB Simulation, Tapered Beam	49
27	Model II Simulation, 10-Grid Plate	50
28	Model IIA Simulation, Plain Beam	50
29	Model IIB Simulation, Tapered Beam	50
30	Model III Simulation, 20-Grid Plate	51
31	Model IIIA Simulation, Plain Beam	51
32	Model IIIB Simulation, Tapered Beam	51
33	Model IV Simulation, 80-Grid Plate	52
34	Model IVA Simulation, Plain Beam	52

LIST OF ILLUSTRATIONS (Continued)

<u>Figure</u>	<u>Title</u>	<u>Page</u>
35	Model IVB Simulation, Tapered Beam	52
36	Nonlinear Plate Deflections for 1000-Lb Load	56
37	Elastic Plate Deflections for 1000-Lb Load	59
38	Nonlinear Cantilever Plate Tip Deflec- tion vs Grid Size	61
39	Elastic Cantilever Plate Tip Deflection vs Grid Size	62
40	Cantilever Plate Deflections for a Quadrilateral Shaped Grid Compared to the Regular Rectangular Grid	64
41	Horizontal Normal Stresses for the Canti- lever Plate, Element Number 2, Model IV	66
42	Horizontal Normal Stresses for the Canti- lever Plate, Element Number 2, Model III	66
43	Horizontal Normal Stresses for the Canti- lever Plate, Element Number 3, Model IV	67
44	Horizontal Normal Stresses for the Canti- lever Plate, Element Number 3, Model III	67
45	Horizontal Normal Stresses for the Cantilever Plate, Element Number 4, Model IV	68
46	Horizontal Normal Stresses for the Canti- lever Plate, Element Number 4, Model III	68

LIST OF ILLUSTRATIONS (Continued)

<u>Figure</u>	<u>Title</u>	<u>Page</u>
47	Horizontal Normal Stresses for the Cantilever Plate, Element Number 5, Model IV	69
48	Horizontal Normal Stresses for the Cantilever Plate, Element Number 5, Model III	69
49	Nonlinear Beam Deflections for 4000-Lb Load	71
50	Elastic Beam Deflections for 4000-Lb Load	73
51	Nonlinear Tip Deflection for the Cantilever Beam vs Grid Size	74
52	Horizontal Normal Stresses for the Cantilever Beam, Element Number 2, Model IVA	75
53	Horizontal Normal Stresses for the Cantilever Beam, Element Number 2, Model IIIA	75
54	Horizontal Normal Stresses for the Cantilever Beam, Element Number 3, Model IVA	76
55	Horizontal Normal Stresses for the Cantilever Beam, Element Number 3, Model IIIA	76
56	Nonlinear Tapered Beam Tip Deflections for 4000-Lb Load	80
57	Elastic Tapered Beam Tip Deflections for 4000-Lb Load	81
58	Tip Deflection for the Tapered Cantilever Beam Plotted vs Grid Size	83

LIST OF ILLUSTRATIONS (Continued)

<u>Figure</u>	<u>Title</u>	<u>Page</u>
59	Nonlinear Flange Stresses, Element Number 4 Shear Webs	84
60	Nonlinear Flange Stresses, Element Number 2 Shear Webs	84

ABSTRACT

Advancements in the area of nonlinear stress analysis have been made through the development of a new finite element, a quadrilateral plate, and the definition and affirmation of practical applications of this element along with the bar, triangle, and rectangle elements used in previous nonlinear stress analyses.

Two quadrilateral plate elements were developed during the course of the study. Each of the quadrilateral plate elements was developed by use of four constant stress triangles. In one, a midpoint node was added and the deflections and stresses were averaged; in the other, the constant stress triangles were overlapped and the stresses were not averaged. The average deflection/average stress quadrilateral produced excellent results; results produced by the overlapping triangles were disappointing.

The method of analysis used in this study is one that relies upon the solution of a system of nonlinear ordinary differential equations to obtain the nonlinear deflections. This method, which was first developed for use with

the constant stress bars and beams and then extended to include constant stress triangles, was shown to be more accurate when used with the more complex finite elements, namely the rectangles and quadrilaterals.

The standard rectangular element was found to give the best results for problems that can utilize a rectangular grid, and the new element developed from four constant stress triangles produced the best results in problem areas that require a quadrilateral-shaped finite element.

Each of the elements discussed, the constant stress bar, the constant stress triangle, the rectangular element, the midpoint quadrilateral and the overlapping quadrilateral were used to solve a standard nonlinear shear-lag problem and three nonlinear cantilever problems. Actual test data are available for the shear-lag problem and these correlate well with the nonlinear analytical solutions obtained. Plots of the cantilever solutions show that the location of the point of maximum nonlinear action for a cantilever beam with a flange is located just at the point where the flange joins the web rather than at the extreme fiber as is often assumed.

It is shown that although the beam deflections in elastic problems always converge to the true value as a

lower bound as the grid is refined, deflections in nonlinear problems do not necessarily follow the same pattern. Sometimes the nonlinear deflections approach from the lower side; then, as the grid is made more fine, they tend to diverge, jump to the higher side, and give an over-estimation of the correct answer.

A prior understanding of the stress field is, therefore, quite valuable in determining the fineness of the finite element grid.

The quadrilateral element developed in this study and the rectangular element investigated permit an extension of finite element analysis to certain nonlinear structures that could not easily be handled by this method previously. The applications made in this study indicate that these elements and the constant stress bar and constant stress triangle can be adapted to the nonlinear stress analysis of complex structural systems by the matrix methods of analysis.

The RQ1 computer program utilized in this study was developed by Richard and Blacklock. A listing of this program is appended to this paper to encourage further studies into the solution of nonlinear engineering problems.

CHAPTER 1

INTRODUCTION

Analysis of many current structural systems involves the solution of nonlinear problems. The determination of the stresses, strains, and displacements in a structure in which the stresses exceed the proportional limit of the material presents a difficult problem to the analyst. Solution of such problems requires the use of some form of approximate nonlinear analysis.

One method that is currently being used to analyze nonlinear plane stress structures was presented by Richard and Blacklock (1968). This method represents the stressed elements by an assembly of isotropic triangular plate and bar elements. The displacement components, in both the bar and plate elements, are assumed to vary linearly so that the stress and strain in the element is of constant value throughout the element. These elements, though simple and direct, are limited in their application; and their use in the finite element solution of complex structures imposes a penalty on the analyst.

In elastic analysis, finite element development has proceeded beyond the constant stress variety so that the analyst now has at his disposal a selection of finite elements which include beams, rectangular plates, and quadrilateral plates.

Little data now exists on the practical application and evaluation of finite elements for nonlinear analysis. If stiffness matrix methods are to be utilized in the solution of nonlinear problems, then new elements applicable to nonlinear structures must be developed and investigated.

The scope of this dissertation is limited, primarily, to the advancement of existing nonlinear methods. The principal contributions of this paper are in two areas. First, the utility of current nonlinear stiffness matrix computer programs has been enhanced by the development of certain complex finite elements for use in these programs; and, second, a systematic study of the applications of five selected finite elements has provided a basis for utilization of these elements.

The method of nonlinear stress analysis may be divided into three categories: the initial strain methods, the incremental methods, and the differential methods.

These methods are introduced in Chapter 2. The three basic finite elements--the triangle, the rectangle, and the bar--are presented in Chapter 3. The triangular element utilization may be extended by substructural arrangements into quadrilateral plates. Two quadrilateral elements are developed in Chapter 4. These elements are produced from two arrangements of four constant stress triangles.

In Chapter 5, a brief study of a shear lag problem is presented. Each of the five elements presented in Chapters 2 and 3 are used to obtain the nonlinear solution to this problem.

The cantilever problem, presented in Chapter 6, provides a basis for the final evaluation of the nonlinear finite elements. The three basic elements plus two quadrilateral elements are used to solve problems related to cantilever plates, cantilever beams and tapered cantilever beams.

CHAPTER 2

NONLINEAR STRESS ANALYSIS METHODS

Since the advent of high speed digital computers, the accurate solution of nonlinear problems has become a reality. In the pre-computer era, the analysis of large indeterminate structural systems for ultimate load capacity was dependent primarily upon the less accurate, perfectly elastic-perfectly plastic schemes of analysis. The ultimate load criteria method of structural analysis, imposed in the aerospace industry, necessitates the use of nonlinear methods to produce accurate failure load predictions. This requirement has furnished the stimulus for the funds which have supported the reported nonlinear research programs. This study is an example of the continuing effort in quest for more accurate methods of nonlinear analysis.

2.1 Basis of Nonlinear Methods

In nonlinear matrix analysis, solution methods are based on several distinguishable steps:

1. Abstraction of the real problem
2. Idealization into a finite number of discrete elements
3. Formulation of the nonlinear stress-strain relationships for the discrete elements
4. Formulation and solution of the set of governing equations
5. Interpretation of results.

The formulation of the nonlinear relationships and the formulation and solution of the governing equations have been exhaustively investigated and well documented. The other tasks are seldom reported comprehensively in the literature; however these steps should be considered equally important to the end results.

2.2 Initial Strain Methods

A general method of analysis, the initial strain method, using finite elements and incremental loading has been developed (Padlog, Huff, and Holloway 1960; Galagher, Padlog, and Bijlaard 1962). In this method, plastic and creep strains for each element are estimated on the basis of specific values of stress and treated as initial strains for the subsequent evaluation of the true stress, strains,

and displacements for each increment of load. For biaxial states of stress, the von Mises yield criterion and the Prandtl-Reuss flow relations are used. Extensive studies of this method have been made, and the method has been extended to include anisotropic elements. Percy, Loden, and Navaratna (1963) and Lansing, Jensen, and Falby (1965) have reported studies based upon the step-by-step procedure with the constant stress or constant strain method.

2.3 Incremental Methods

In the incremental method of analysis, the nonlinear stress-strain relationship is followed by generating a linear solution for each consecutive load interval. This method has been described by Wilson (1963); Argyris, Kelsey, and Kamel (1964); Pope (1965); and Denke (1956). The analysis of certain elastic-plastic systems has been performed using the direct stiffness method by combining the linear analysis with incremental loading procedure. The relevant properties of the elements are modified for each load increment and thus the procedure comprises a series of linear analyses.

2.4 Differential Methods

In the differential methods of analysis an approximate simple analytical expression is used as a substitute for the stress-strain relationship. This leads to a set of differential equations which, in turn, may be integrated by one of the available numerical algorithms, for instance the Runge-Kutta method.

The computer studies reported in this paper were made using the differential procedure presented by Richard and Blacklock (1968). This method is a generalization of the direct stiffness method for truss and frame systems subjected to proportional loading (Goldberg and Richard 1963). In this method, a differential point of view, which represents an exact approach to the truss system, is taken. The result is a system of differential equations which can be integrated to obtain the stresses, strains and displacements.

For the biaxial state of stress, the concepts of a generalized stress and isotropic hardening are used to evaluate the effective modulus and Poisson's ratio (Richard and Callabresi 1967). The surface of plasticity

approximates the von Mises surface when the generalized stress is set equal to the von Mises stress (Richard and Blacklock 1968).

This method of analyzing a nonlinear structural system is similar to an initial value problem wherein the stresses, strains, and displacements are treated as functions of the applied loading. In this case, however the accuracy of the equation solution may be ascertained by back substitution methods.

CHAPTER 3

BASIC NONLINEAR FINITE ELEMENTS

The three basic nonlinear finite elements included in this study are a constant stress bar, a constant stress triangle, and a linear stress rectangle. Each of these elements was developed for use in basic stiffness matrix computer programs for elastic stress analysis. The triangular element used is the basic Turner triangle (Turner et al. 1956). The element derivations and FORTRAN computer listings have been published numerous times and therefore, are not repeated in this paper.

The element stiffness matrices are first developed in their local coordinate systems; then, for addition into the master stiffness matrix, these are transformed into the datum coordinate system. The coordinate transformation method detailed by Przemieniecki and Berke (1964) was followed and used in developing the elements for the RQ1 computer program (Richard and Blacklock 1968). A listing of the RQ1 computer program is provided in Appendix I.

3.1 Bar Element Number 1

The displacement distribution in the pin-jointed bar element, shown in Figure 1, is assumed to be

$$U = C_1 + C_2x \quad , \quad (1)$$

where C_1 and C_2 are constants to be determined from the boundary conditions. The first element stiffness matrix to be developed in the local coordinate system is a 4 by 4 matrix containing coordinates U_1 through U_4 . When it is expanded for inclusion in the master stiffness matrix it becomes a 6 by 6 matrix containing datum coordinates \bar{U}_1 through \bar{U}_6 .

3.2 Triangular Plate Element Number 2

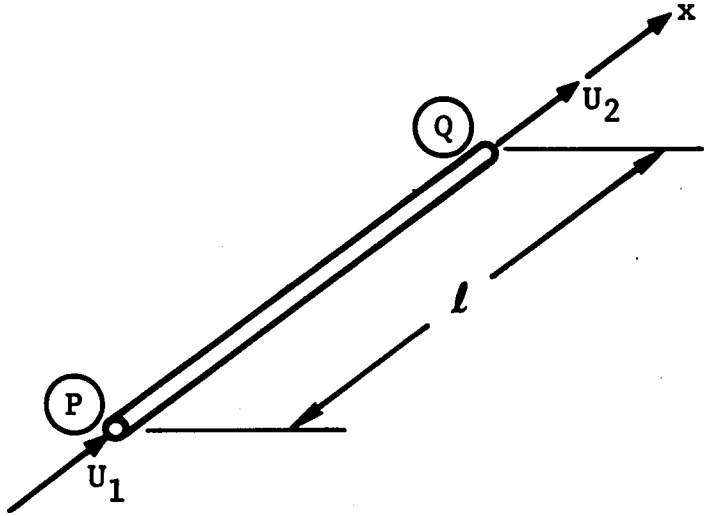
The displacement distribution in the plane stress triangular element, shown in Figure 2, is assumed to be

$$U_x = C_1x + C_2y + C_3 \quad (2)$$

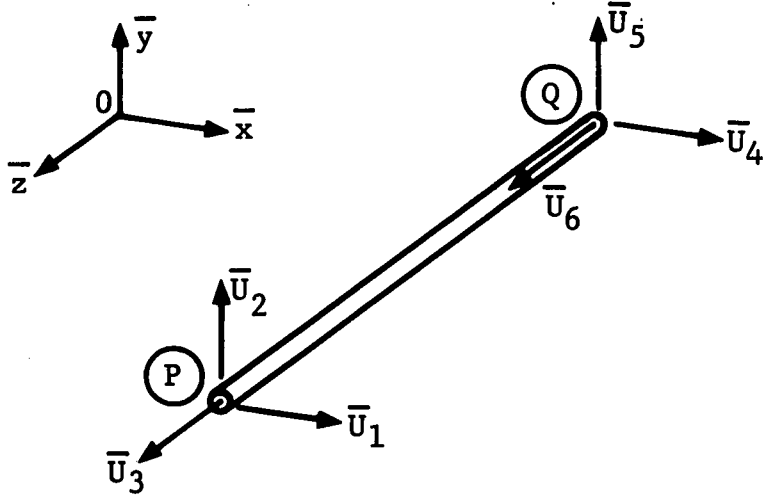
and

$$U_y = C_4x + C_5y + C_6 \quad , \quad (3)$$

where C_1 through C_6 are arbitrary constants to be determined from the boundary conditions. The first element

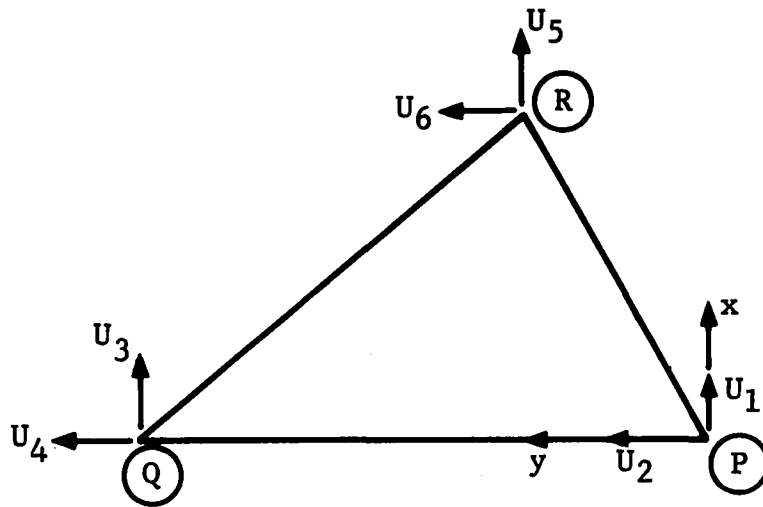


Local Coordinate System

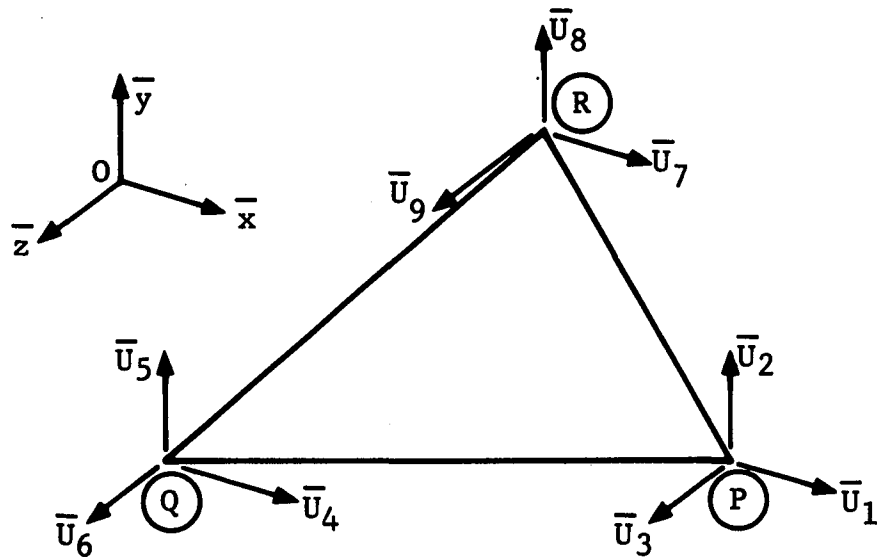


Datum Coordinate System

Figure 1 Bar Element Number 1



Local Coordinate System



Datum Coordinate System

Figure 2 Triangular Plate Element Number 2

stiffness matrix to be developed in the local coordinate system is a 6 by 6 matrix containing coordinates U_1 through U_6 . The stiffness matrix in the datum coordinate system is a 9 by 9 matrix containing coordinates \bar{U}_1 through \bar{U}_9 .

3.3 Rectangular Plate Element Number 3

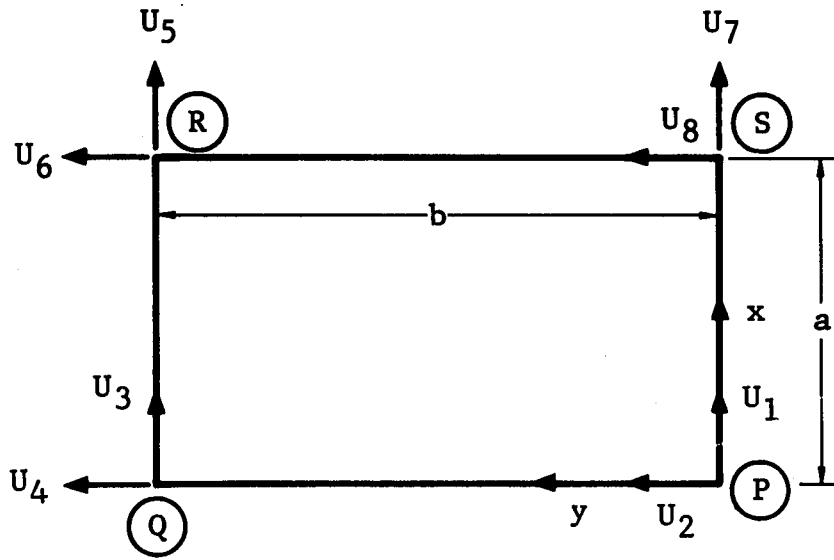
The rectangular plate displacements, which satisfy the assumption of linearly varying boundary displacements, may be assumed to be of the form

$$U_x = C_1 \frac{x}{a} + C_2 \frac{xy}{ab} + C_3 \frac{y}{b} + C_4 \quad (4)$$

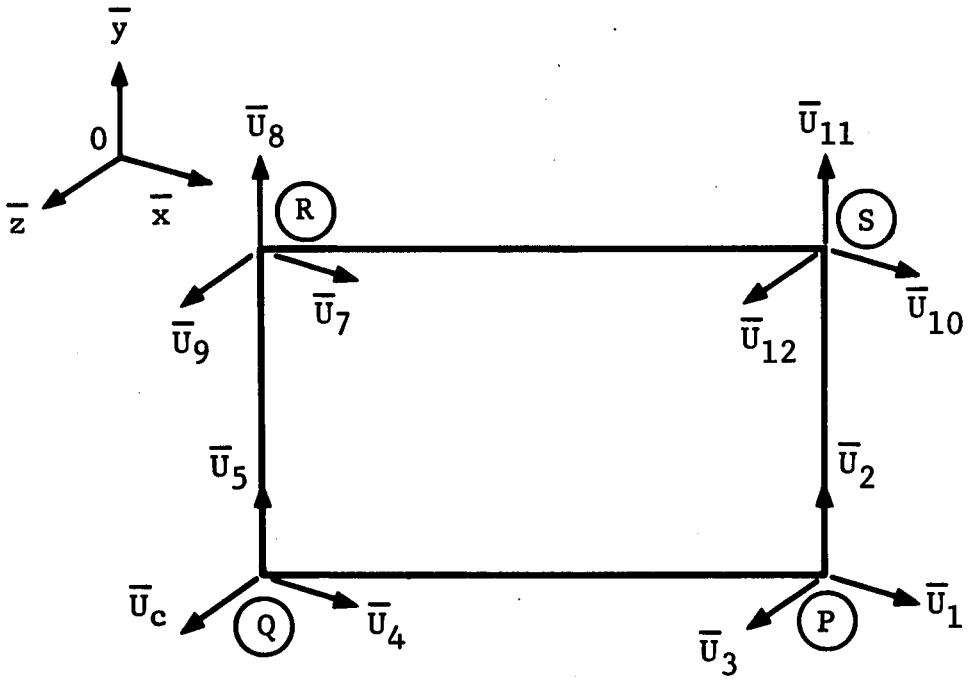
and

$$U_y = C_5 \frac{x}{a} + C_6 \frac{xy}{ab} + C_7 \frac{y}{b} + C_8 \quad , \quad (5)$$

where the arbitrary constants C_1 through C_8 are determined from the boundary conditions. The element stiffness matrix first developed in the local coordinate system is an 8 by 8 matrix containing coordinates U_1 through U_8 . The stiffness matrix in the datum coordinate system is a 12 by 12 matrix containing coordinates \bar{U}_1 through \bar{U}_{12} . The rectangular plate element number 3 is shown in Figure 3.



Local Coordinate System



Datum Coordinate System

Figure 3 Rectangular Plate Element Number 3

CHAPTER 4

NONLINEAR FINITE ELEMENT DEVELOPMENT

The constant stress triangular plate elements, used in sufficient numbers, will provide accurate results in nonlinear analysis. By combining four such elements into small substructures, the engineer can make more efficient use of these elements. If, in addition, a technique for averaging the element stresses within the substructure can be developed, this smoothing should create a more representative element. It is well known that triangular elements tend to produce somewhat irregular stress patterns, and most users of constant stress triangles have developed schemes for calculating more accurate distributions by use of the nodal force data. An example of such a scheme is given by Lansing, Jensen, and Falby (1965).

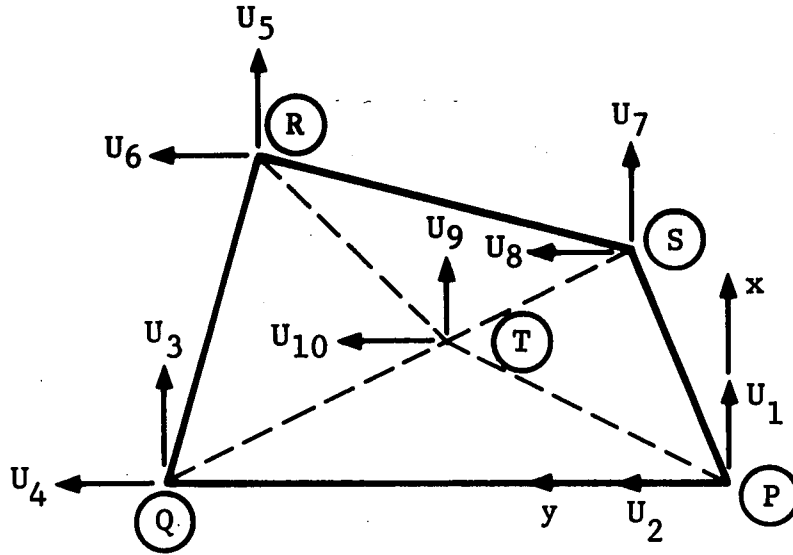
In the nonlinear program it is necessary to have good stress approximations within the stress solution in order to produce the proper inelastic action. The work in this chapter will provide the bases for such an element.

4.1 Quadrilateral Plate Element Number 4

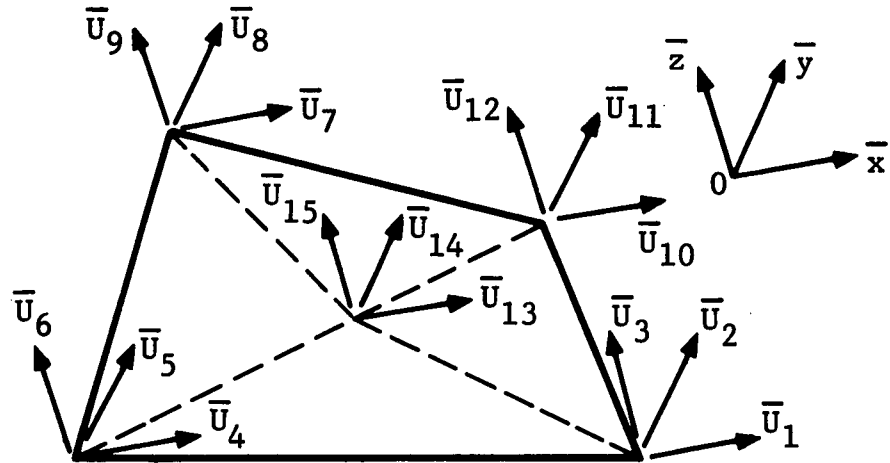
The quadrilateral plate element number 4 is constructed from four constant stress triangles with a common midpoint node as shown in Figure 4. The element is described by the computer input data quite similarly to the way that one describes a standard rectangle. The four corner nodes are established from the input geometry data, and then the element thickness and material properties are specified. The computer program averages the corner node locations in order to establish the location of the common midpoint node, designated node T in Figure 4. The quadrilateral stiffness matrix is a size 12 by 12 matrix in the datum coordinate system containing coordinates \bar{U}_1 through \bar{U}_{12} .

The development of the element stiffness matrix is accomplished in five distinct steps:

1. Using the geometry of the T node, the stiffness matrix of each of the four constant stress triangles is calculated in datum coordinates and added into a size 15 by 15 storage matrix, TT, containing coordinates \bar{U}_1 through \bar{U}_{15} .
2. Using the appropriate transformation matrix, the TT matrix is transformed into the local coordinates



PQT Local Coordinates



Datum Coordinate System

Figure 4 Quadrilateral Plate Element Number 4

of triangle PQT. It thereby becomes the size 10 by 10 stiffness matrix, SS, containing coordinates U_1 through U_{10} . This method of transformation matrix development and utilization was patterned after the one described by Przemieniecki and Berke (1964).

3. Using the elementary scheme of coordinate elimination, the two local coordinates U_9 and U_{10} located at node T are eliminated from SS. The stiffness matrix thereby becomes the size 8 by 8 matrix, RR, containing coordinates U_1 through U_8 .
4. Using the appropriate transformation matrix, the RR matrix is expanded from the PQT local coordinate system to the structure datum coordinate system. The resulting matrix, QQ, is a size 12 by 12 stiffness matrix of the quadrilateral plate containing coordinates \bar{U}_1 through \bar{U}_{12} .
5. The QQ stiffness matrix is then added into the structure master stiffness matrix.

The development of the average stress value for the quadrilateral plate is divided into four steps:

1. The structural datum coordinate system deflections are established for each of the four quadrilateral plate corner nodes. These deflection numbers are averaged to obtain the approximate value of \bar{x} , \bar{y} , and \bar{z} deflections of the common midpoint node in datum coordinates.
2. The datum coordinates of the five nodes are next used to calculate the σ_x , σ_y , and τ_{xy} stresses for each of the four triangles shown in Figure 5.
3. Using the appropriate transformation equations, the stresses are all rotated into the stress system of the PQT triangle.
4. The stresses are averaged to obtain assigned values of σ_x , σ_y , and τ_{xy} for the quadrilateral plate.

The results of averaging the deflections to obtain the average stresses were compared, in several example problems, to the results obtained when stresses were calculated by use of the actual values for the midpoint deflections and then only the stresses were averaged. In each case studied, the elastic stress results agreed remarkably well.

One problem used in this study is shown in Figure 6. Average deflection-average stress results are shown in

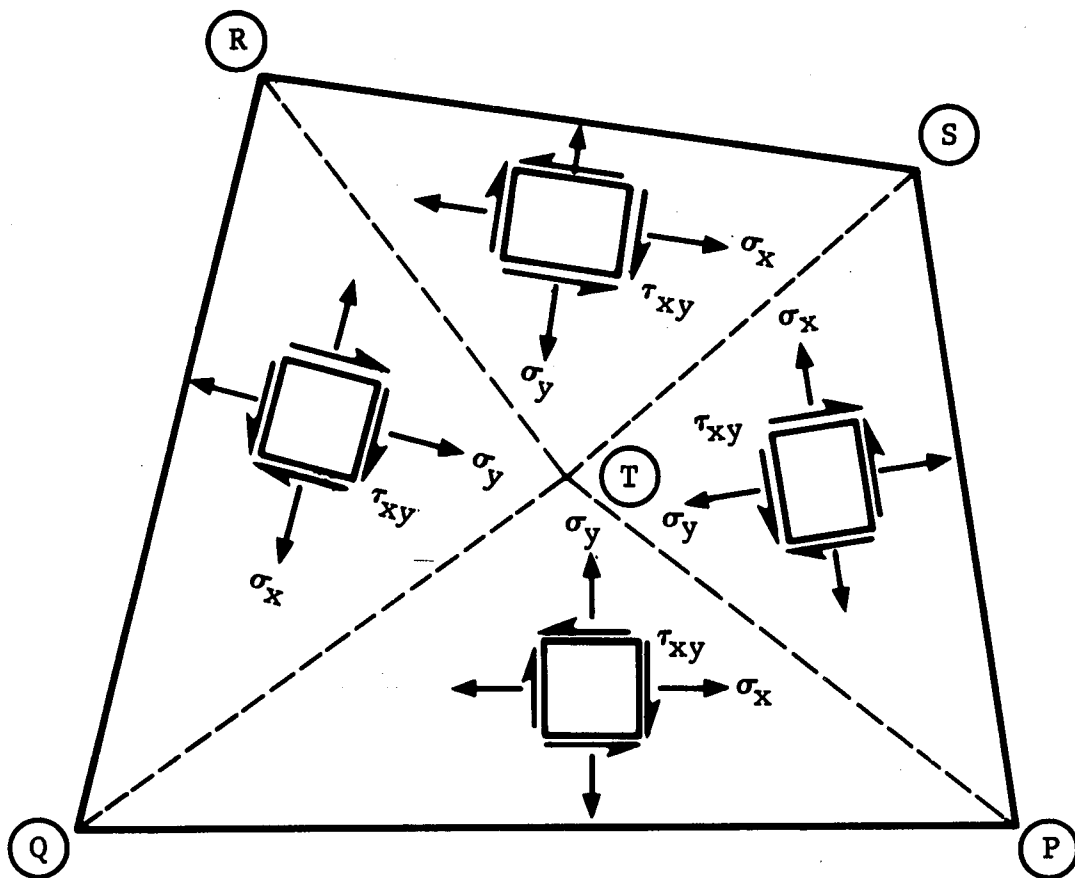


Figure 5 Quadrilateral Plate Local Stress Conventions

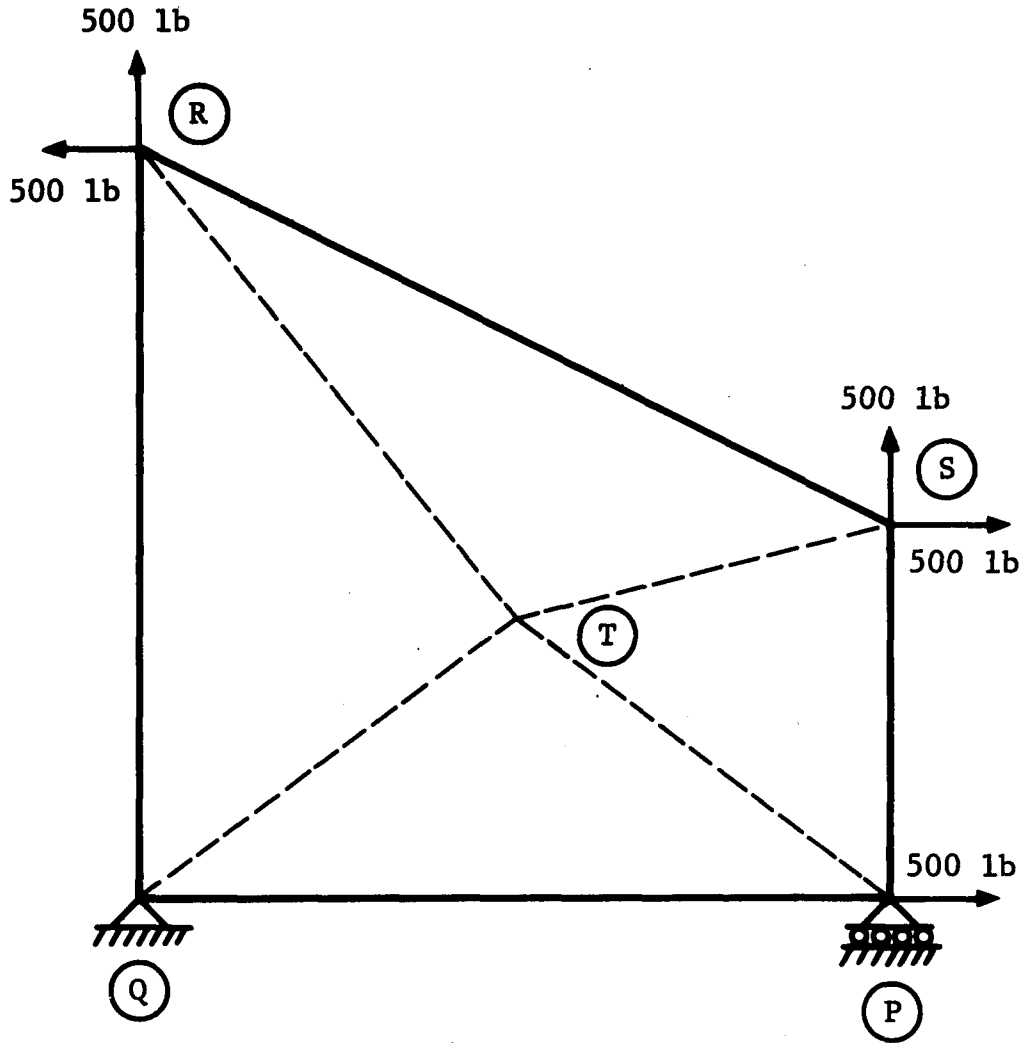


Figure 6 Quadrilateral Study Problem

Figure 7, and actual deflection-average stress results are shown in Figure 8. This problem is typical of the type of study problems used in developing this element.

It is interesting to note that, even though the actual common midpoint node deflections and the average common midpoint node deflections show considerable disagreement, the average stress results agree within a very small percent.

Since the average deflection-average stress method requires significantly fewer calculations, this procedure was selected for development of the quadrilateral plate element for inclusion in the RQ1 nonlinear computer program.

4.2 Quadrilateral Plate Element Number 5

The constant stress triangular plate is, in reality, a very versatile analytical tool. Many of its shortcomings can be eliminated when groups of triangles are combined into small substructures. Such a grouping was illustrated in the development of quadrilateral plate element number 4. The numerical results of the number 4 element are quite accurate, and the computation time for its utilization is satisfactory; however, the elimination

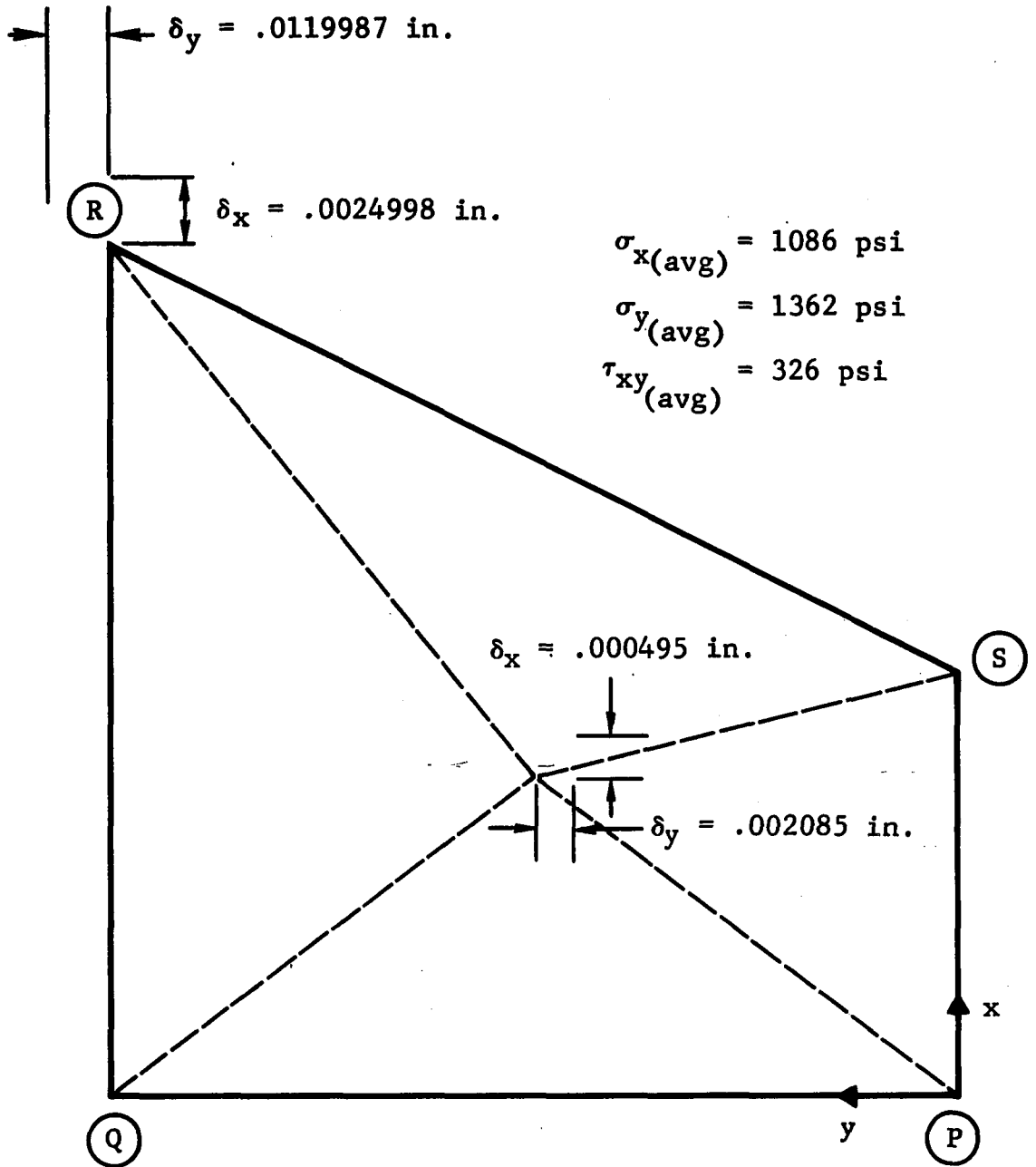


Figure 7 Quadrilateral Plate Stresses, Average Deflection - Average Stress

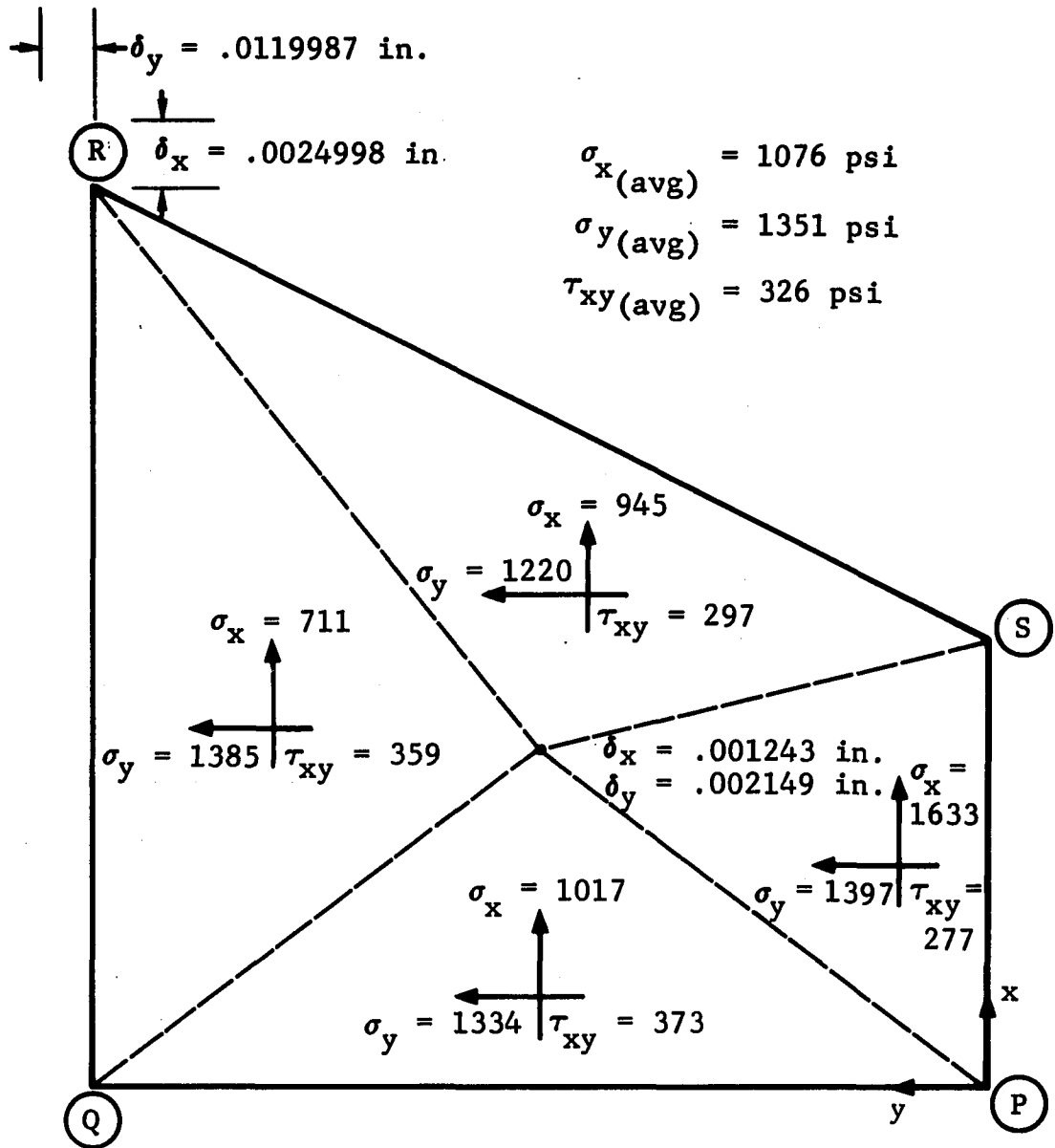


Figure 8 Quadrilateral Plate Stresses, Actual Deflection - Average Stress

procedure required for its use increases the computation time. The development of the element number 5 quadrilateral plate was begun to see if a technique of overlapping the four triangles, thus eliminating the need for the center node, would provide an element that would be equally as accurate as the element number 4.

The element developed for study is shown in Figure 9. Each constant stress triangle is given a thickness of one-half of the thickness of the plate. This element does not require averaging of the stresses until the final step, immediately prior to the print function. In other words, the computer program treats element number 5 as if it were four separate triangles placed in an overlapping fashion within the quadrilateral space. The results obtained with this technique are a little disappointing, especially after splendid results were obtained with the number 4 element. Although the overlapping element is faster in the execution phase of the computer program, it will not give the same degree of accuracy as that obtained with element number 4. In fact, element number 5, with its four triangles, produces only slightly better results than those obtained with two constant stress triangles.

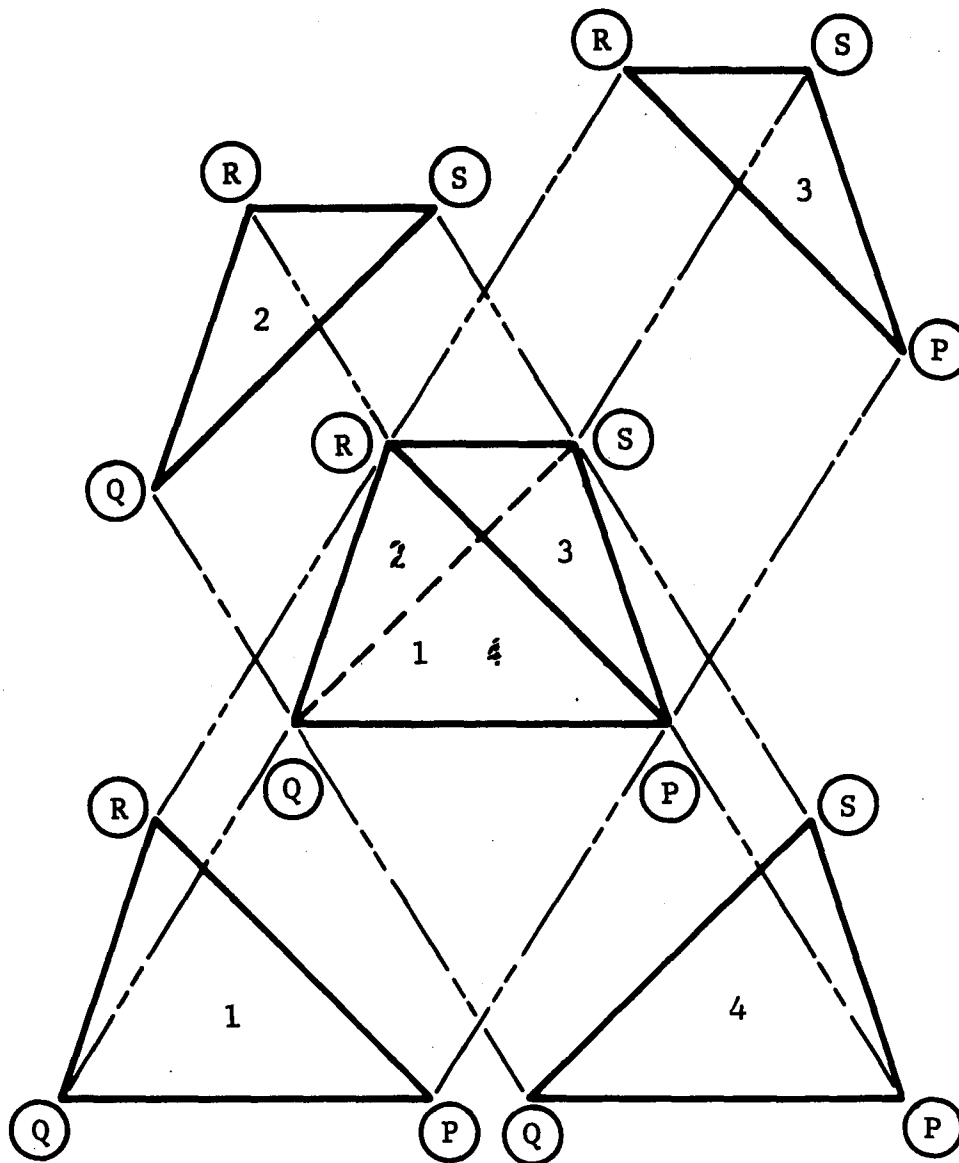


Figure 9 Quadrilateral Plate Element Number 5

The results obtained from studies made with this element are compared with results obtained using other elements in the next two chapters 5 and 6.

CHAPTER 5

THE SHEAR-LAG PROBLEM

The shear-lag problem, though seemingly only a simple laboratory or textbook type problem, is one which engineers encounter time and again in actual practice. A typical critical shear-lag problem occurred in the design of the Saturn V booster. The designers were faced with the problem of distributing the engine thrust loads into the thin skins of the booster skirt by use of tapered thrust beams. Millions of pounds of engine thrust had to be reacted correctly to prevent overstressing the skins and failure of the system. Calculation of the safety factor for such a problem, where the safety factor is based upon an ultimate load criteria, usually requires the accurate solution of a nonlinear problem in order to predict failure and determine the correct stress distribution.

5.1 Problem Definition

The shear-lag problem selected for presentation in this study was first presented by Percy, Loden, and Navaratma

(1963). The specimen design is illustrated in Figure 10. Tensile coupon stress-strain data taken from both the longitudinal and transverse direction are presented in Figure 11. The X-axis coincides with the longitudinal direction. The structure, which was an integrally machined part of 2024-T4 aluminum alloy, stiffened along the loading axis. The material properties essential to this analysis were the modulus of elasticity, E , the plastic stress, σ_0 , Poisson's ratio, μ , and the nonlinear Richard's parameter, n . The values obtained from the stress strain data shown in Figure 11 are $E = 10,000,000$ psi, $\sigma_0 = 52,000$ psi, and $n = 5$ for the transverse specimens and $E = 10,000,000$ psi, $\sigma_0 = 54,000$ psi, and $n = 8$ for the longitudinal specimens. Poisson's ratio was equal to one-third.

The test specimen was instrumented with a number of Budd metal film strain gauges on both faces of the panel. All of the two-gauge rosettes were mounted with their elements oriented in the vertical and horizontal directions. An exact explanation of the strain gauge types, locations, and orientations has been reported by Percy, Loden, and Navaratna (1963).

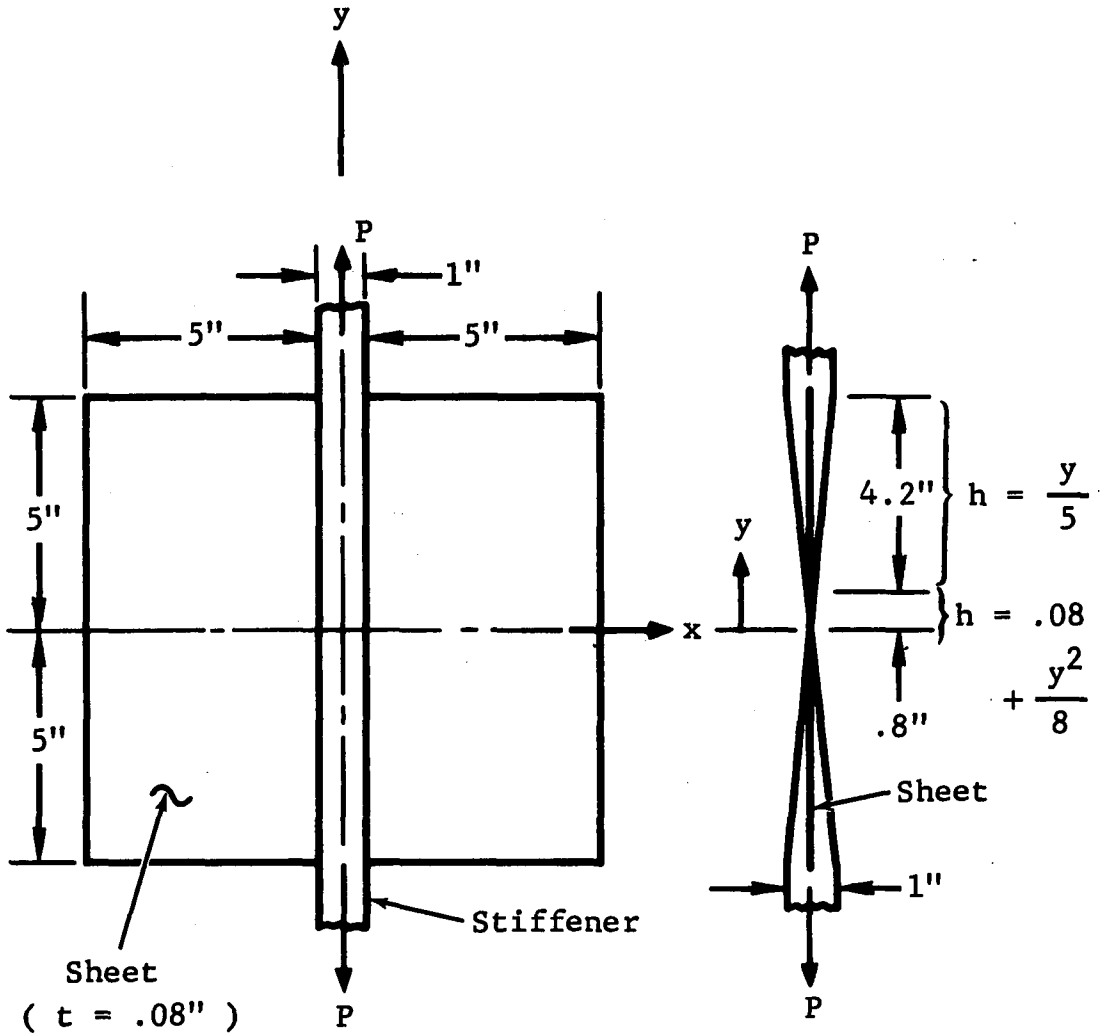


Figure 10 Shear-Lag Specimen

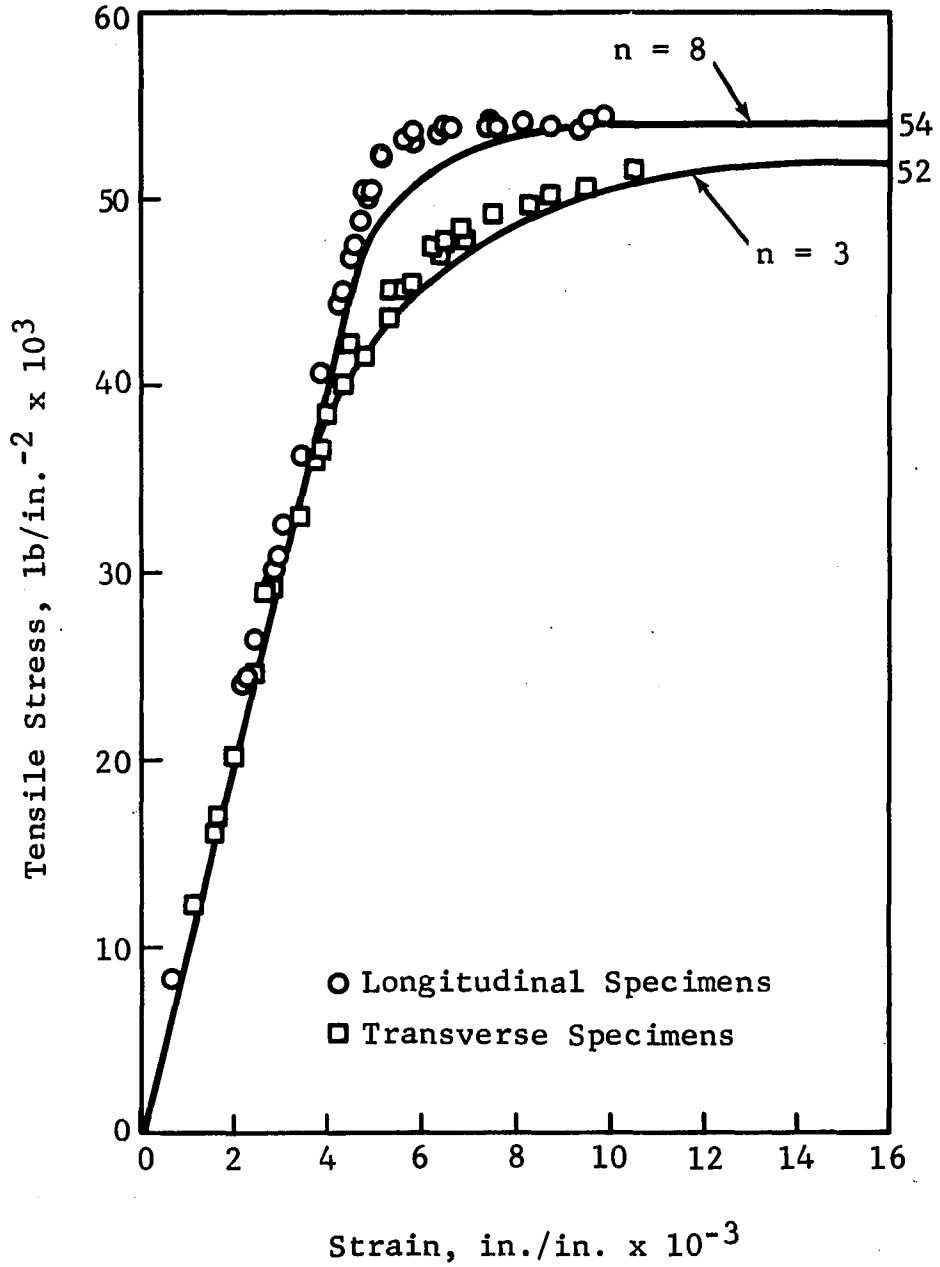


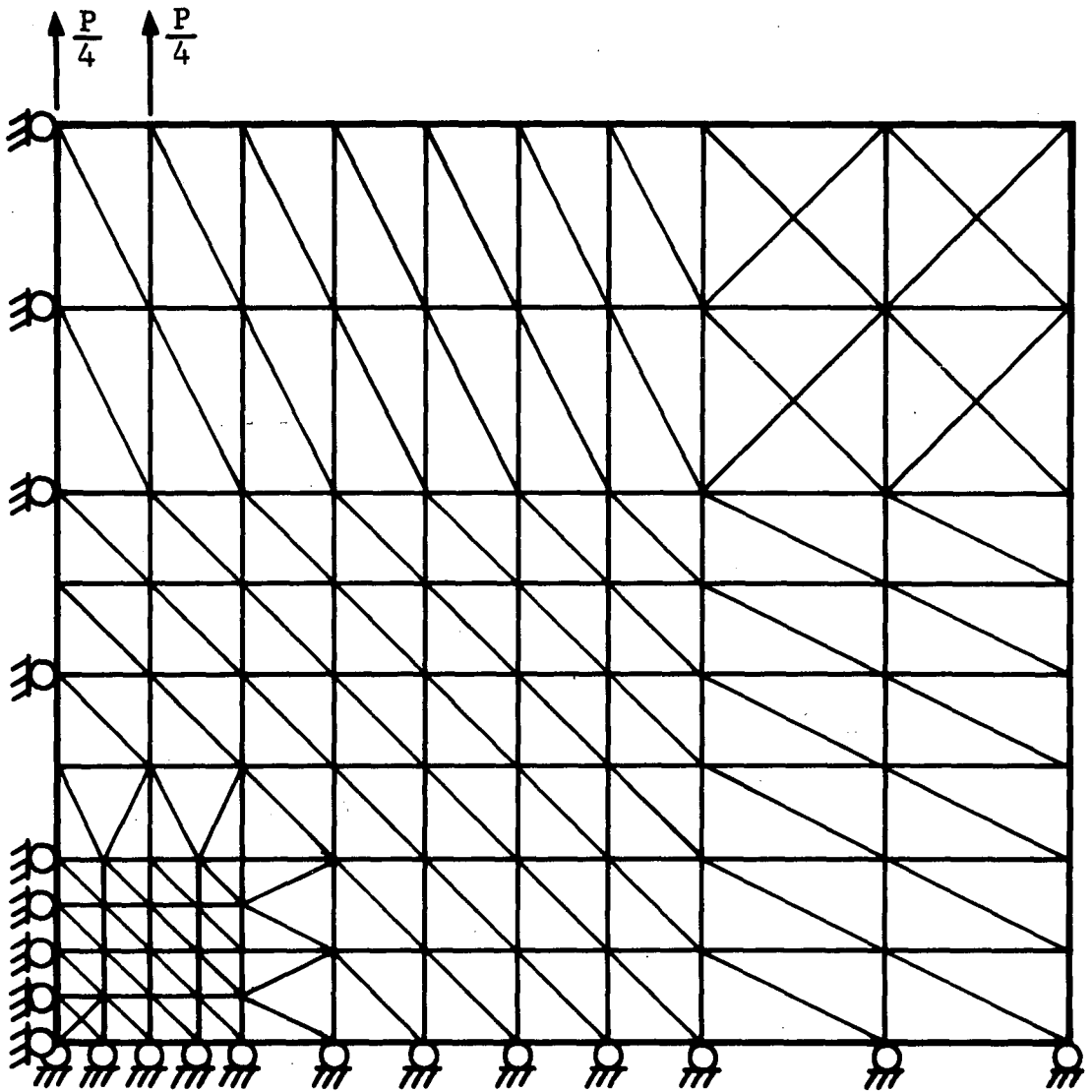
Figure 11 Stress Strain Plot of Test Data

5.2 Fine Grid Solution

The fine grid structural idealization for one quadrant of the structure is shown in Figure 12. Element number 2 triangular plate elements were used to represent the structural material of both the sheet and the stiffener. The grid was arranged to take the best advantage of the 182 elements, so more elements were placed in the areas of higher stress gradients. For this model the transverse tensile specimen data were used.

The boundary conditions applied to the stiffness matrix are pictured in Figure 12. By modeling only one quadrant of the structure and then fixing the X-coordinates along the vertical centerline and the Y-coordinates along the horizontal centerline and applying one-half of the load, the solution is identical to the one that would be obtained if the total structure were simulated.

To obtain the nonlinear solution, loads equal to one-fourth P were each applied in five equal steps. Figure 13 is a plot of the center strains versus the applied loads for both the analytical and test results. The good correlation between the computer solution and the test results



(182 Element Number 2 Triangles)

Figure 12 Fine Grid Simulation

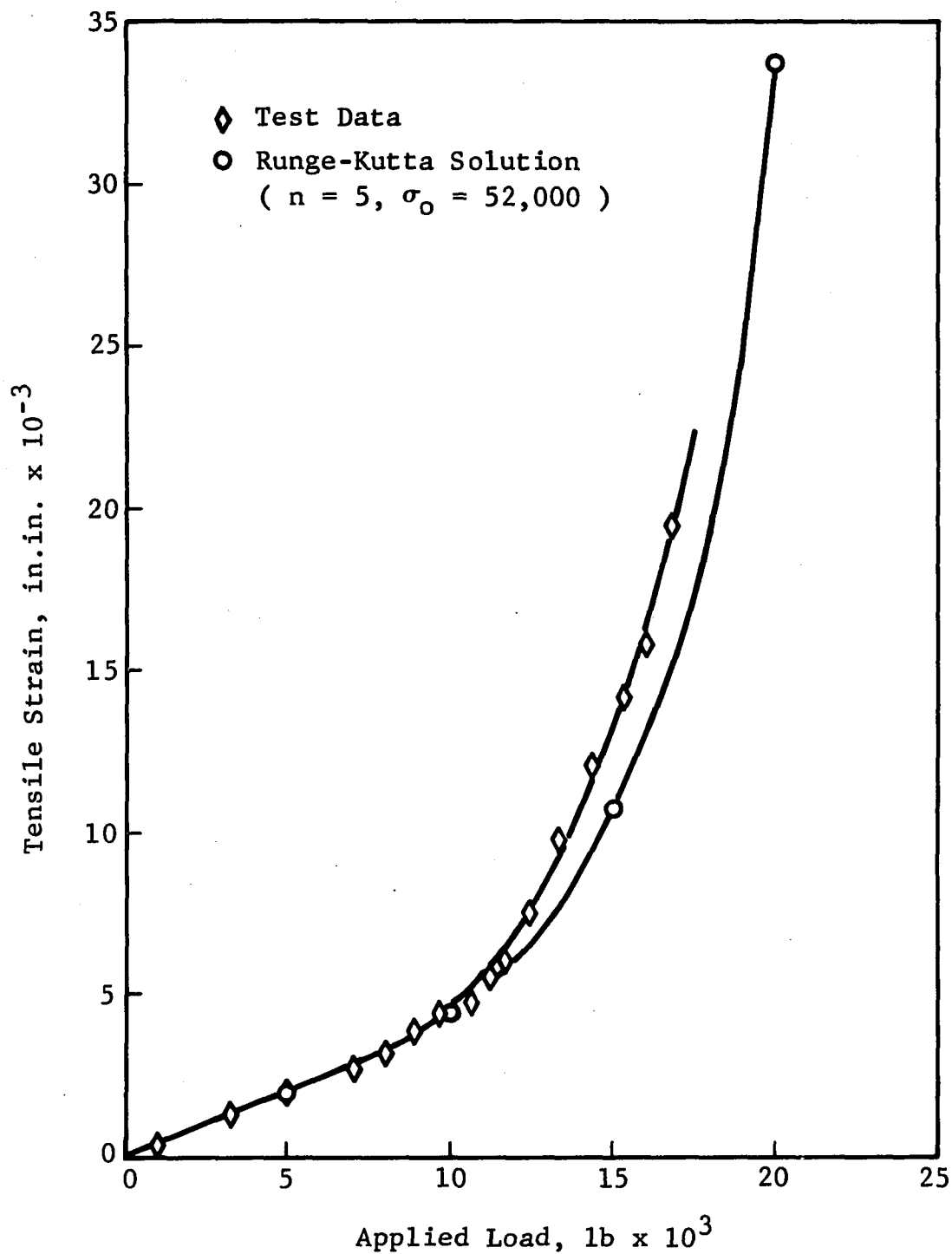


Figure 13 Center Strain vs Applied Load (Fine Grid)

was not achieved with the first model attempted. The particular fine grid used to determine these results was the best of several that were investigated. The steep stress gradients around the center of the plate are very severe and require more grid fineness than might at first be expected. Other model studies are reported elsewhere (Richard and Blacklock 1968).

In Figures 14 and 15, the ϵ_y and ϵ_x strains are plotted along the structure centerline at $Y = 0.0$. It can be seen in these plots that the general strain distribution in the Y-direction is very accurate whereas the stress distribution in the X-direction is less accurate. The difference in accuracy may be due to the fact that the Y-direction elastic properties were used. However, noting the difference in the magnitudes of the strains, the percent of errors are quite acceptable when compared to the maximum values.

5.3 Coarse Grid Solution

The coarse grid simulation was developed in order to evaluate the accuracy of the different elements under consideration. No attempt was made in the coarse grid arrangement to account for the areas of higher stress

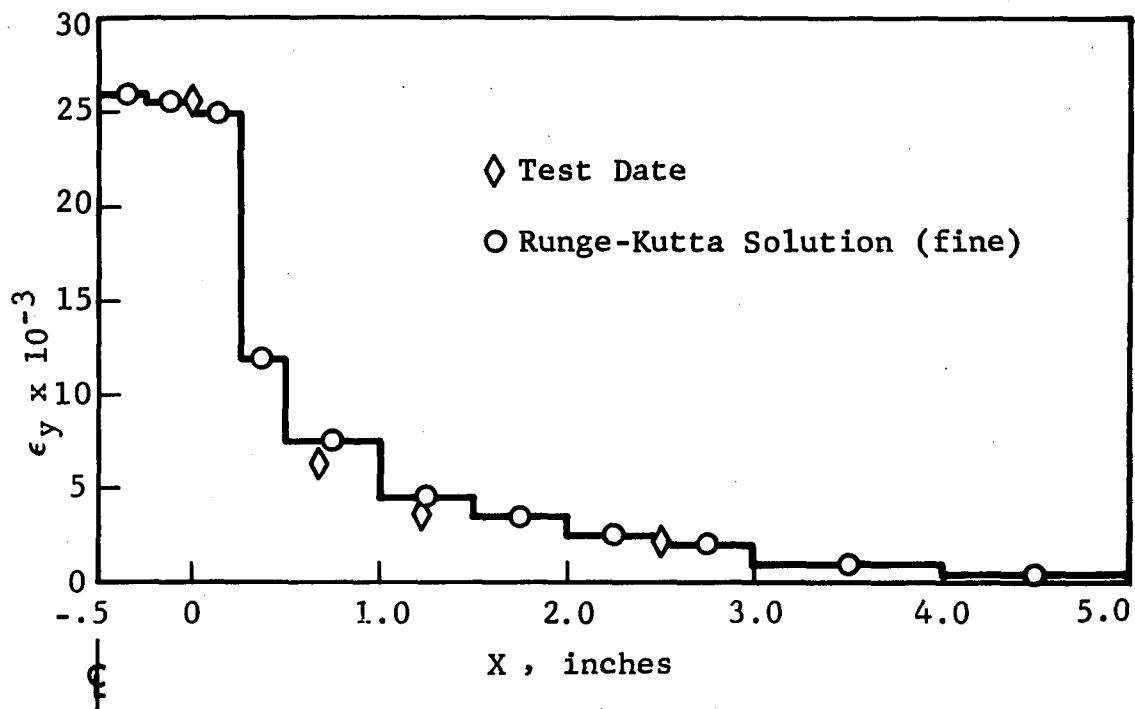


Figure 14 Strain (ϵ_y) Distribution Along the Line $y = 0.0$

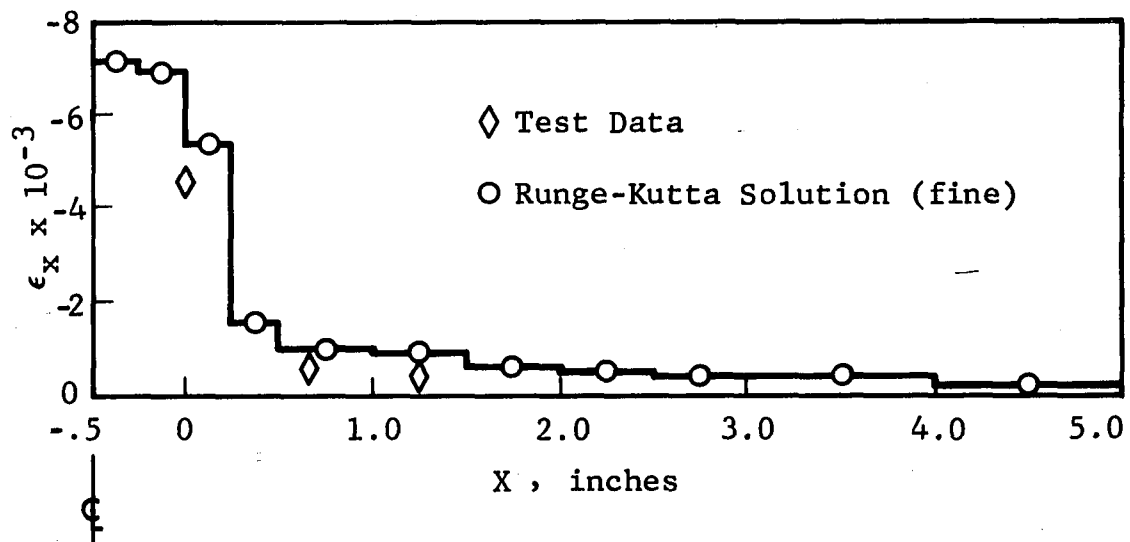


Figure 15 Strain (ϵ_x) Distribution

gradients. The coarse grid depicted in Figure 16 is made up of 30 rectangles. The problem was solved five times, once with each element. The solution with element number 1 was obtained with the formation of Hrennikoff rectangular plate elements. In each case the load conditions and boundary conditions were the same.

Figure 17 is a presentation of the nonlinear deflected shape. The dotted lines represent the shape of the grid lines after they have deformed. The table shown at the top of Figure 17 reflects the actual values for δ_{\max} for each of the models. Model number 3 gave the largest deflection and the Hrennikoff model was the stiffest. The nonlinear deflection obtained with the Hrennikoff model was less because of the nonlinear algorithm within computer program. In this algorithm, the von Mises effective stresses are used to predict the amount of nonlinear action. In the Hrennikoff model, the number 1 bars can only carry axial loads, so the effective stress principle is eliminated. This principle could be incorporated by additional programming; however, the good results obtained with the other elements will probably discourage this additional effort.

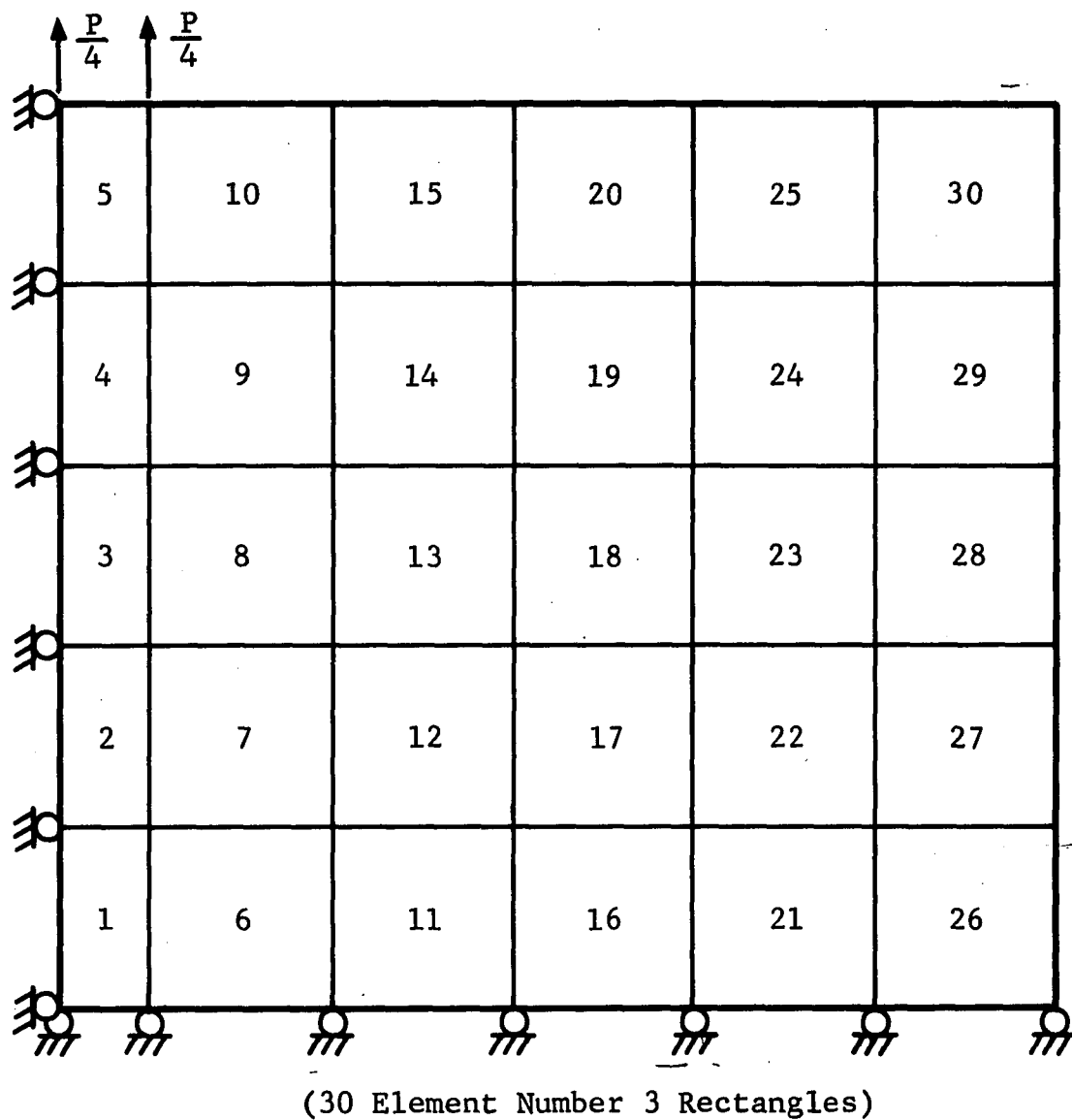


Figure 16 Coarse Grid Simulation

Element	δ_{\max}
Hrennikoff	.01442"
Elem. No. 2	.01557"
Elem. No. 3	.01607"
Elem. No. 4	.01597"

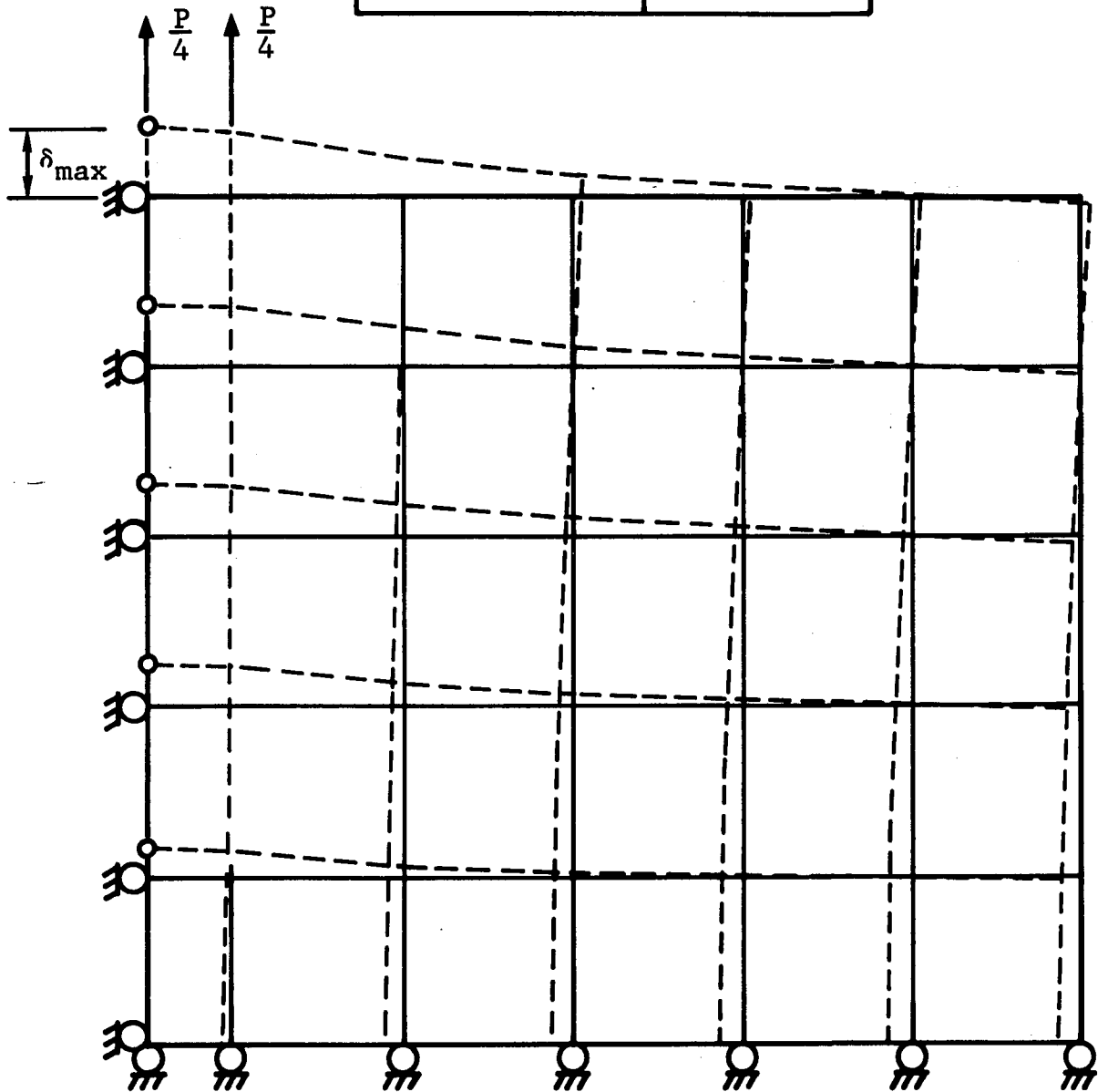


Figure 17 Nonlinear Deflected Shape

In Figure 18, the average center stress in the center-most element is plotted versus applied load. Element numbers 3 and 4 gave nearly identical results, and element numbers 2 and 5 gave nearly identical results. The results obtained with element numbers 3 and 4 were slightly more accurate than the others.

In Figure 19, the σ_y stresses are plotted along the centerline at $Y = 0.0$. The results from each of the element analyses are so similar that one may conclude that, for this simulation, any one of the elements may be used satisfactorily.

5.4 Final Remarks on the Shear-Lag Problem

The computer study reported in this chapter should give the reader some idea of the grid fineness required for an accurate solution of stress concentration problems. This is especially important in the fatigue analysis of brittle materials. For rough analysis of ductile structure, the coarse grid solution may be adequate.

The element study has shown that any one of the elements is adequate for solving the shear-lag problem; however, the high stress concentration can only be accurately analyzed with a very fine grid. Fewer elements are required

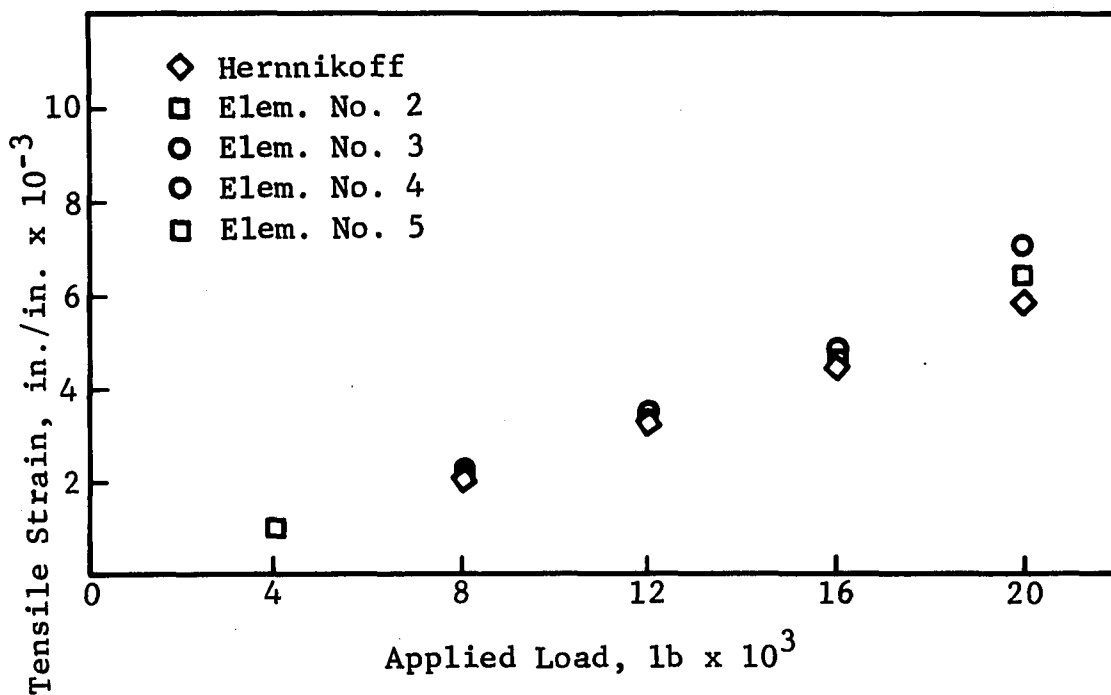
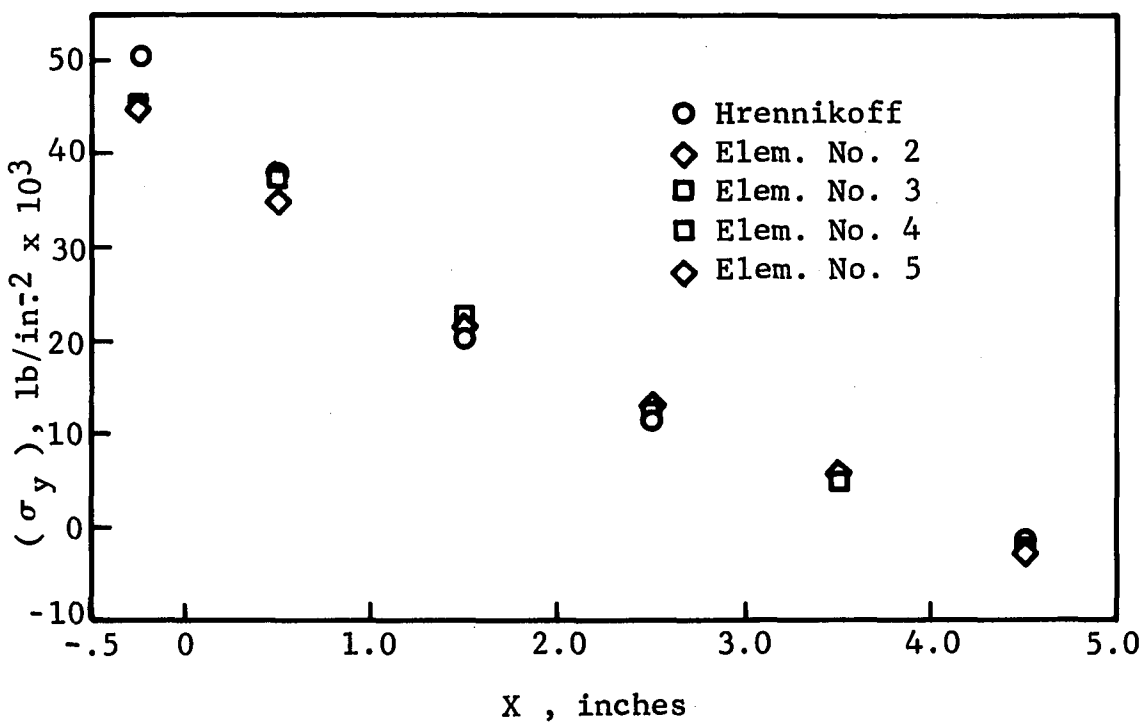


Figure 18 Average Center Stress vs Load

Figure 19 Stress (σ_y) Along Line $y = 0.0$

when the rectangular and quadrilateral elements are used; however, if a computer program has only triangular elements available, the problem can still be solved with only a small penalty in computer time.

CHAPTER 6

THE CANTILEVER PROBLEM

The cantilever problem is perhaps one of the most interesting of the classical structural problems. One early attempt to obtain a solution for the cantilever beam problem was carried out by the French physicist Mariotte (1620-1684). Following the earlier work of Galileo (1564-1642), Mariotte erroneously took the neutral axis to be tangent to the boundary at the concave side; however, he was the first to present correctly the idea of linearly increasing tension and compression stresses above and below the beam centerline. Parent (1666-1716) is recognized as the first to locate the neutral axis and present a correct solution for the elastic stress analysis of the cantilever beam problem.

The considerable success achieved by Parent and others with the cantilever beam problem is barely mentioned in "A Treatise on Civil Engineering," an early American textbook (1880) by D. H. Mahan, LL.D., a professor of Civil Engineering at West Point. The analytical treatment of such

problems was completely omitted from the main text, which consisted of 543 pages devoted to the more important "descriptive matter." Items concerned with "mathematical analysis," which included three cantilever examples, were relegated to a 76-page appendix.

The engineers who made these early attempts to analyze the cantilever problem were particularly handicapped since they were challenged to predict failing loads rather than the elastic stress distribution. Present-day strain measuring devices were not available to these men, so they directed their attention to the failing loads, which could be substantiated, rather than to elastic analysis.

It is interesting to note that even with today's technology one of the most challenging engineering problems is to predict the ultimate or failing load of complex engineering structures. It has become quite apparent that in order to predict failing loads one must be able to examine the state of nonlinear stress which occurs within the structure.

This chapter on nonlinear analysis of the cantilever problem is presented with the hope of encouraging engineers

to take a critical look at the accepted plastic solutions of these and other engineering problems to see whether, as in the case of Galileo and Mariotte, the proverbial neutral axes may have been mislocated.

6.1 Problem Definition

The work reported in this chapter was conducted for use in the evaluation of the new nonlinear elements. It has, however, also afforded the writer the opportunity to rediscover, by use of modern matrix analytical tools, the solution of the cantilever beam. Some of the findings have been quite surprising, while others have merely confirmed that which has already been stated.

The three classes of problems chosen for examination were the cantilever plate (Figure 20), the cantilever beam (Figure 21), and the tapered cantilever beam (Figure 22). In seeking to find the critical variables to validate the study of the cantilever beam, approximately 12 models were chosen originally. Variables in these models included long beams as well as short beams; heavy, medium and light flanges; and small, medium, and steep tapers. Summing up these possibilities and considering the different stress-strain curves possible, it became apparent that several hundred computer

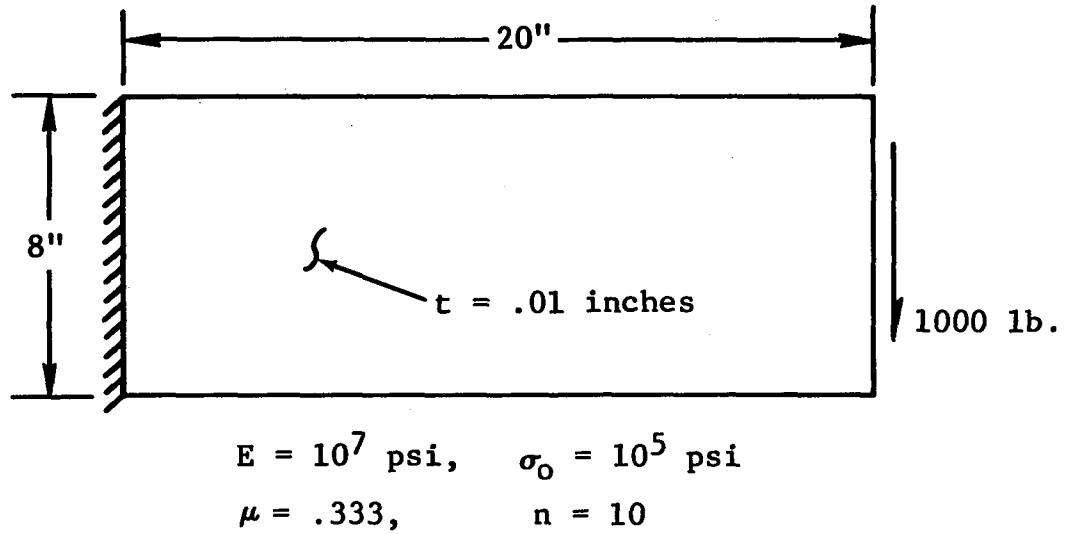


Figure 20 Cantilever Plate Problem, Models I Through IV

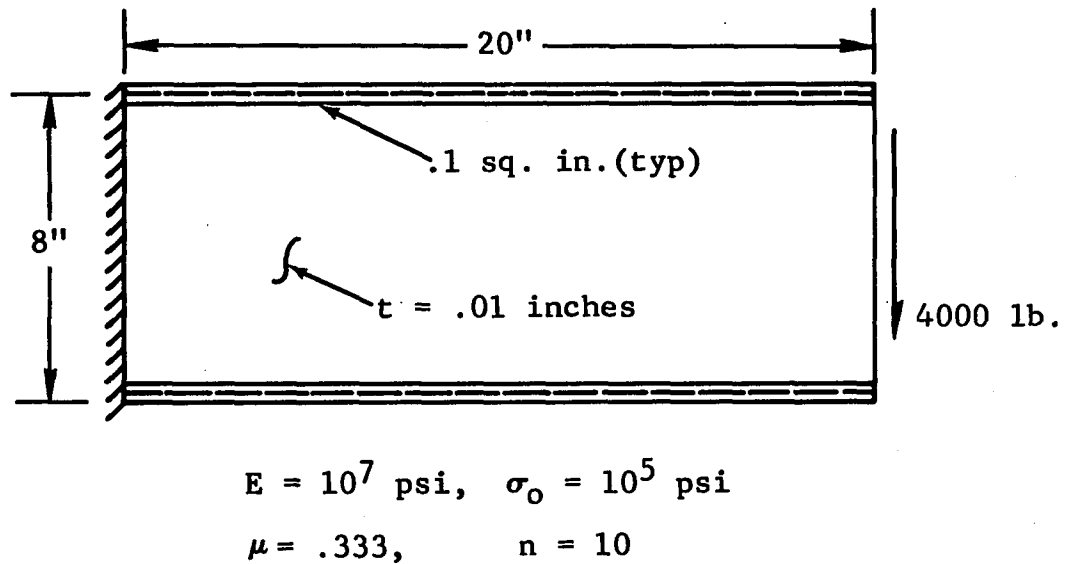
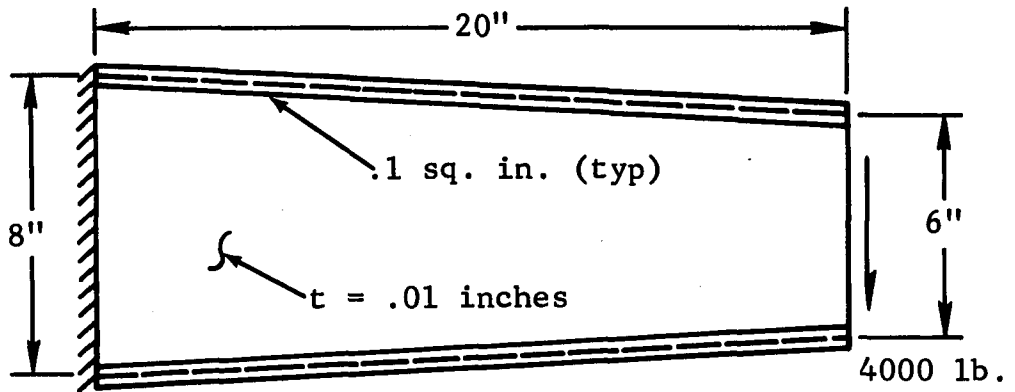


Figure 21 Cantilever Beam Problem, Models IA Through IVA



$$E = 10^7 \text{ psi}, \sigma_0 = 10^5 \text{ psi}$$

$$\mu = .333, \quad n = 10$$

Figure 22 Tapered Cantilever Beam Problem. Models IB Through IVB

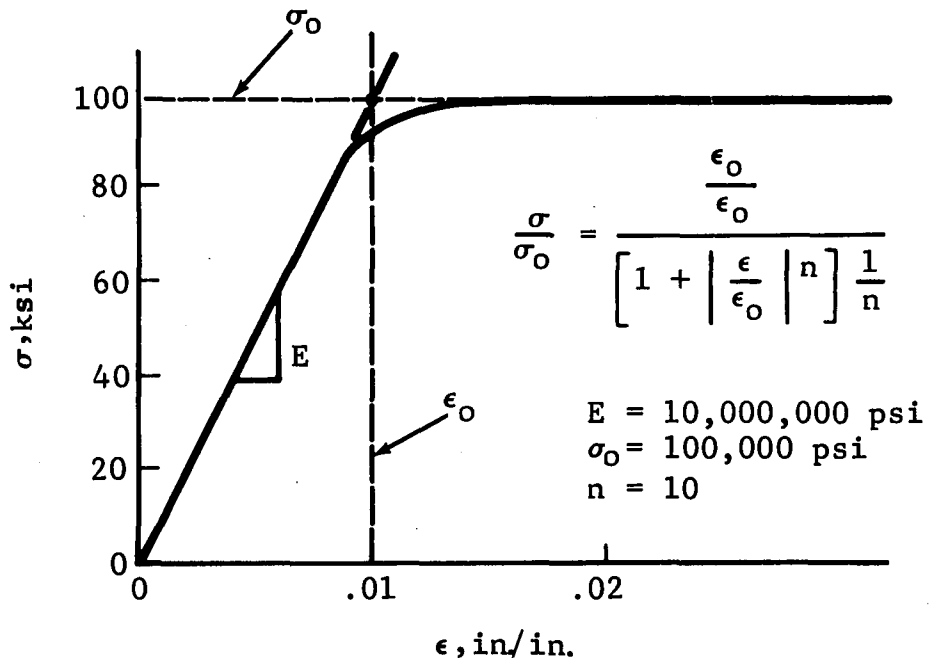


Figure 23 Nonlinear Stress-Strain Curve

runs would be required to complete such an ambitious study. It was finally decided that by selecting the medium range of all of the variables and utilizing the stress-strain curve shown in Figure 23, 48 problems would provide a fairly accurate evaluation of the nonlinear elements and grids chosen for examination.

6.2 Problem Simulation

The three cantilever problems were simulated by various systems of bars, triangles, rectangles, and quadrilaterals. The number of these elements necessary for each simulation depended on the grid mesh size. The grids varied from a minimum of five divisions to a maximum of 80 divisions. Four grid simulations were made for each problem as shown in Figures 24 through 35. The boundary conditions are illustrated along the left edge of the beams in each figure.

The five-division grid is of particular importance in solving practical engineering problems since it represents the type of simulation that can be used for very large plate-like structure, where one layer of shear elements can be used to represent the full depth of the shear web.

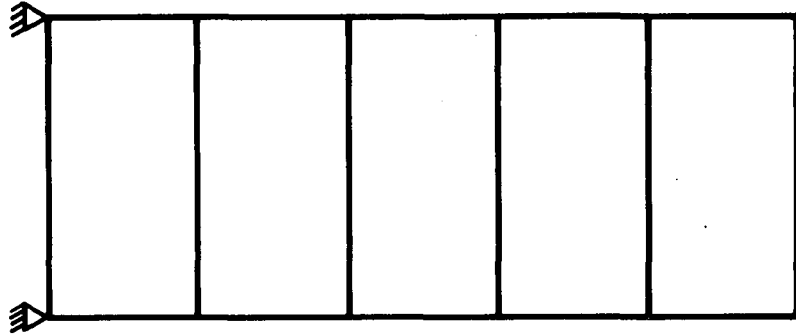


Figure 24 Model I Simulation, 5-Grid Plate

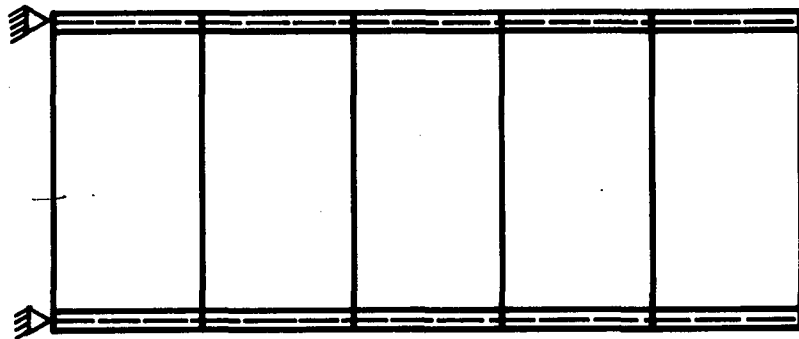


Figure 25 Model IA Simulation, Plain Beam

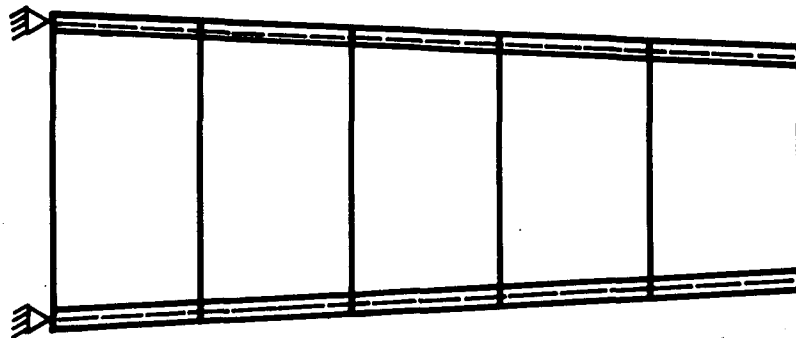


Figure 26 Model IB Simulation, Tapered Beam

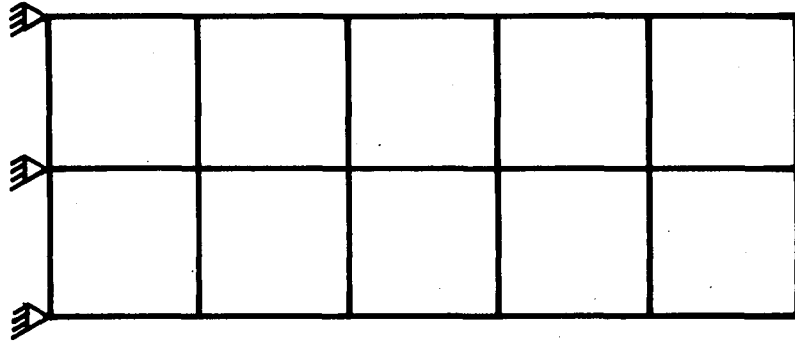


Figure 27 Model II Simulation, 10-Grid Plate

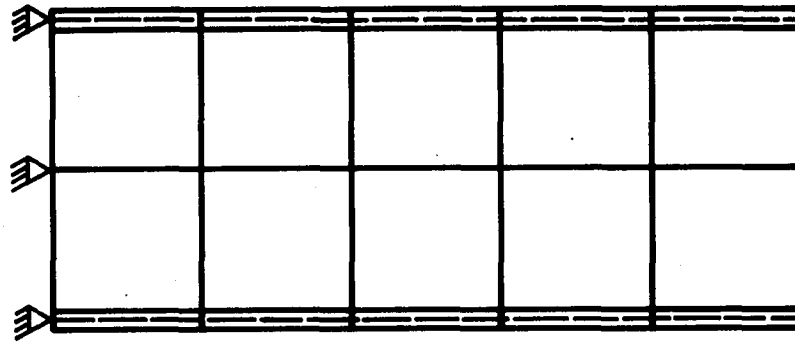


Figure 28 Model IIA Simulation, Plain Beam

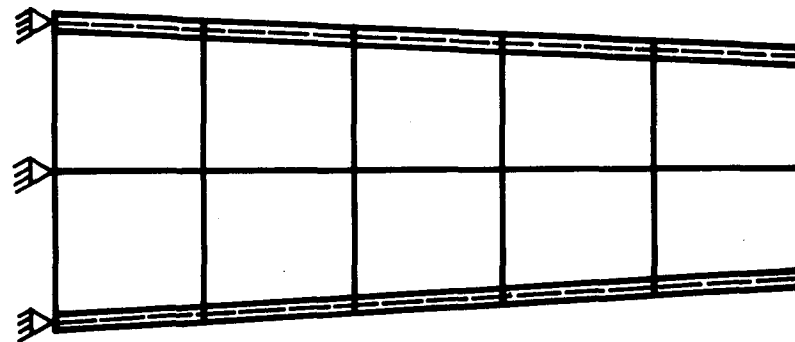


Figure 29 Model IIB Simulation, Tapered Beam

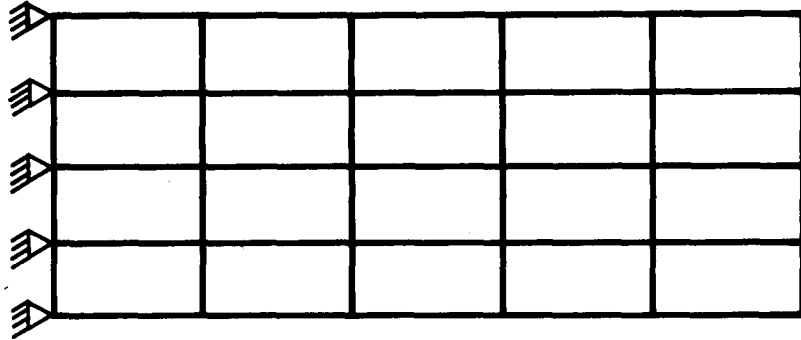


Figure 30 Model III Simulation, 20-Grid Plate

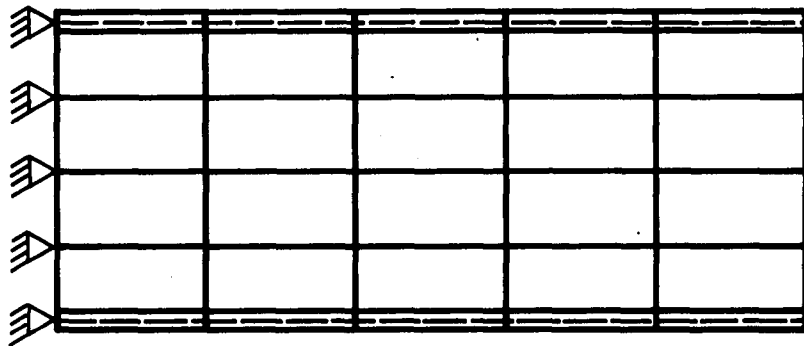


Figure 31 Model IIIA Simulation, Plain Beam

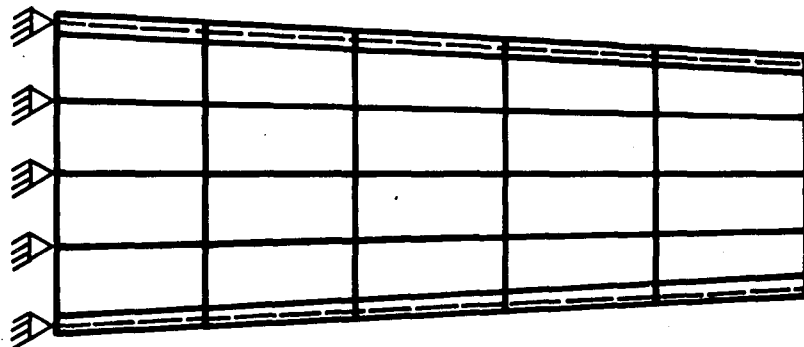


Figure 32 Model IIIB Simulation, Tapered Beam

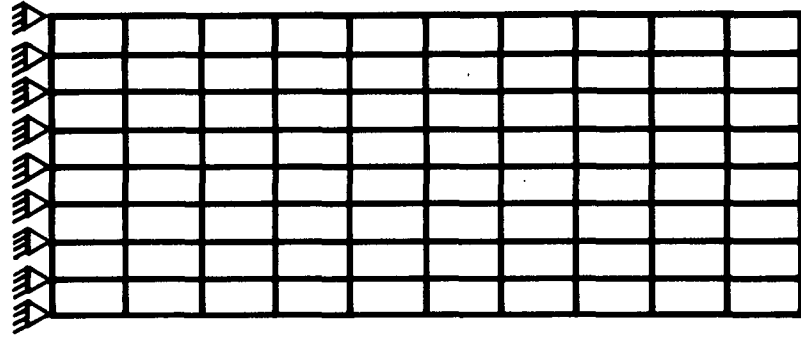


Figure 33 Model IV Simulation, 80-Grid Plate

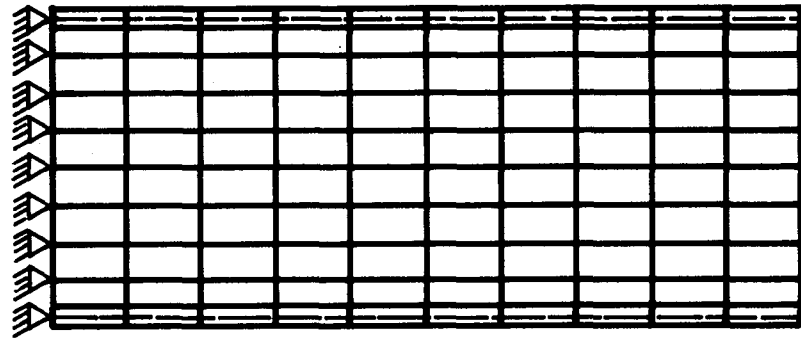


Figure 34 Model IVA Simulation, Plain Beam

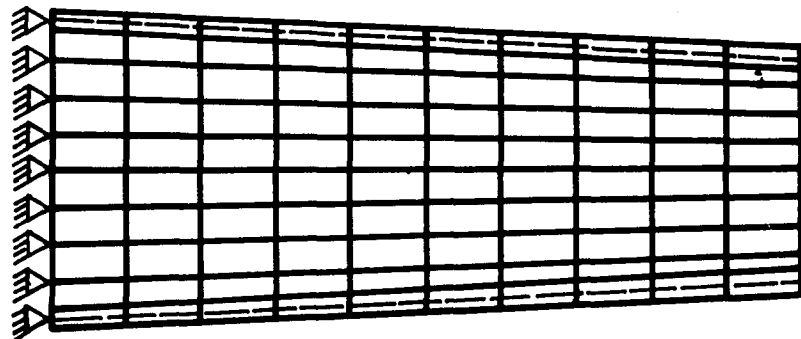


Figure 35 Model IVB Simulation, Tapered Beam

The 80-division grid was chosen to represent the base line solution. Since an exact analytical solution to such problems is not available, the author felt that the 80-grid problems would provide the best measuring stick for the correctness of the nonlinear solutions.

Both the 10- and 20-division grids were chosen because these were considered to approach the ideal grid for the nonlinear solution of a series of problems such as these.

The choice of boundary conditions for these studies presented a problem since a proper boundary condition for one of the problems was either impossible or impractical for one of the other problems. The boundary conditions finally chosen (shown in the Figures 24 through 35) proved to be quite manageable, and the effects of the boundary conditions on the results were not considered important provided these were consistent.

The use of the constant stress bar to represent the outstanding flange proved to be a slight handicap in examining the various elements. While the constant stress bar and the constant stress triangle are quite compatible, the use of this same bar with the more sophisticated rectangular elements subjected the flange to a discontinuous load

distribution. The effects of this unknown variance on the solution was not ascertained.

Loads were applied in a more or less parabolic shaped distribution. The load applied to Model I was divided into two equal parts; however, a more accurate application was possible in the other problems. The parabolic distribution was selected to minimize the effects of redistribution near the load; this was an important item in the study of the short beams. In each of the nonlinear solutions the load is applied in two equal increments, and the stresses and deflections were found by use of two intervals of Runge-Kutta integration.

The rectangular elements were not used for the analysis of the tapered beams. Although the computer program will accept rectangular plates in quadrilateral grids, the answers will always be out of moment balance. One point, which perhaps should be mentioned is the importance of using adequate checking procedures to ensure correct operation of the computer program. For instance, it is easy to show that the summation of forces in the X- and Y-axis directions are exactly in balance while, due to improper selection of ele-

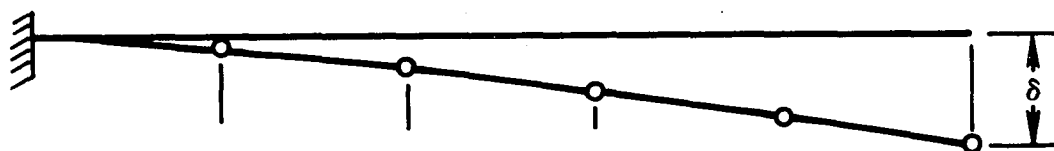
ments such as rectangles for quadrilaterals, the solution may be completely out of moment balance.

6.3 The Cantilever Plate Analysis

The cantilever plate, shown in Figure 20, is 20 inches long and 8 inches deep. The assumed stress strain diagram for this plate was shown in Figure 23. The problem was solved for a 1000-pound load applied parabolically at the right edge while the nodes along the left edge remained fixed. Element numbers 2, 3, 4, and 5 were each used to simulate the plate material; these simulations are shown by Models I, II, III, and IV.

6.3.1 Deflection Analysis

The nonlinear plate deflections for the 1000 pound load are shown plotted along the plate length in Figure 36. It is easy to see from these results that, in every model, the element number 3 rectangle gives the highest deflection values. Because the procedure gives a lower bound to the correct answer for these solutions, the deflection for element number 3 which varies from 0.574 inch for Model I to 1.205 inches for Model IV is the most accurate value calculated for each grid.



Model I

ELEM No. 2	.024	.064	.115	.175	.240
ELEM No. 3	.041	.131	.258	.410	.574
ELEM No. 4	.036	.111	.217	.342	.477
ELEM No. 5	.023	.061	.113	.172	.236

Model II

ELEM No. 2	.036	.100	.190	.295	.409
ELEM No. 3	.048	.141	.275	.436	.611
ELEM No. 4	.046	.136	.265	.420	.588
ELEM No. 5	.036	.100	.188	.293	.405

Model III

ELEM No. 2	.046	.137	.259	.402	.557
ELEM No. 3	.061	.173	.330	.514	.712
ELEM No. 4	.056	.158	.302	.472	.656
ELEM No. 5	.051	.143	.266	.411	.566

Model IV

ELEM No. 2	.121	.339	.600	.890	1.195
ELEM No. 3	.121	.336	.600	.895	1.205
ELEM No. 4	.096	.271	.493	.744	1.011
ELEM No. 5	.104	.280	.499	.745	1.007

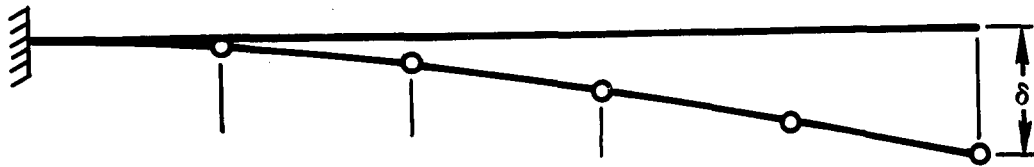
Figure 36 Nonlinear Plate Deflections for 1000-Lb Load

Several interesting observations may be made upon examination of the results obtained with the remaining three elements:

1. The deflections of Model III element number 2 analysis are more or less identical to the Model I element number 3 analysis. This would seem to indicate that for this type of problem one layer of the number 3 elements is as accurate as four layers of the number 2 elements.
2. The number 3 and 4 elements give almost the same answers for Models I, II, and III, with element number 4 being the stiffer of the two.
3. In each of the models the number 2 and 5 elements give more or less identical deflections. It is interesting to note that although the number 5 element is made of double overlapped triangles, i.e., twice the number of triangles, the deflections do not show any improvement.
4. The next point is one of great importance, and it recurs in each of the cantilevers analyzed. Throughout Models I, II, and III, the number 2 element deflections lag those of the number 3 and 4 elements

and then pass the number 4 element deflections and all but pass the number 3 element deflections in the Model IV analysis. What has happened is that the far left triangle, nearest the boundary where the highest stresses occur, has become plastic. This is the beginning of a plastic hinge, and, thus, the structure is only slightly short of collapse. This same effect does not show up in results obtained with the number 4 elements and shows up only slightly in results obtained with the number 3 element because the nonlinear action of these elements is monitored by the midpoint stresses, which are closer to the neutral axis. The warning here is that once a plastic hinge begins to form the accuracy of the results deteriorates rapidly. In this particular problem, the structure would suffer complete collapse if only a very small additional load were applied.

The elastic plate deflections for the 1000-pound load are shown plotted along the plate length in Figure 37.



Model I

ELEM No. 2	.024	.064	.115	.175	.239
ELEM No. 3	.041	.131	.258	.410	.574
ELEM No. 4	.036	.111	.216	.342	.477
ELEM No. 5	.022	.062	.113	.172	.236

Model II

ELEM No. 2	.035	.099	.186	.290	.403
ELEM No. 3	.048	.140	.274	.435	.609
ELEM No. 4	.046	.136	.265	.419	.587
ELEM No. 5	.033	.095	.181	.282	.392

Model III

ELEM No. 2	.042	.119	.228	.358	.499
ELEM No. 3	.050	.145	.282	.446	.625
ELEM No. 4	.049	.141	.273	.431	.603
ELEM No. 5	.040	.117	.225	.354	.493

Model IV

ELEM No. 2	.050	.148	.288	.455	.636
ELEM No. 3	.054	.157	.305	.481	.674
ELEM No. 4	.053	.154	.299	.472	.660
ELEM No. 5	.050	.146	.282	.446	.623

Figure 37 Elastic Plate Deflections for 1000-Lb Load

In comparison with the nonlinear results, the elastic results seem quite stable. For each model, the elements always remain in the same order with regards to the amount of predicted deflection. The elements are rated thus: Element number 5 is the least accurate, element number 2 next, element number 4 next, with element number 3, the rectangular plate with the linear edge displacement assumption, producing the best results.

In Figures 38 and 39 are shown the plots of the nonlinear and elastic tip deflections for the cantilever plate versus the grid size. Figure 38 shows graphically the before-mentioned plastic hinge effect of the number 2 and 3 element solutions. In the plot, this is noted as divergence, which is meant to indicate that the deflections are no longer converging as a lower bound solution but are diverging, which indicates that a collapse mechanism is being formed for this load. The results of the number 4 and 5 element solutions, because their stresses are lagging those of the other elements, seem to be stable up to this point. Perhaps for a 900-pound load all elements would be stable, and for an 1100-pound load all elements would diverge. At

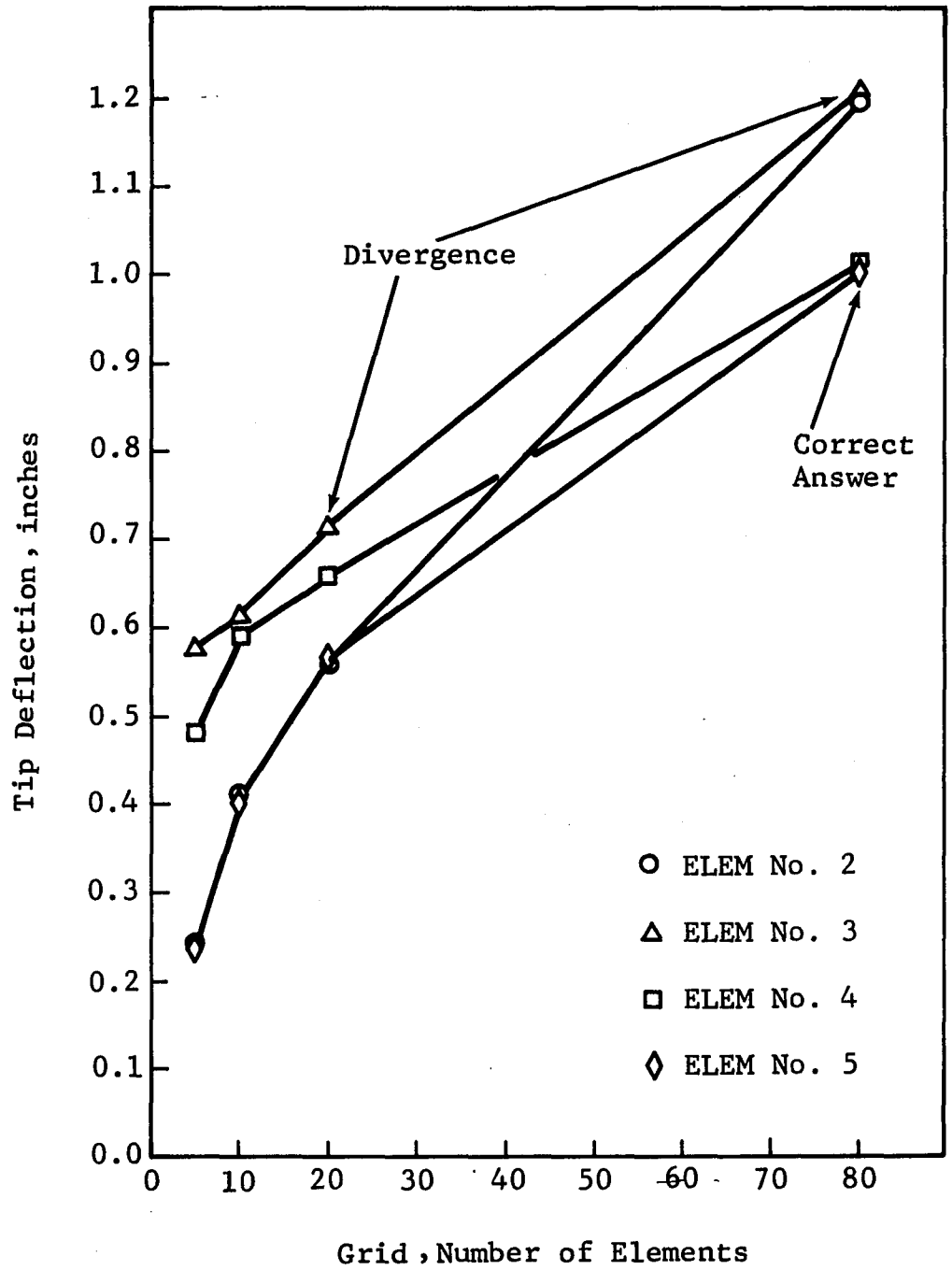


Figure 38 Nonlinear Cantilever Plate Tip Deflection vs Grid Size

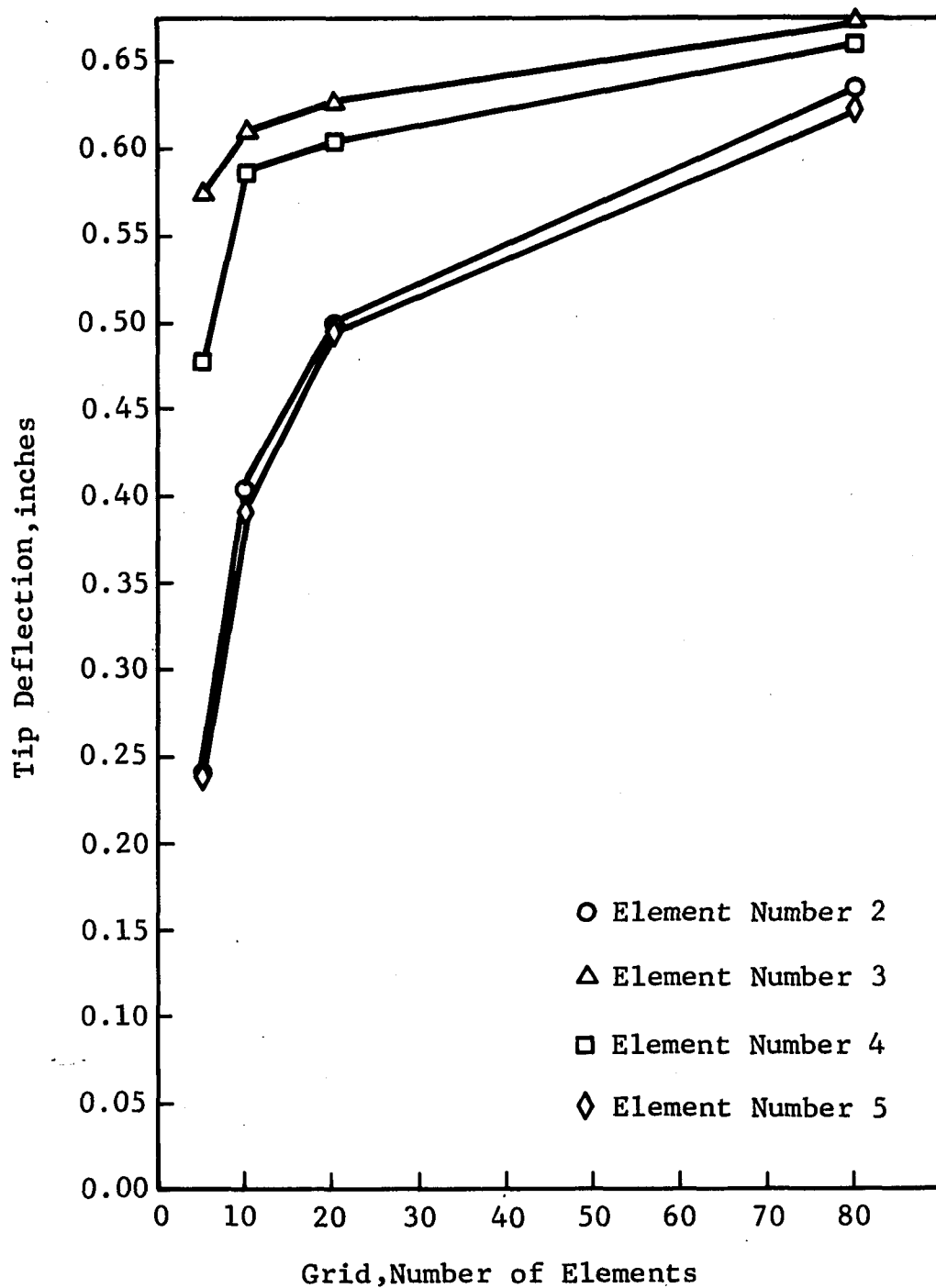


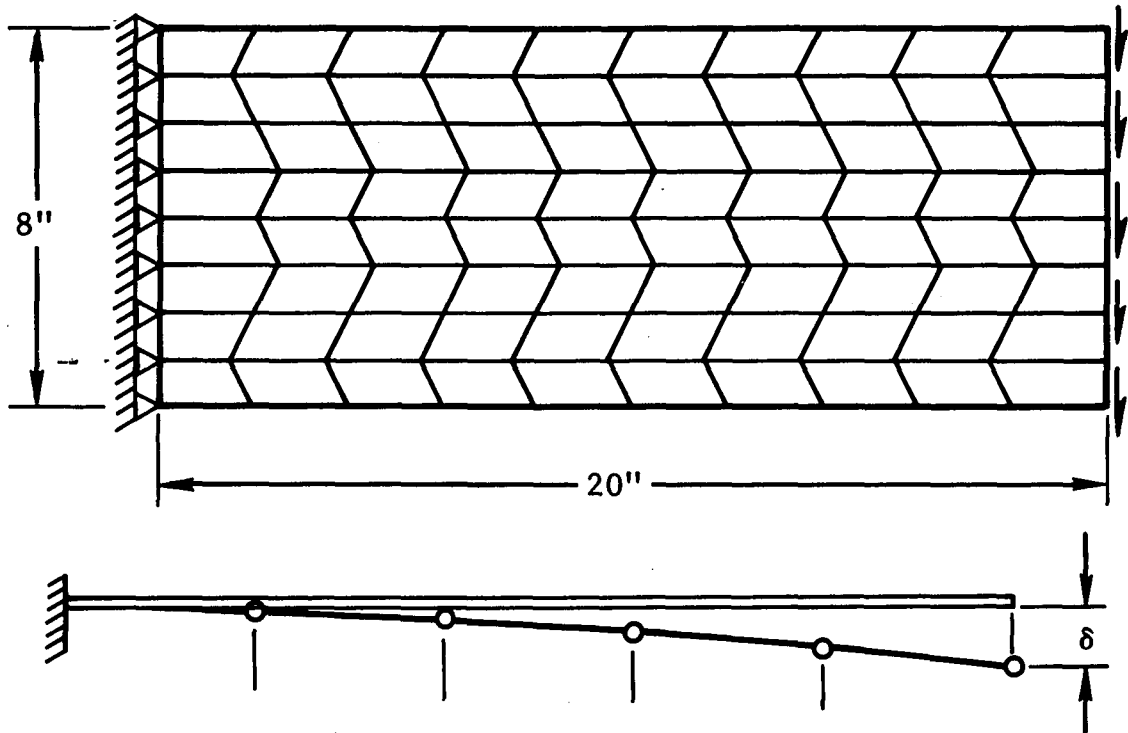
Figure 39 Elastic Cantilever Plate Tip Deflection vs Grid Size

least the existing data seem to indicate that this would be true.

Close examination of the elastic results, plotted in Figure 39, reveals a picture of consistency, convergence, and numerical stability. Interpolation between Figures 38 and 39 supports the above conclusions.

6.3.2 Special Deflection Problem

The results shown in Figure 40 were obtained in a special study problem, which was set up for the purpose of determining whether or not the element number 4 quadrilateral plate would perform satisfactory while described in various nonrectangular shapes. The work in the preceding section showed that element number 4 performed very satisfactorily when it was described in a rectangular shape. This study, although not extensive, indicates that the deflections along the beam are more or less identical for the quadrilateral grid shown in the same figure. The results obtained in this problem were quite reassuring since the major justification for the development of this element was its use in numerous applications that can be simulated only by a quadrilateral grid.



1000 lb. Elastic Deflections , inches

Rectangular Grid	.053	.154	.299	.472	.660
Quadrilateral Grid	.053	.154	.297	.469	.657

500 lb. Nonlinear Deflections , inches

Rectangular Grid	.027	.773	.150	.236	.331
Quadrilateral Grid	.027	.770	.149	.235	.329

1000 lb Nonlinear Deflections , inches

Rectangular Grid	.096	.272	.494	.745	1.011
Quadrilateral Grid	.091	.257	.470	.711	.969

Figure 40 Cantilever Plate Deflections for a Quadrilateral Shaped Grid Compared to the Regular Rectangular Grid.

6.3.3 Plate Stress Analysis

The horizontal normal stress σ_x is shown in Figures 41 through 48. In each figure, the σ_x stress has been plotted at four different cross-sections. The cross-sections investigated are located at 2, 6, 10 and 14 inches from the fixed end. No attempt was made to plot the data from either Models I or II since these models did not present enough data points for a meaningful evaluation.

The shape of the nonlinear curves are very much as might be expected. It is apparent that at the highest stressed cross-section for each of the elements only a small amount of reserve strength remains to prevent a complete collapse. The differences in accuracy noted in the Model III and IV deflection curves also appeared in the Model III and IV stress curves.

An overlay of the stress pictures will show that the results obtained with elements number 2 and 5 are more or less identical and the results obtained in the element 3 and 4 solutions are almost exactly identical. It is reassuring to find that element number 4, which can be used as a quadrilateral plate as well as a rectangular plate, gives such good agreement with the linear stress rectangular element.

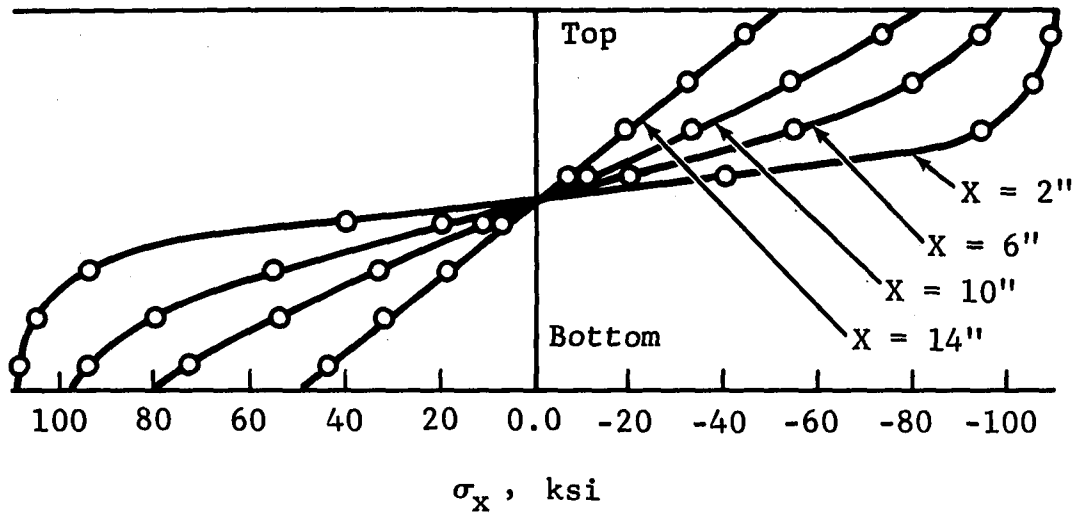


Figure 41 Horizontal Normal Stresses for the Cantilever Plate, Element Number 2, Model IV

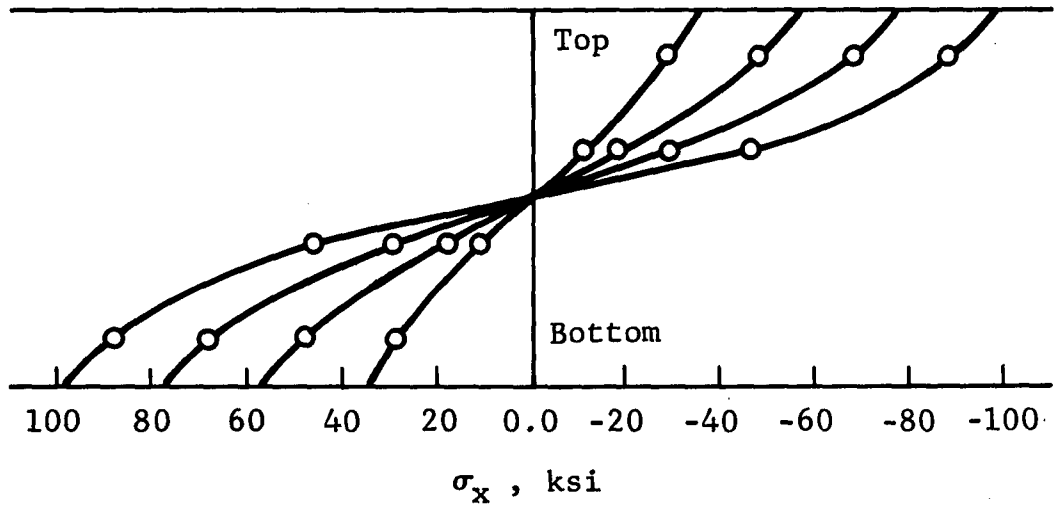


Figure 42 Horizontal Normal Stresses for the Cantilever Plate, Element Number 2, Model III

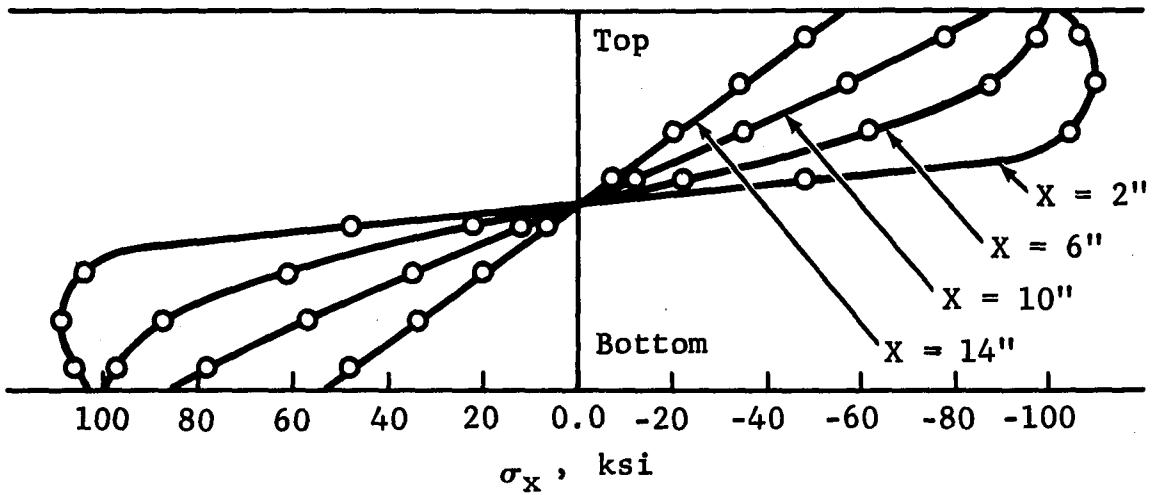


Figure 43 Horizontal Normal Stresses for the Cantilever Plate, Element Number 3, Model IV

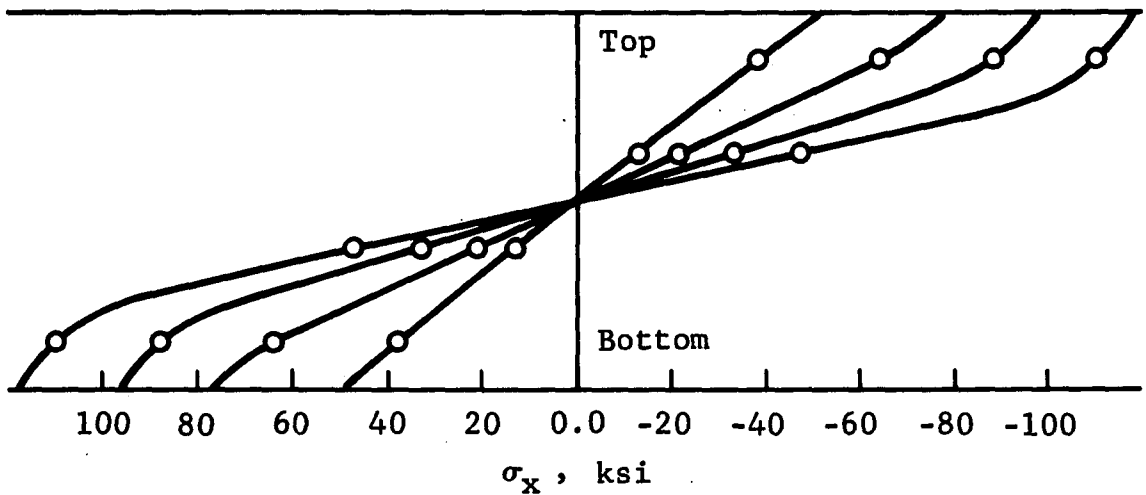


Figure 44 Horizontal Normal Stresses for the Cantilever Plate, Element Number 3, Model III

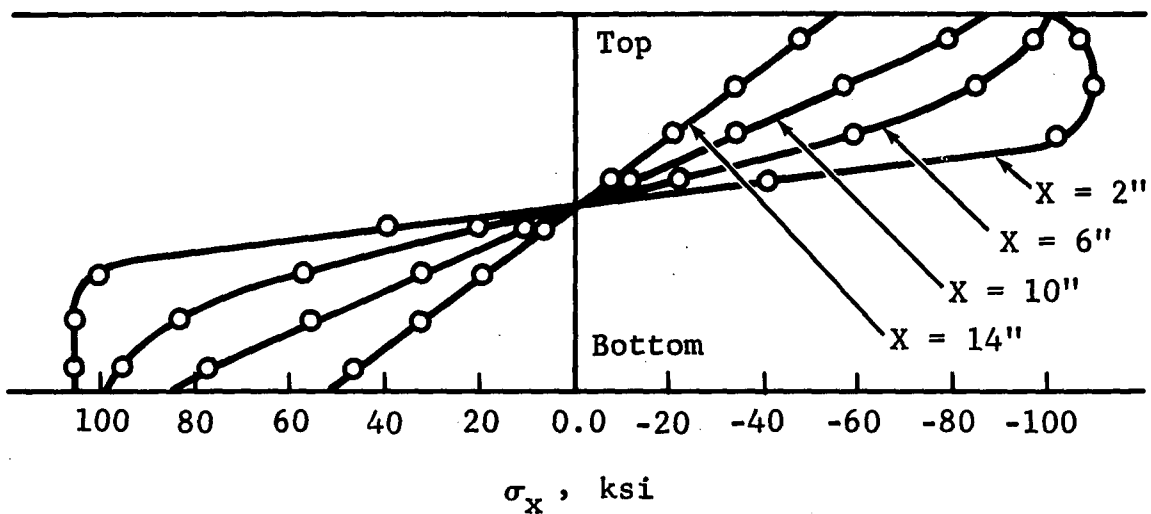


Figure 45 Horizontal Normal Stresses for the Cantilever Plate, Element Number 4, Model IV

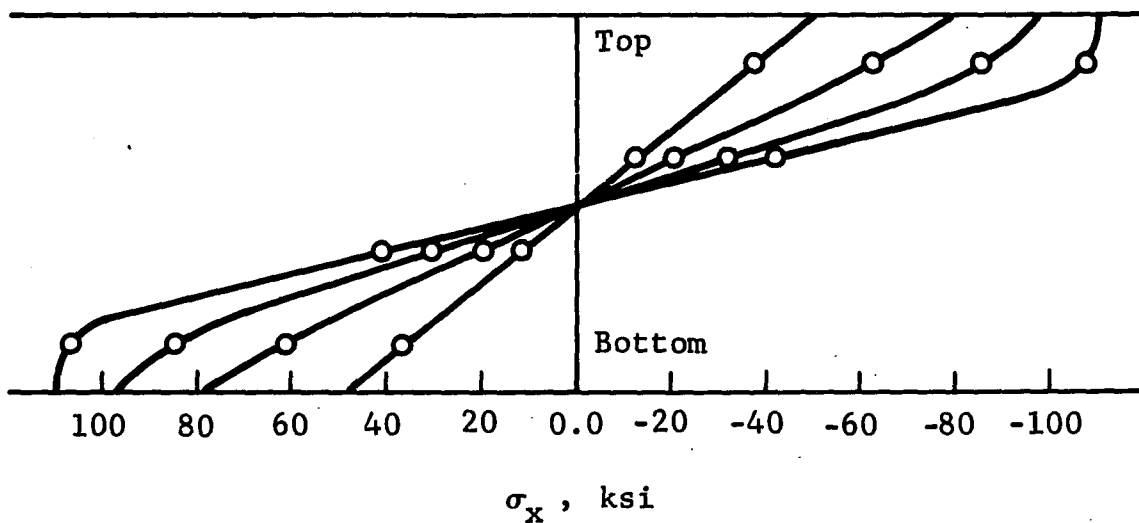


Figure 46 Horizontal Normal Stresses for the Cantilever Plate, Element Number 4, Model III

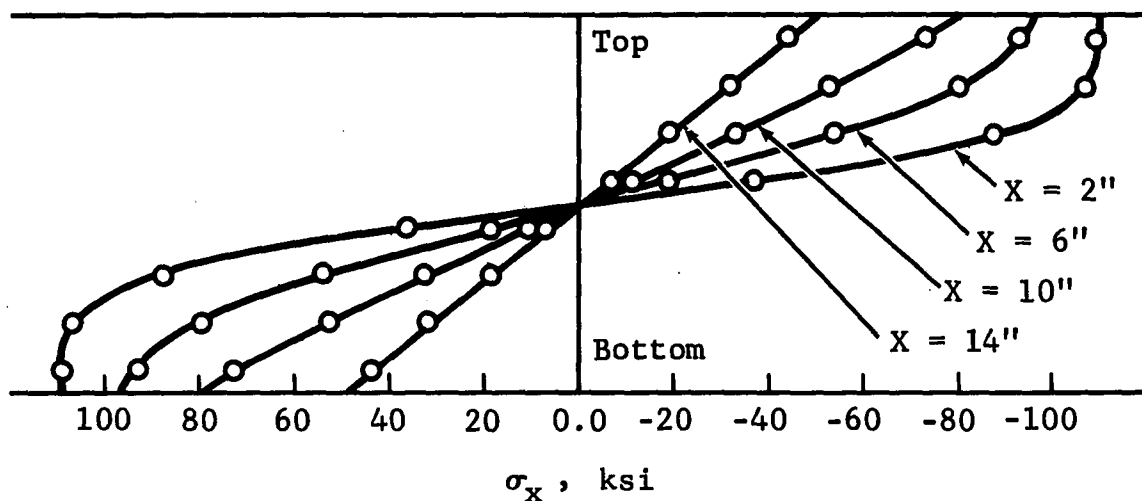


Figure 47 Horizontal Normal Stresses for the Cantilever Plate, Element Number 5, Model IV

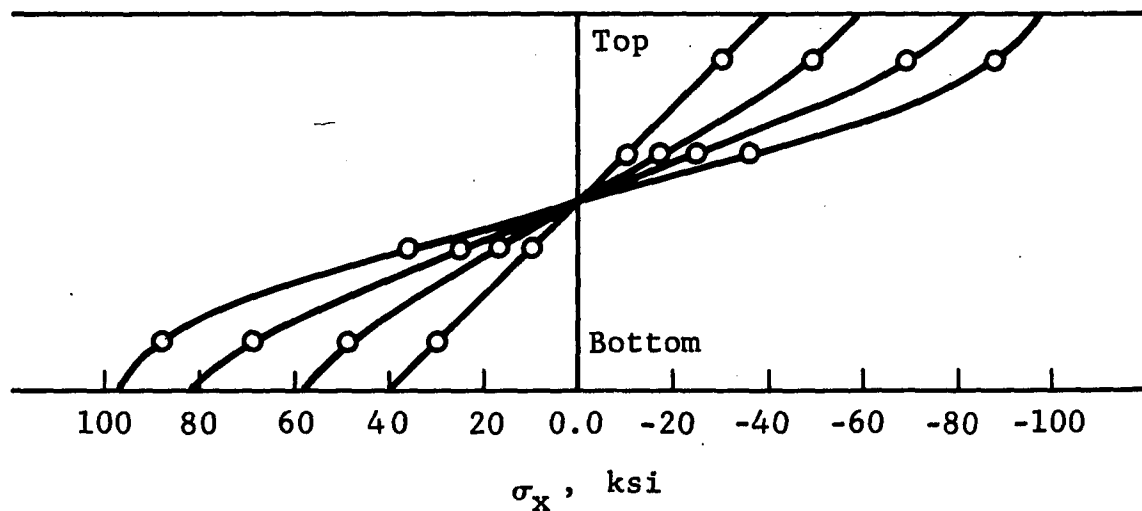


Figure 48 Horizontal Normal Stresses for the Cantilever Plate, Element Number 5, Model III

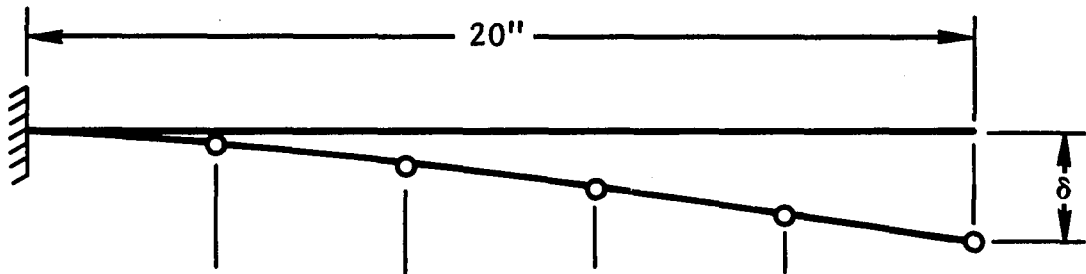
6.4 The Cantilever Beam Analysis

The second class of cantilever problems examined is the beam with a constant area flange equal at the top and bottom. A good example of this problem is the typical wide-flange beam. The particular problem presented here was carefully selected to avoid the plastic hinge formation that appeared in the plate study. Of the several combinations examined it seemed that in general the web would go nonlinear and cause collapse because of the critical biaxial stress just beneath the flange.

Since the beam problem is a rough idealization of an aircraft wing, this study has particular importance. The data presented show that, although slight improvements may be obtained by use of better elements, for this particular flange-web ratio the difference between the solutions is too small to be of much consequence.

6.4.1 Deflection Analysis

The nonlinear cantilever beam deflections for the 4000-pound load are shown plotted along the length of the beam in Figure 49. Since the answers obtained all agree to two significant figures, no effort will be made to select



Model IA

ELEM No. 2	.095	.196	.307	.427	.552
ELEM No. 3	.071	.169	.288	.421	.561
ELEM No. 4	.070	.167	.284	.415	.552
ELEM No. 5	.097	.200	.311	.431	.555

Model IIA

ELEM No. 2	.084	.186	.303	.432	.568
ELEM No. 3	.077	.176	.296	.430	.570
ELEM No. 4	.077	.176	.296	.430	.569
ELEM No. 5	.091	.195	.315	.446	.582

Model IIIA

ELEM No. 2	.087	.192	.313	.446	.584
ELEM No. 3	.079	.179	.300	.434	.573
ELEM No. 4	.079	.178	.300	.433	.571
ELEM No. 5	.088	.193	.315	.448	.587

Model IVA

ELEM No. 2	.081	.184	.306	.442	.583
ELEM No. 3	.080	.182	.304	.440	.580
ELEM No. 4	.080	.181	.302	.437	.577
ELEM No. 5	.083	.185	.307	.442	.583

Figure 49 Nonlinear Beam Deflections for 4000-Lb Load

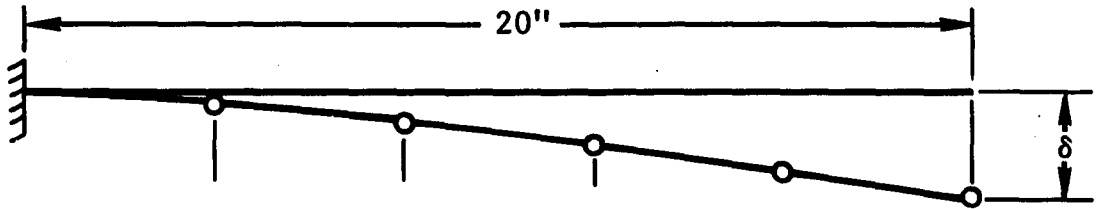
the best element for this problem. The important item to note is that, once a flange has been placed on the web and the web is forced to carry mainly shear, the large differences seen in the element performance for the plates no longer seems to exist.

The values for elastic beam deflections with the 4000-pound load, shown in Figure 50, agree to the same accuracy, as did the nonlinear results; however, in addition they tend to show a definite pattern. If it is assumed that a lower bound solution has been obtained and that in each case where no divergence exists the highest value is the most nearly correct, then element number 3 is the best for each model.

In Figure 51, the nonlinear tip deflections are plotted versus grid size. The average value of all of the elements in the Model IA and IIA results is improved about 4 percent; however, the differences recorded in the Model IIA, IIIA, and IVA results are too slight to be noticeable.

6.4.2 Stress Analysis

The horizontal normal stresses for the cantilever beams are shown in Figures 52 through 55. These figures



Model IA

ELEM No. 2	.067	.154	.258	.372	.491
ELEM No. 3	.069	.165	.282	.413	.550
ELEM No. 4	.068	.163	.278	.406	.541
ELEM No. 5	.065	.152	.255	.369	.488

Model IIA

ELEM No. 2	.070	.163	.276	.400	.532
ELEM No. 3	.072	.167	.284	.415	.553
ELEM No. 4	.072	.167	.284	.414	.552
ELEM No. 5	.070	.162	.274	.398	.530

Model IIIA

ELEM No. 2	.071	.166	.281	.409	.543
ELEM No. 3	.073	.168	.285	.416	.552
ELEM No. 4	.072	.167	.284	.415	.550
ELEM No. 5	.071	.166	.280	.408	.542

Model IVA

ELEM No. 2	.072	.168	.286	.417	.554
ELEM No. 3	.073	.169	.287	.420	.557
ELEM No. 4	.072	.169	.286	.418	.555
ELEM No. 5	.072	.169	.286	.417	.554

Figure 50 Elastic Beam Deflections for 4000-Lb Load

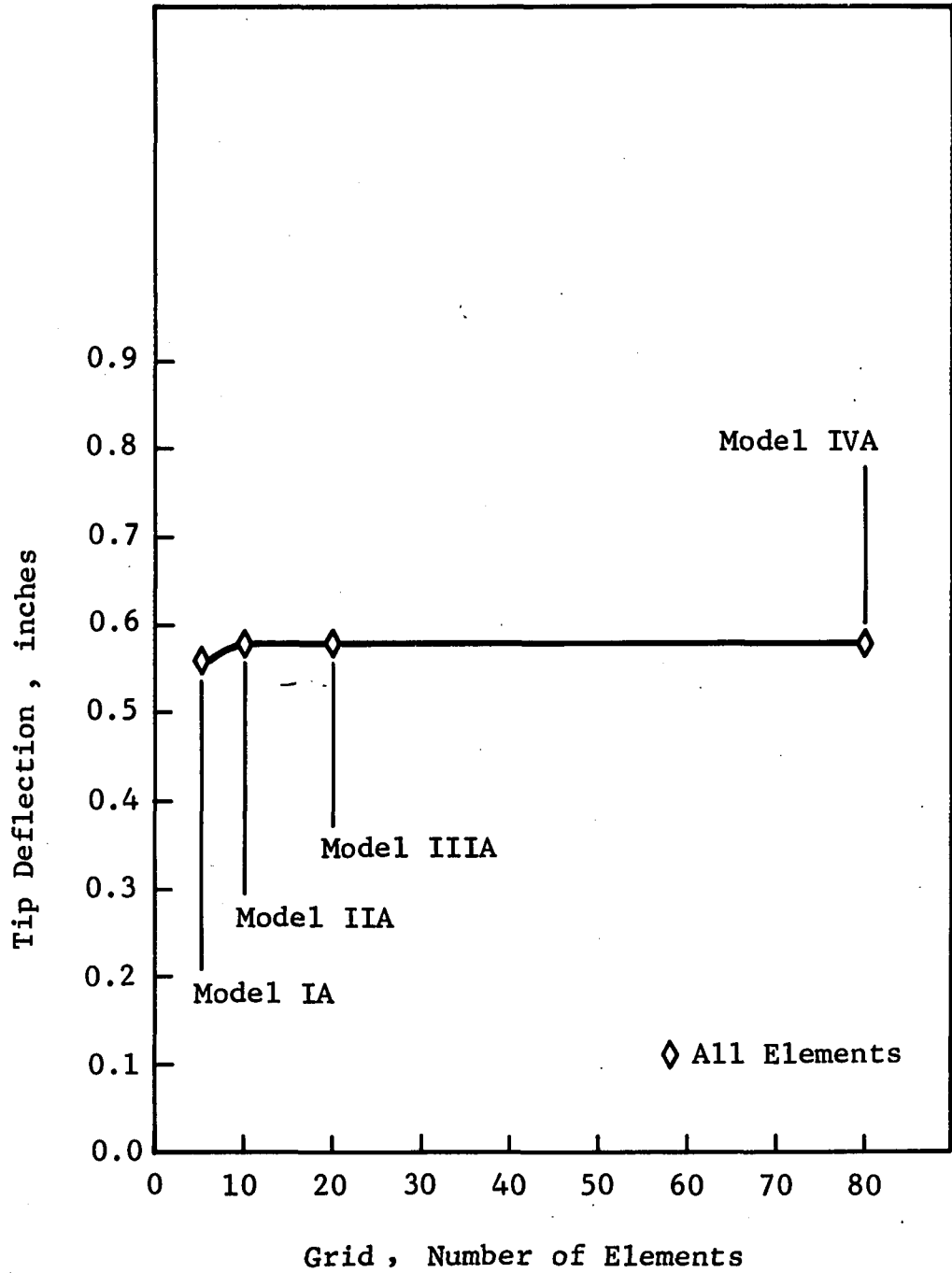


Figure 51 Nonlinear Tip Deflection for the Cantilever Beam vs Grid Size

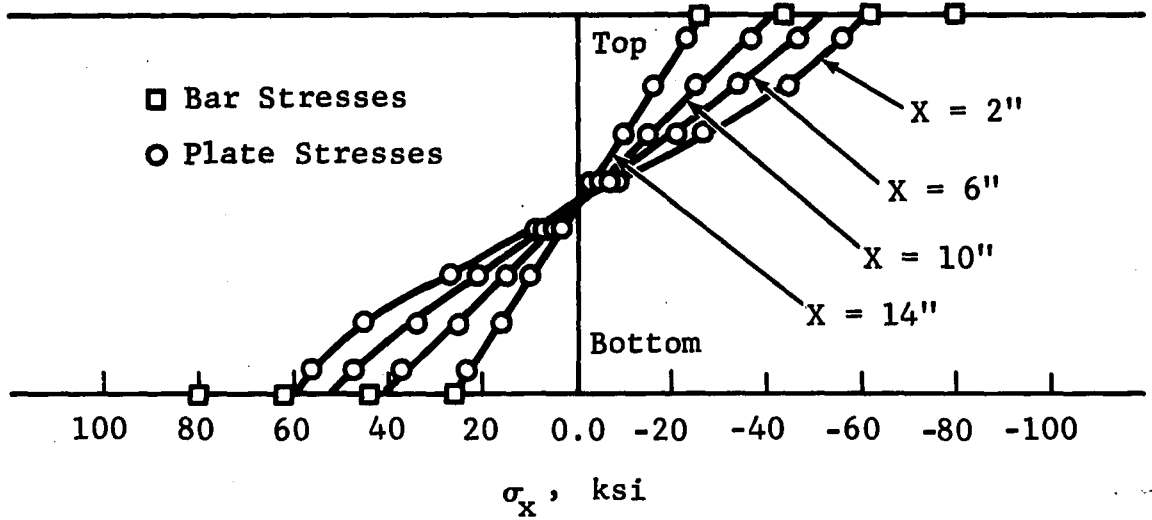


Figure 52 Horizontal Normal Stresses for the Cantilever Beam, Element Number 2, Model IVA

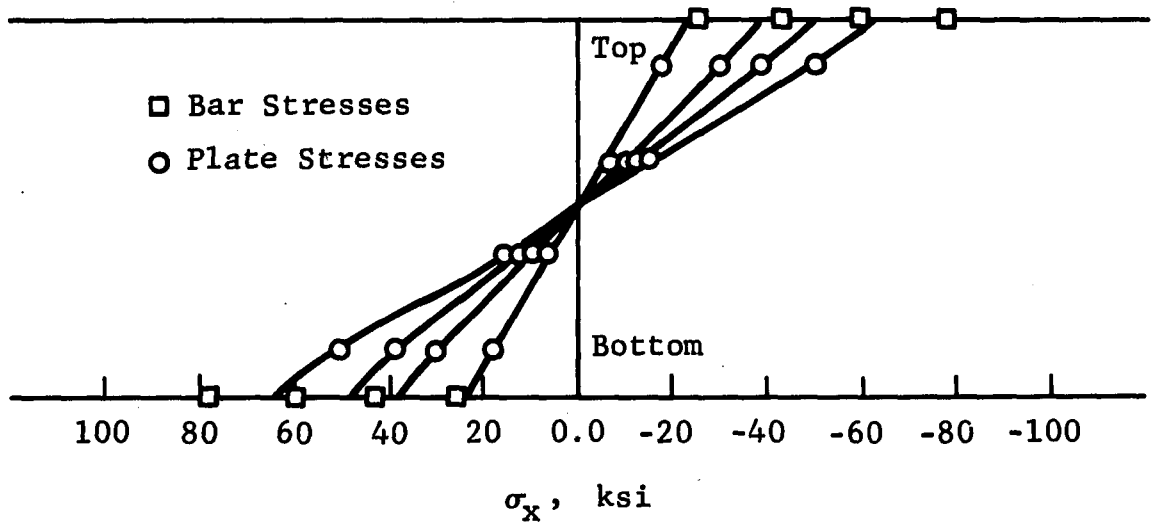


Figure 53 Horizontal Normal Stresses for the Cantilever Beam, Element Number 2, Model IIIA

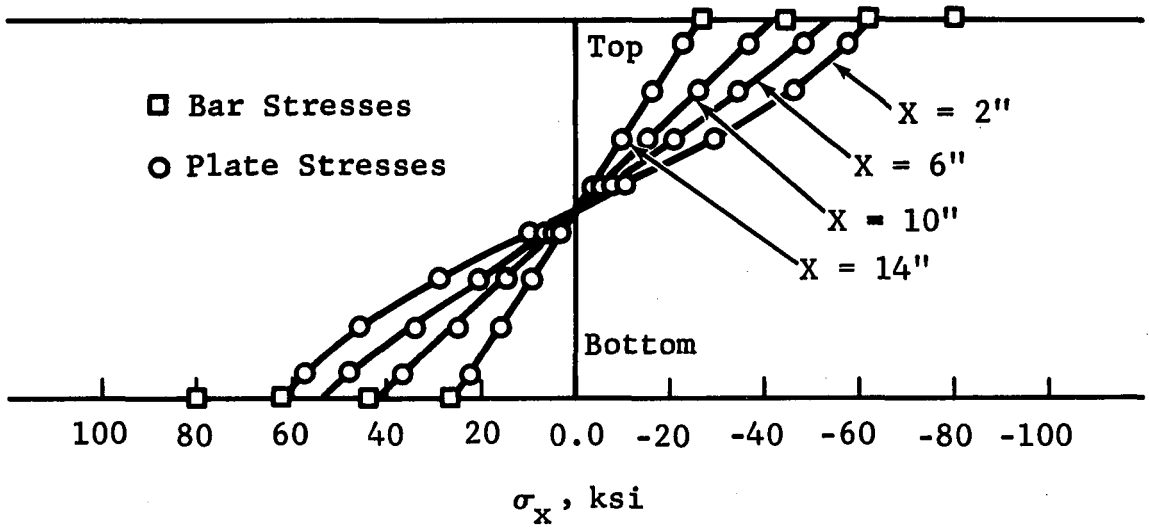


Figure 54 Horizontal Normal Stresses for the Cantilever Beam, Element Number 3, Model IVA

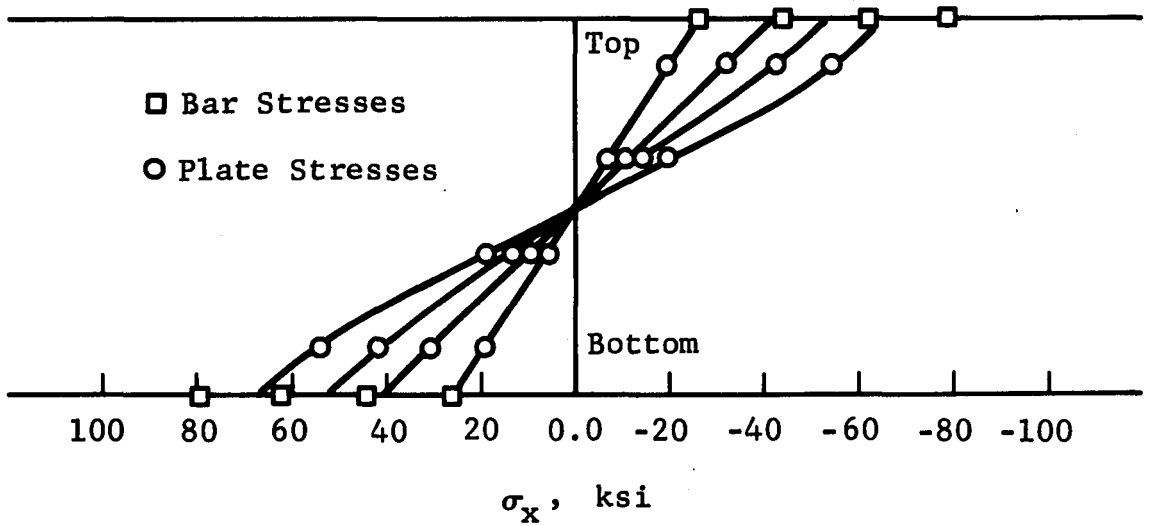


Figure 55 Horizontal Normal Stresses for the Cantilever Beam, Element Number 3, Model IIIA

show the Model IIIA and IVA results plotted at four different cross-sections on each beam for elements number 2 and 3.

In order to point out the discontinuity between the horizontal normal stress in the flange and that just beneath the flange in the web, different symbols are used to indicate bar and plate stresses. Looking at Figures 54 and 55, one can see that the discontinuity all but disappears at $X = 14$ inches, whereas at $X = 2$ inches the discontinuity is as much as 20,000 psi. To understand this difference, one must remember that the initiation of plastic action is caused by the von Mises stress rather than the horizontal normal stress. Since the shear stress in a wide flange beam approaches zero in the flange while it has a high value just beneath the flange, the effects of this stress will cause most of the plastic action to occur at the point just beneath the flange, rather than on the extreme fibers as is often assumed. For the ratio of flange area-to-web thickness and bending moment-to-vertical shear occurring in this particular problem, the beam becomes almost completely plastic in the extreme fiber of the web, while the flange is stressed to only 80 percent of its capability. Thus we can

see the true stress distribution in a wide flange beam cross-section as it undergoes plastic straining action.

In each case, whether the stresses are low or high, the elements seem to give approximately the same degree of accuracy. Of particular interest is the fact that without exception the stresses from elements number 2 and 5 were identical and the stresses from elements 3 and 4 were identical. The stress plots for element number 2 are the results of the triangular stresses in each rectangle being averaged. An attempt was made originally to use the data points from the triangles without averaging them; however, no apparent correlation could be made of the results when this practice was followed. This particular characteristic of triangular elements is not only true for the constant stress triangles used in this analysis but also for triangles of a higher order, which the author has used in other analyses.

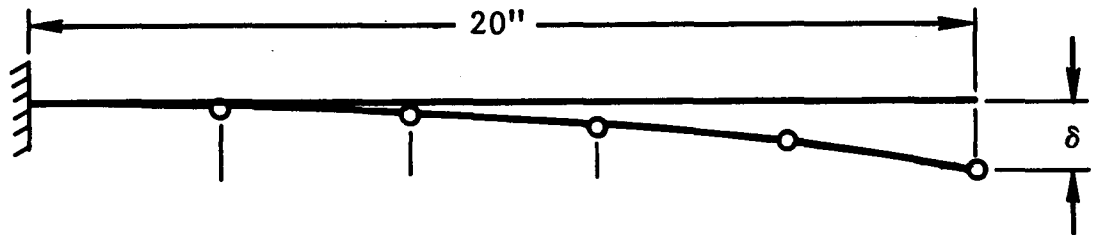
6.5 The Tapered Cantilever Beam Analysis

The tapered beam depicted in Figure 22 is 20 inches long and tapers from 8 inches in height at the fixed end to 6 inches at the free end. The assumed stress-strain diagram is shown in Figure 23. The problem was solved for a 4000-pound load which was applied parabolically at the right edge

while all coordinates at each of the nodes along the left edge remained fixed. Elements number 2, 4, and 5 were each used to simulate the web material while the flanges were simulated by element number 1 bars. The tapered beam simulations are shown by Models IB, IIB, IIIB, and IVB.

The nonlinear vertical deflections are shown in Figure 56 for the 4000-pound load plotted at five stations along the length. Except for the added taper, these problems are identical to those for the nontapered beam; however, the results are somewhat different from those presented for the nontapered beam, where the deflections were almost identical for Models IIA, IIIA, and IVA. The data presented in Figure 56 indicate that more layers of elements are necessary for the analysis of tapered beams.

The elastic tapered beam deflections, shown in Figure 57, tend to be more regular than the nonlinear deflections, with the order of elements identical to the order noted for the plate and straight beam problem. Elements number 2 and 5 results are more or less identical while element number 4 results seem to be slightly better.



Model IB

ELEM No. 2	.065	.156	.271	.410	.613
ELEM No. 4	.059	.150	.270	.418	.636
ELEM No. 5	.064	.155	.270	.408	.614

Model IIB

ELEM No. 2	.063	.155	.275	.422	.636
ELEM No. 4	.062	.153	.276	.425	.646
ELEM No. 5	.066	.160	.281	.428	.644

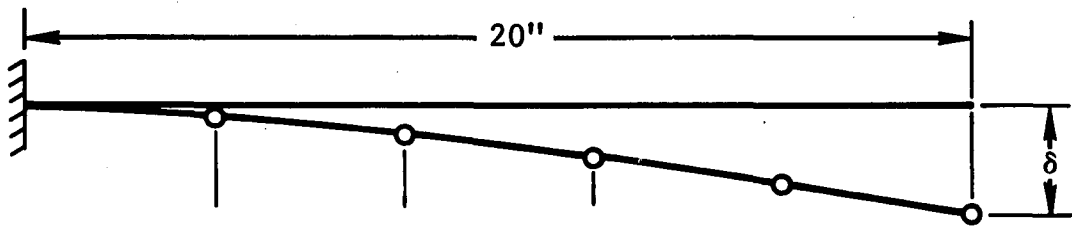
Model IIIB

ELEM No. 2	.064	.159	.282	.432	.658
ELEM No. 4	.063	.154	.277	.428	.659
ELEM No. 5	.065	.160	.284	.434	.662

Model IVB

ELEM No. 2	.063	.157	.281	.435	.741
ELEM No. 4	.063	.156	.279	.432	.724
ELEM No. 5	.064	.158	.282	.436	.739

Figure 56 Nonlinear Tapered Beam Tip Deflections for 4000-Lb Load



Model IB

ELEM No. 2	.059	.144	.251	.377	.514
ELEM No. 4	.059	.149	.267	.407	.562
ELEM No. 5	.058	.142	.249	.374	.512

Model IIB

ELEM No. 2	.060	.149	.264	.400	.549
ELEM No. 4	.061	.151	.271	.412	.569
ELEM No. 5	.060	.148	.263	.399	.549

Model IIIB

ELEM No. 2	.061	.151	.268	.407	.560
ELEM No. 4	.061	.152	.271	.413	.568
ELEM No. 5	.061	.150	.267	.407	.560

Model IVB

ELEM No. 2	.061	.152	.273	.416	.573
ELEM No. 4	.061	.153	.273	.416	.577
ELEM No. 5	.061	.153	.273	.416	.575

Figure 57 Elastic Tapered Beam Tip Deflections for 4000-Lb Load

In Figure 58 the tip deflection for elements number 2 and 4 have been plotted versus grid size for both the linear and nonlinear results.

The shear stress data for the tapered beams reflected essentially the same results as those obtained for the straight beam problem. These data are not included in this paper.

The flange stress data for the Model IB, Model IIB, and Model IVB tapered beams are plotted in Figures 59 and 60. The data presented in Figure 59 are for beams with element number 4 shear webs; these data show that for this tapered beam problem the percent error between the 5-division grid and the 80-division grid is less than 5 percent. The data in Figure 60 are for beams with element number 2 shear webs; these data show that for this tapered beam the percent error in the flange stress between the 5-division grid and the 80-division grid is approaching 20 percent. Again we see that element number 4 is much more accurate than element number 2.

6.6 Final Remarks on the Cantilever Problem

The particular stress field of the beam problem i.e., flexural normal stresses and shear stresses, can be

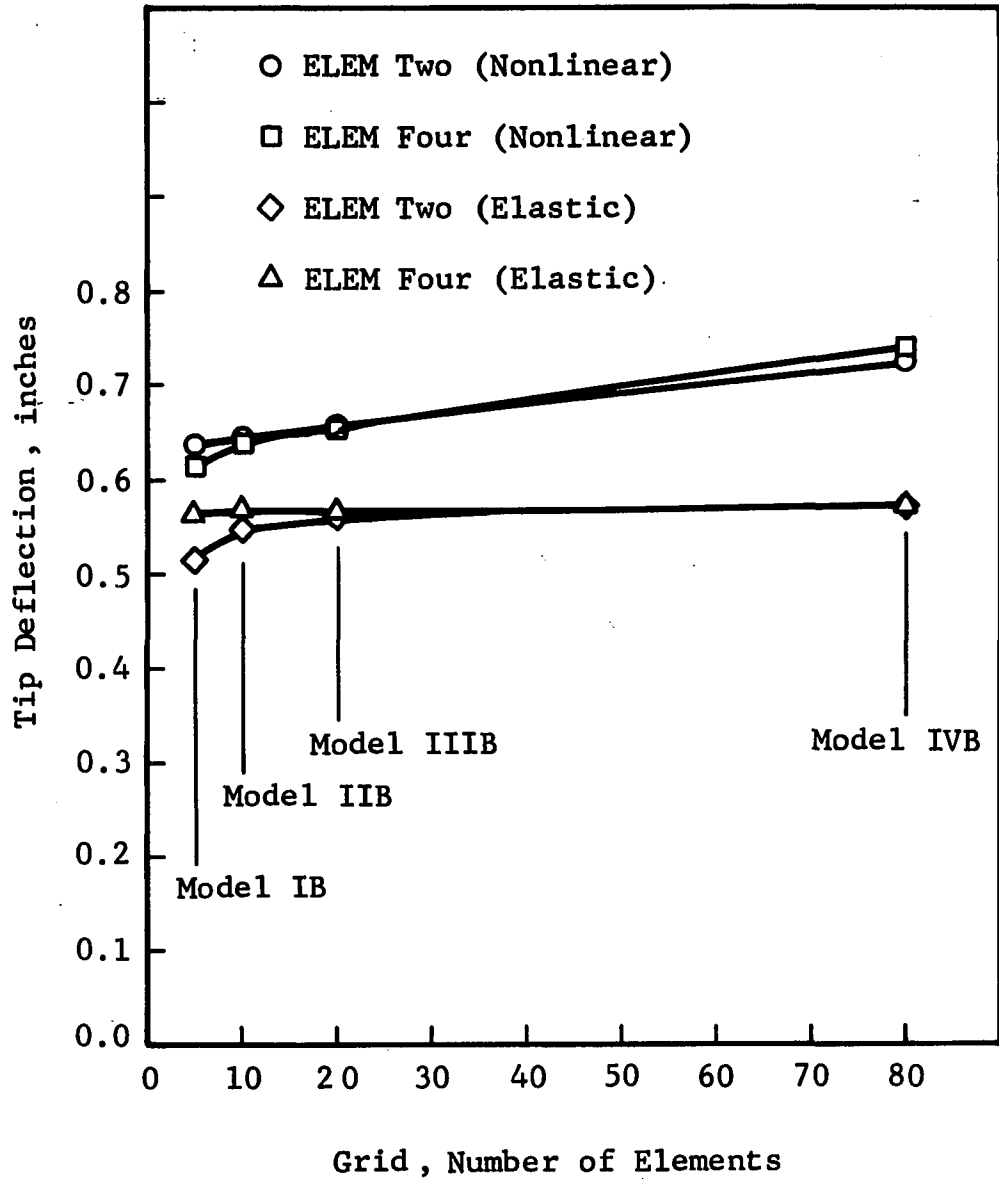


Figure 58 Tip Deflection for the Tapered Cantilever Beam Plotted vs Grid Size

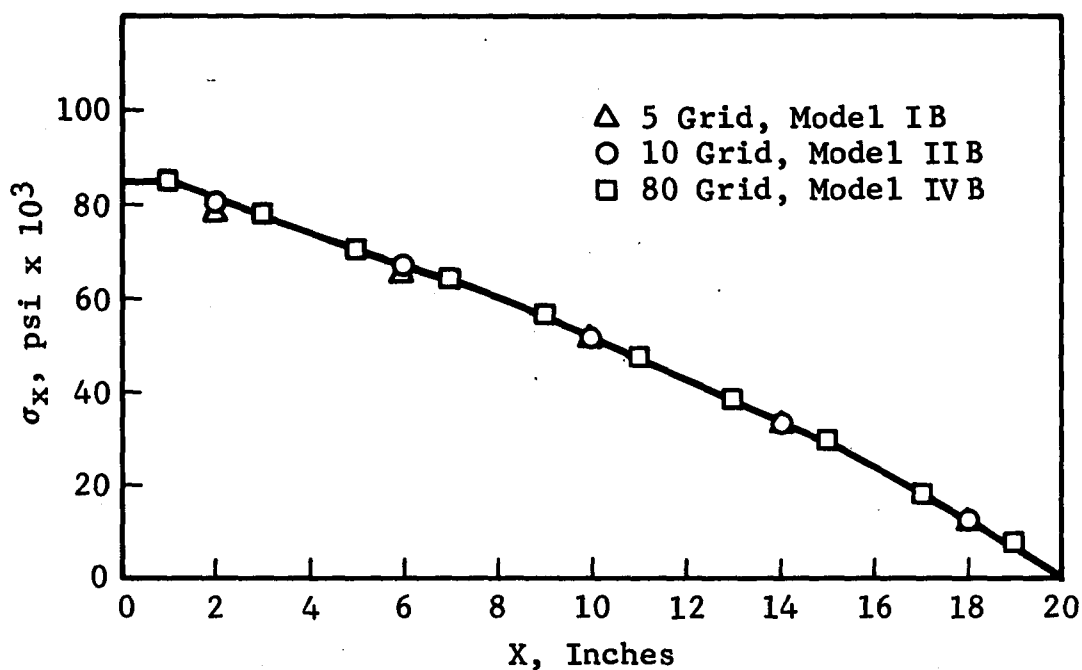


Figure 59 Nonlinear Flange Stresses, Element Number 4 Shear Webs

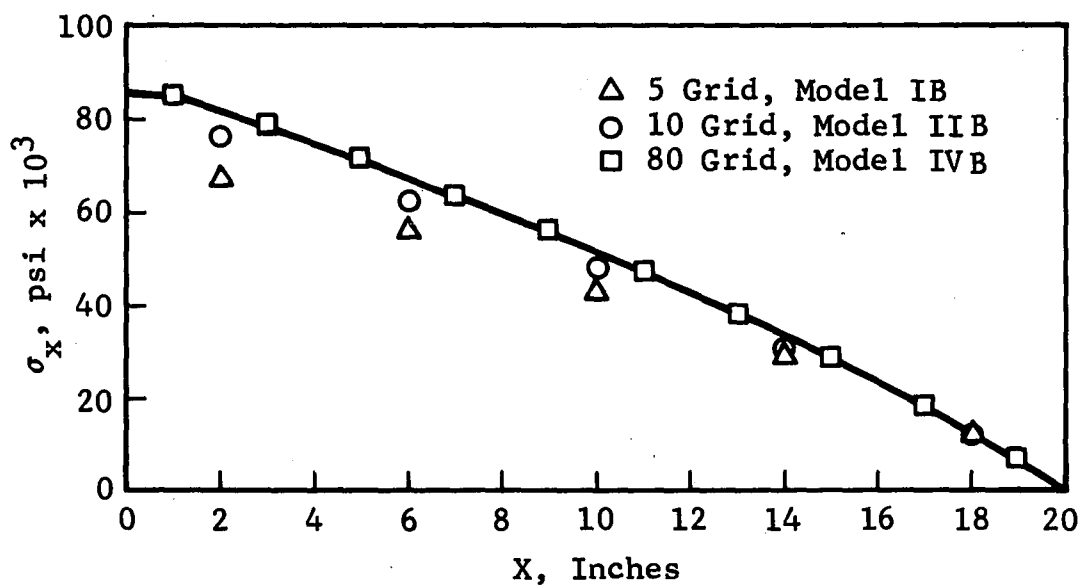


Figure 60 Nonlinear Flange Stresses, Element Number 2 Shear Webs

well represented by any of the four plate element types investigated when the geometric and material parameters are identical to those used in this study and the grid is adequate. For a more complex stress field, the elements may or may not give satisfactory answers; however, there is no question but that the more complex the state of stress, the finer the grid must be. In addition, more caution must be exercised in evaluating the results.

CHAPTER 7

DISCUSSION

The problems solved in this dissertation have been presented to demonstrate the accuracy and applicability of the nonlinear finite element method of structural analysis. The average stress value general quadrilateral plate element developed during the study has been shown to be a valuable tool for the solution of nonlinear problems.

Two types of quadrilateral plates were investigated. One, element number 4, makes use of an averaging technique while the other, element number 5, uses overlapping constant stress triangles with no averaging technique. In all applications conducted during this study, the element number 4 quadrilateral finite plate element was superior to the element with the overlapping triangles. Thus, element number 4 may be used with confidence in nonlinear finite element computer programs. Further work with element number 5 has been discontinued.

Of particular interest in the study is the work described in Chapter 6, where the results of 48 cantilever beam

problems are presented. The interplay of stress gradients, grid fineness, and element types for each of the three cantilever beams investigated leads to the conclusion that some nonlinear solutions require a bit more engineering judgment than identical elastic problems. However, since the nonlinear solution method described herein encompasses several important engineering structures, its importance warrants the additional effort required for its use. Very simple problems, such as those presented by the straight wide flange beam, can be processed by the uninitiated; however, prior experience with the procedure is essential for the nonlinear analysis of complex shapes and fittings. By examining the problems presented in this text, the structures analyst should be able to avoid some of the early pitfalls in nonlinear finite element analysis and proceed to the solution of meaningful problems at a more rapid pace.

7.1 Significance of the Method

The nonlinear finite element method of analysis is relative simple in its application mechanics. The structural systems to be analyzed are represented by finite element models composed of bars and plates just as in the elastic

finite element method. Additional nonlinear parameter input data are required, of course; however, the procedure used to establish nodal geometry, material size, and elastic constants is much the same as that learned for elastic solutions. The accuracy demonstrated with the solution of the shear-lag structure (Chapter 5) gives additional confidence in the accuracy of the method for predicting stresses, strains, and internal load distribution of complex structural systems subjected to static loadings into the nonlinear material range.

7.2 Implication for Solution of Other Problems

Although all of the problems presented are relatively simple and only partially typical of real design problems, the program is not limited to the solution of this class of problems. In related experience in the aircraft industry the author has used the method for the analysis of large complex structures constructed of plastic and metallic materials. Of particular interest has been the solution of nonlinear stress concentrations around bolt holes.

Using a technique of stepped down grid fineness, a coarse grid is first used for the total structure to obtain the internal displacement distribution. The local regions

are then resimulated with a much finer grid while using the internal nodal displacements as boundary values. Then an area inside of this local region can be resimulated and the same procedure with the deflections applied once again until the right fineness of grid is reached. This technique extends the method to a new class of problems and greatly enhances its value as an analytical tool.

7.3 Recommendations

As with most research undertakings, the knowledge gained in this study has indicated several areas in which further work is desirable. Some of these areas, enumerated and discussed below, are simply extensions of the present studies while others are the extensions of the method to other classes of problems.

1. A study of the effects of length, web-flange ratio, taper rate, Richard parameter, and shear-moment ratios would probably be beneficial. These additional problems should add validity to the results of this study.
2. A search should be made for additional nonlinear structural test data. There is definitely a shortage of available nonlinear test data for analytical

problem correlation. The shear-lag problem has probably been overworked; thus, the challenge is to obtain data from a nonlinear structural test of other representative real structural problems.

3. New finite elements for nonlinear stress analysis of fastener systems--which may account for bolt slip, prestress, and bearing failure--should be the subject of future research. The method presented in this dissertation can be relied upon to give good results only in regions away from such areas.
4. Finally, the value of the method would be greatly enhanced by the documentation of procedures for automatic input generation and meaningful visual presentation of the input and output data. One goal of such a study would be to develop an automatic plotting routine for stress contours, deflection contours, and deflected shapes. Such a routine would allow the computers to do one of the time-consuming tasks that now consumes valuable engineering manpower.

APPENDIX I.

RQ1 FORTRAN LISTING

```

C      NONLINEAR FINITE ELEMENT ANALYSIS BY R.M.RICHARD AND J.R.BLACKLOCKRQ1$001
C      MODE=0 FOR FOURTH ORDER RUNGE KUTTA INTEGRATION RQ1$002
C      MODE=1 FOR FIRST ORDER EULER INTEGRATION RQ1$003
C RQ1$004
C RQ1$005
C LMODE=1 SPECIFIC LOAD COEFFICIENTS MUST BE SUPPLIED IN PMODE RQ1$006
C LMODE=2 FOR 1/2,1/4,1/8,ETC INCREMENTS OF LOAD RQ1$007
C LMODE=3 FOR EQUAL INCREMENTS OF LOAD RQ1$008
C RQ1$009
      DIMENSION ALAM(15,15),ALAMT(15,15),R(12),U(12),UU(10),AL(3), RQ1$010
      1SIGMA(3),LP(333),NS(666),AL2(3),DSK(8,8),PMODE(10),QXY(333), RQ1$011
      2PXY(750),P(750),P1(750),PE(750),IX(750),JL(750),JR(750), RQ1$012
      3NSP(750),SS(87,750),NPT(250),X(250),Y(250),Z(250),IS(1000), RQ1$013
      4SE(1000),S1(1000,3),S2(1000,3),S3(1000,3),IE(1000),IP(1000), RQ1$014
      5IQ(1000),IR(1000),NTYPE(1000),EM(20),PR(20),SY(20),PNL(20), RQ1$015
      6MATYPE(1000),A(1000),SAFTY(1000),VE(1000),S4(1000,3),S7(1000,3), RQ1$016
      7EMM(20),G(20),THETA(20),ZZ(15,15), RQ1$017
      8TT(15,15),T11(8,8),T22(2,2),T12(8,2),T21(2,8),T22INV(2,2) RQ1$018
      9,SIG(3),ZIGMA(3),TMA TR X(3,3),DENSE(20) RQ1$019
      COMMON SS,IX,JL,JR,AE1,NBAND,ALAM,ALAMT,R,RR,D1,AL,X21,X31,X32,Y21 RQ1$020
      1,Y31,Y32,A123,U,UU,SIGMA,SYE,PN,EME,A,NLP,BM,SE,S1,S2,S3,P1, RQ1$021
      2NTYPE,N,IM,NPASS,NN,NPT,X,Y,Z,IE,IP,IQ,IR,AE,NODES,II,JJ,AL2,DSK, RQ1$022
      3P,SAFTY,VE,S4,S7,PE,MID,NSP,IS,D2, RQ1$023
      4EMM,G,THETA,BETA,S,C,SB,CH,GT,PR1,PR2,E1,E2 RQ1$024
      5,LP,PR,NS,SY,PMODE,PNL,PXY,EM,MATYPE, RQ1$025
      6TT,T11,T22,T12,T21,T22INV,ZZ,NPASS1,NTRI,XIT,YIT,ZIT,ILAM,JLAM RQ1$026
      7,DIR1,DIR2,DIR3,THETA1,QXY RQ1$027
      CALL GSTART(3HRQ1,MID) RQ1$028
800 CALL PROB RQ1$029
600 FORMAT(8I7) RQ1$030
601 FORMAT(8F7.0) RQ1$031
602 FORMAT (1H1,10X,46H RUNGE-KUTTA ELEMENT STRESSES AND STRAINS ) RQ1$032
603 FORMAT(1P3E20.6) RQ1$033
604 FORMAT(15) RQ1$034
605 FORMAT (1H1,5X,16H***** DATA *****) RQ1$035
606 FORMAT(1P8E15.5) RQ1$036
607 FORMAT(9I7,I2) RQ1$037
608 FORMAT(7I10) RQ1$038
609 FORMAT(5I4,4F10.0,F5.0) RQ1$039
610 FORMAT(1I10,5X,3F10.5) RQ1$040
611 FORMAT(3F10.0,F5.0,2F10.0,2F5.0) RQ1$041
612 FORMAT (1H1,10X,46H EULER ELEMENT STRESSES AND STRAINS ) RQ1$042
613 FORMAT(1H1,10X,38HFIRST INTERVAL LINEAR ELEMENT STRESSES/ ) RQ1$043
614 FORMAT(1X,1I3,4I4,1P8E14.5) RQ1$044
615 FORMAT(1H0,56HELEMENT NO. SIGMA XX SIGMA YY SIGMRQ1$045
      1A XY/ ) RQ1$046
616 FORMAT(1H1,10X,44HFIRST INTERVAL LINEAR ELEMENT DISPLACEMENTS / ) RQ1$047
617 FORMAT(1H0,65HCOORD DEFLECTION COORD DEFLECTION COORRQ1$048
      10 DEFLECTION/ ) RQ1$049
618 FORMAT(1H ,15,2X,E13.6,I8,2X,E13.6,I8,2X,E13.6) RQ1$050
619 FORMAT(1H0,104HELEMENT NO. SIGMA XX SIGMA YY SIGMRQ1$051
      1A XY STRAIN XX STRAIN YY STRAIN XY/ ) RQ1$052
620 FORMAT(1H0,74H NUMEL NODES NLOAD NSUPS NRKI NODSEP MODE RQ1$053
      1NOMAT LMODE ITERAT /) RQ1$054
621 FORMAT(1H0,10X,5HLOADS/ ) RQ1$055
622 FORMAT(1H0,10X,11HLOAD POINTS/ ) RQ1$056

```

```

623 FORMAT(1H0,10X,14HSUPPORT POINTS/ )
624 FORMAT(1H1,63H NO. P Q R S NTYPE MATYPE AREARQ1$058
1-THICKNESS /)
625 FORMAT(1H1,44H NUDE POINT X COORD Y COORD Z COORD /)
626 FORMAT(10I7)
630 FORMAT(1H ,15,8X,6E16.7)
632 FORMAT(1H1,16H PNODE ELEMENTS /)
633 FORMAT(1H ,15,8X,3E16.7)
634 FORMAT(1H0,64HCOORD LOAD COORD LOAD COORRQ1$065
1D LOAD /)
635 FORMAT(1H1,17HEQUILIBRIUM CHECK)
636 FORMAT(1H0,44H SUM FORCES-X SUM FORCES-Y SUM FORCES-Z/)
637 FORMAT(1P3E15.5)
638 FORMAT(1H1,10X,46H RESIDUAL STRESSES AND STRAINS )
639 FORMAT(1H1,10X,43HPRINCIPAL STRESSES AND MARGIN OF SAFETY )
640 FORMAT(1H0,115HELEMENT NO. SIGMA ONE SIGMA TWO TAU
1 MAX EFFECTIVE STRES PLASTIC STRESS MARGIN OF SAFETY )
641 FORMAT(1I10,3F10.0)
650 FORMAT(6I5,1I10,F10.5)
651 FORMAT(1I5,5X,3E13.6,5X,1E13.6,3X,2E13.6,3X,1E13.6,1E13.6)
652 FORMAT(1H1,116HMATERIAL NO/ELASTIC MOD/POISSONS RATIO/PLASTIC STRE
1SS/NONLINEAR PARAM/ELASTIC MOD-2/SHEAR MODULUS DENSITY THETA )
653 FORMAT(1H1,10X,46H EULER COORDINATE DISPLACEMENTS )
654 FORMAT(1H1,10X,46H RUNGE-KUTTA COORDINATE DISPLACEMENTS )
655 FORMAT(1H1,10X,46H RESIDUAL COORDINATE DISPLACEMENTS )
656 FORMAT(6I5,1I10,5X,F10.5)
657 FORMAT(1H1)
659 FORMAT(37H * * * NODSEP IS OUT OF BOUNDS * * * )
660 FORMAT(43H * * * NBAND IS GREATER THAN 3*NODES * * * )
661 FORMAT(1H1,10X,46H THE STRUCTURE WEIGHT CALCULATED IN POUNDS )
662 FORMAT(1H0,43H SUM MOMENTS-X SUM MOMENTS-Y SUM MOMENTS-Z /)
C*****READ AND WRITE DATA *****
READ(5,607) NUMEL,NODES,NLOAD,NSUPS,NRKI,NODSEP,MODE,NOMAT,LMODE
1,ITERAT
READ(5,601) (QXY(II),II=1,NLOAD)
READ(5,600) (LP(II),II=1,NLOAD)
READ(5,600) (NS(II),II=1,NSUPS)
READ(5,611)(FM(II),PR(II),SY(II),PNL(II),EMM(II),G(II),DENSE(II),
1 THETA(II),I=1,NOMAT)
DO 97 I=1,NOMAT
97 THETA(I) = 0.0174533*THETA(I)
DO 99 II=1,NODES
READ(5,641) NPT(II),X(NPT(II)),Y(NPT(II)),Z(NPT(II))
99 CONTINUE
DO 102 I=1,NUMEL
READ(5,650) IE(I),IP(IE(I)),IQ(IE(I)),IR(IE(I)),IS(IE(I)),
1 NTYPE(IE(I)),MATYPE(IE(I)),A(IE(I))
C * * * TEST NODSEP FOR PROPER SIZE
IF(NODSEP.LT.0.OR.NODSEP.GT.28) GO TO 1800
GO TO 1810
1800 WRITE(6,659)
CALL SKIPPR
GO TO 800
1810 CONTINUE
NBAND = (6*NODSEP)+5
IF(NBAND.LE.(3 *NODES)) GO TO 1820

```

```

WRITE(6,660)
CALL SKIPPR
GO TO 800
1820 CONTINUE
IBAND = NODSEP
II = IE(1)
JBAND = IABS(IP(II)-IQ(II))
IF(JBAND.GT.IBAND) GO TO 40
IF(NTYPE(II).EQ.1.0) GO TO 102
JBAND = IABS(IP(II)-IR(II))
IF(JBAND.GT.IBAND) GO TO 40
JBAND = IABS(IQ(II)-IR(II))
IF(JBAND.GT.IBAND) GO TO 40
IF(NTYPE(II).EQ.2)GO TO 102
IF(NTYPE(II).EQ.3)GO TO 102
JBAND = IABS(IP(II)-IS(II))
IF(JBAND.GT.IBAND)GO TO 40
JBAND = IABS(IQ(II)-IS(II))
IF(JBAND.GT.IBAND)GO TO 40
JBAND = IABS(IR(II)-IS(II))
IF(JBAND.GT.IBAND)GU TO 40
GO TO 102
40 WRITE(6,50)
50 FORMAT (36H * * * NBAND IS OUT OF ROUNDS * * * )
WRITE(6,600) II
CALL SKIPPR
GO TO 800
102 CONTINUE
1830 CONTINUE
WRITE(6,605)
WRITE(6,620)
WRITE(6,626) NUMEL,NODES,NLOAD,NSUPS,NRKI,NODSEP,MODE,NOMAT,LMODE
1,ITERAT
WRITE(6,621)
WRITE(6,606) (QXY(II),II=1,NLOAD)
WRITE(6,622)
WRITE(6,600) (LP(II),II=1,NLOAD)
WRITE(6,623)
WRITE(6,600) (NS(II),II=1,NSUPS)
WRITE(6,652)
WRITE(6,651) (I,EM(I),PR(I),SY(I),PNL(II),EMM(I),G(I),DENSE(I),
1 THETA(II),I=1,NOMAT)
GO TO(154,155,155),LMODE
154 READ(5,601) (PMODE(II), II=1,NRKI)
WRITE(6,632)
WRITE(6,606) (PMODE(II), II=1,NRKI)
155 CONTINUE
WRITE(6,624)
DO 209 I=1,NUMEL
WRITE(6,650) I,IP(I),IQ(I),IR(I),IS(I),NTYPE(II),MATYPE(II),A(I)
209 CONTINUE
WRITE(6,625)
WRITE(6,610) (II,X(II),Y(II),Z(II),II=1,NODES)
IF(MODE) 116,116,117
116 WRITE(6,613)
WRITE(6,615)
RQ1$113
RQ1$114
RQ1$115
RQ1$116
RQ1$117
RQ1$118
RQ1$119
RQ1$120
RQ1$121
RQ1$122
RQ1$123
RQ1$124
RQ1$125
RQ1$126
RQ1$127
RQ1$128
RQ1$129
RQ1$130
RQ1$131
RQ1$132
RQ1$133
RQ1$134
RQ1$135
RQ1$136
RQ1$137
RQ1$138
RQ1$139
RQ1$140
RQ1$141
RQ1$142
RQ1$143
RQ1$144
RQ1$145
RQ1$146
RQ1$147
RQ1$148
RQ1$149
RQ1$150
RQ1$151
RQ1$152
RQ1$153
RQ1$154
RQ1$155
RQ1$156
RQ1$157
RQ1$158
RQ1$159
RQ1$160
RQ1$161
RQ1$162
RQ1$163
RQ1$164
RQ1$165
RQ1$166
RQ1$167
RQ1$168

```

117	NODES=3*NODES	RQ1\$169
	WEIGHT = 0.0	RQ1\$170
1103	DO 103 II=1,NODES	RQ1\$171
	NSP(II)=0	RQ1\$172
	PXY(II) = 0.0	RQ1\$173
103	P(II)=0.0	RQ1\$174
	DO 104 II=1,NSUPS	RQ1\$175
	JJ=NS(II)	RQ1\$176
104	NSP(JJ)=1	RQ1\$177
	DO 105 JJ=1,NLOAD	RQ1\$178
	II = LP(JJ)	RQ1\$179
	GO TO(5110,5110,1105),LMODE	RQ1\$180
1105	ANRKI=NRKI	RQ1\$181
	PXY(II) = QXY(JJ)/ANRKI	RQ1\$182
	GO TO 105	RQ1\$183
5110	PXY(II) = QXY(JJ)	RQ1\$184
105	CONTINUE	RQ1\$185
	DO 108 II=1,NODES	RQ1\$186
108	P1(II) = 0.	RQ1\$187
	DO 121 II=1,NUMEL	RQ1\$188
	SE(III)=0.	RQ1\$189
	DO 121 JJ=1,3	RQ1\$190
	S3(II,JJ)=C.	RQ1\$191
	S1(II,JJ)=0.	RQ1\$192
121	S2(II,JJ)=0.	RQ1\$193
	GO TO(501,502,503),LMODE	RQ1\$194
501	TLC=1./PMODE(1)	RQ1\$195
	GO TO 504	RQ1\$196
502	TLC=2.	RQ1\$197
	GO TO 504	RQ1\$198
503	TLC=NRKI	RQ1\$199
504	CONTINUE	RQ1\$200
C*****	SET UP BAND INDEXING VECTORS	*****RQ1\$201
	NBSYM=(NBAND+1)/2	RQ1\$202
	KOUNT=1	RQ1\$203
	DO 370 II=1,NODES	RQ1\$204
	IF(II-KOUNT*NBSYM) 371,371,372	RQ1\$205
371	IX(III)=II-NBSYM*(KOUNT-1)	RQ1\$206
	GO TO 370	RQ1\$207
372	IX(III)=II-NBSYM*KOUNT	RQ1\$208
	KOUNT=KOUNT+1	RQ1\$209
370	CONTINUE	RQ1\$210
	JRT=(NBAND-1)/2	RQ1\$211
	JS=NODES-JRT	RQ1\$212
	ISI = JRT+1	RQ1\$213
	DO 340 II=1,NODES	RQ1\$214
	IF(II-ISI) 350,350,352	RQ1\$215
350	JLT=1	RQ1\$216
	JRT=JRT+1	RQ1\$217
	GO TO 356	RQ1\$218
352	IF(II=JS) 351,353,353	RQ1\$219
351	JLT=JLT+1	RQ1\$220
	JRT=JRT+1	RQ1\$221
	GO TO 356	RQ1\$222
353	JLT=JLT+1	RQ1\$223
	JRT=NODES	RQ1\$224

```

356 JL(III)=JLT
JR(III)=JRI
340 CONTINUE
IRK=1
IF(NRK1.EQ.1.0) GO TO 401
IF(LMODE.GE.2.0) GO TO 401
DO 152 I=2,NRK1
J = NRK1 +2-1
152 PMODE(J) = PMODE(J)/PMODE(J-1)
C***** START THE INTEGRATION SCHEME
401 DO 300 JRK=1,NRK1
DO 182 II=1,NUMEL
DO 182 JJ=1,3
S3(II,JJ)=S2(II,JJ)
182 S1(II,JJ)=S2(II,JJ)
GO TO (151,119,100),LMODE
151 DO 153 II =1,NUDES
153 PXY(II) = PXY(II)* PMODE(JRK)
GO TO 100
119 DO 118 II =1,NUDES
118 PXY(III)=PXY(II)/2.
100 DO 106 II=1,NUDES
P(II)=PXY(II)
DO 106 JJ=1,NBSYM
106 SS(JJ,II)=0.
NPASS=1
NPASS1= 1
DO 107 IM=1,NUMEL
NN=IM
NTYP=NTYPE(NN)
MATYP = MATYPE(IM)
GO TO (1108,1108,1109,1108,1108),NTYP
1108 SYE = SY(MATYP)
PN = PNL(MATYP)
NLP=PN
HM=1.+(ABS(SE(IM)/SYE))*NLP
EME=EM(MATYP) /BM**((PN+1.)/PN)
IF(EME-EM(MATYP)/100.0) 1106,1106,1107
1106 EME = EM(MATYP)/100.0
1107 CONTINUE
RR =.5-(.5-PR(MATYP))*(EME/EM(MATYP))
AE=A(IM)
GO TO 1110
1109 PN =PNL(MATYP)
NLP=PN
E1 = EM(MATYP)
E2 =EM(MATYP)
PR1= PR(MATYP)
PR2=PR1*E2/E1
SYE = SY(MATYP)
HM=1.+(ABS(SE(IM)/SYE))*NLP
GT=G(MATYP)/BM**((PN+1.)/PN)
AE=A(IM)
BETA = THETA(MATYP)
1110 CONTINUE
C***** COMPUTE ELEMENT STIFFNESS COEFFICIENTS AND STORE

```

```

RQ1$225
RQ1$226
RQ1$227
RQ1$228
RQ1$229
RQ1$230
RQ1$231
RQ1$232
RQ1$233
*****RQ1$234
RQ1$235
RQ1$236
RQ1$237
RQ1$238
RQ1$239
RQ1$240
RQ1$241
RQ1$242
RQ1$243
RQ1$244
RQ1$245
RQ1$246
RQ1$247
RQ1$248
RQ1$249
RQ1$250
RQ1$251
RQ1$252
RQ1$253
RQ1$254
RQ1$255
RQ1$256
RQ1$257
RQ1$258
RQ1$259
RQ1$260
RQ1$261
RQ1$262
RQ1$263
RQ1$264
RQ1$265
RQ1$266
RQ1$267
RQ1$268
RQ1$269
RQ1$270
RQ1$271
RQ1$272
RQ1$273
RQ1$274
RQ1$275
RQ1$276
RQ1$277
RQ1$278
RQ1$279
*****RQ1$280

```

CALL ELEMS	RQ1\$281
CALL STORE	RQ1\$282
107 CONTINUE	RQ1\$283
C*****SOLVE THE SIMULTANEOUS EQUATIONS	*****RQ1\$284
DO 420 II=1, NODES	RQ1\$285
IF (NSP(II)) 420, 425, 420	RQ1\$286
425 KB=IX(II)	RQ1\$287
IF (SS(KB, II).NE.0.0) GO TO 1400	RQ1\$288
1401 FORMAT (45H * * * THERE IS A ZERO ON THE DIAGONAL * * * /)	RQ1\$289
WRITE (6, 1401)	RQ1\$290
1402 FORMAT (10H COORD NO.)	RQ1\$291
WRITE (6, 1402)	RQ1\$292
1403 FORMAT (17)	RQ1\$293
WRITE(6, 1403) IV	RQ1\$294
CALL ERROR (107)	RQ1\$295
1400 CONTINUE	RQ1\$296
AA=1./SS(KB, II)	RQ1\$297
JRT=JR(II)	RQ1\$298
DO 434 JJ=II, JRT	RQ1\$299
434 SS(KB, JJ)=SS(KB, JJ)*AA	RQ1\$300
P(II)=P(II)*AA	RQ1\$301
II=II+1	RQ1\$302
DO 424 LL=II, JRT	RQ1\$303
LB=IX(LL)	RQ1\$304
IF (NSP(LL)) 424, 421, 424	RQ1\$305
421 BB=SS(KB, LL)/AA	RQ1\$306
IF (BB) 423, 424, 423	RQ1\$307
423 DO 422 JJ=LL, JRT	RQ1\$308
422 SS(LB, JJ)=SS(LB, JJ)-SS(KB, JJ)*BB	RQ1\$309
P(LL)=P(LL)-P(II)*BB	RQ1\$310
424 CONTINUE	RQ1\$311
420 CONTINUE	RQ1\$312
DO 452 II=2, NODES	RQ1\$313
JJ=NODES+1-II	RQ1\$314
IF (NSP(JJ)) 451, 451, 452	RQ1\$315
451 JB=IX(JJ)	RQ1\$316
KIK=II-1	RQ1\$317
LL=JL(II)	RQ1\$318
DO 450 MN=LL, KIK	RQ1\$319
NN=NODES+1-MN	RQ1\$320
450 P(JJ)=P(JJ)-SS(JB, NN)*P(NN)	RQ1\$321
452 CONTINUE	RQ1\$322
IF (MODE) 141, 141, 251	RQ1\$323
251 IF (NRK I-1) 261, 252, 261	RQ1\$324
252 DO 263 N=1, NODES	RQ1\$325
263 PE(N)=P(N)	RQ1\$326
261 DO 262 N=1, NODES	RQ1\$327
262 P1(N)=P1(N)+P(N)	RQ1\$328
GO TO 140	RQ1\$329
141 GO TO (136, 137, 138, 139), IRK	RQ1\$330
136 IF (JRK-1) 143, 143, 142	RQ1\$331
143 DO 144 N=1, NODES	RQ1\$332
144 PE(N)=P(N)	RQ1\$333
142 DO 132 N=1, NODES	RQ1\$334
132 P1(N)=P1(N)+P(N)/6.	RQ1\$335
GO TO 140	RQ1\$336

```

137 DO 133 N=1, NODES
133 P1(N)= P1(N)+P(N)/3.
GO TO 140
138 DO 134 N=1, NODES
134 P1(N) = P1(N) +P(N)/3.
GO TO 140
139 DO 135 N=1, NODES
135 P1(N) = P1(N)+P(N)/6.
140 NPASS = 2
DO 111 N=1, NUMEL
NN=N
MATYP=MATYP(N)
NTYP=NTYP(N)
GO TO(1111,1111,1112,1111,1111), NTYP
1111 SYE = SY(MATYP)
EME = EM(MATYP)
RR = PR(MATYP)
AF=A(N)
GO TO 1113
1112 SYE = SY(MATYP)
E1 = EM(MATYP)
E2 =EMM(MATYP)
PR1 = PR(MATYP)
PR2=PR1*E2/E1
GT = G(MATYP)
AF=A(N)
BETA=THETA(MATYP)
1113 CONTINUE
C***** COMPUTE ELEMENT COMPATIBILITY ARRAY
CALL ELEMS
C***** COMPUTE ELEMENT STRESSES
CALL STRES
IF(MODE) 70, 70, 71
C***** ENTER EULER INTEGRATION SCHEME
71 DO 72 J=1, 3
72 S1(N, J) = S1(N, J)+SIGMA(J)
GO TO 111
C***** ENTER RUNGE-KUTTA INTEGRATION SCHEME
70 GO TO (74, 75, 76, 77), IRK
74 IF(IRK-JRK) 83, 82, 83
82 DO 8200 J=1, 3
8200 SIGMA(J) = SIGMA(J)*TLC
WRITE(6, 633) N, (SIGMA(J), J=1, 3)
DO 8201 J=1, 3
8201 SIGMA(J) = SIGMA(J)/TLC
DO 288 J=1, 3
288 S4(N, J)=SIGMA(J)
83 DO 78 J=1, 3
S1(N, J)=S1(N, J)+SIGMA(J)/6.
78 S2(N, J)=S3(N, J)+SIGMA(J)/2.
GO TO(1178,1178,1179,1178,1178), NTYP
1178 CONTINUE
SE(N)=(S2(N, 1)**2+S2(N, 2)**2-S2(N, 1)*S2(N, 2)+3.*S2(N, 3)**2)**.5
GO TO 1180
1179 SE(N)=S2(N, 3)
1180 CONTINUE

```

```

RQ1$337
RQ1$338
RQ1$339
RQ1$340
RQ1$341
RQ1$342
RQ1$343
RQ1$344
RQ1$345
RQ1$346
RQ1$347
RQ1$348
RQ1$349
RQ1$350
RQ1$351
RQ1$352
RQ1$353
RQ1$354
RQ1$355
RQ1$356
RQ1$357
RQ1$358
RQ1$359
RQ1$360
RQ1$361
RQ1$362
RQ1$363
RQ1$364
RQ1$365
RQ1$366
RQ1$367
RQ1$368
RQ1$369
RQ1$370
RQ1$371
RQ1$372
RQ1$373
RQ1$374
RQ1$375
RQ1$376
RQ1$377
RQ1$378
RQ1$379
RQ1$380
RQ1$381
RQ1$382
RQ1$383
RQ1$384
RQ1$385
RQ1$386
RQ1$387
RQ1$388
RQ1$389
RQ1$390
RQ1$391
RQ1$392

```

```

      GO TO 111
75 DO 79 J=1,3
      S1(N,J)=S1(N,J)+SIGMA(J)/3.
79 S2(N,J)=S3(N,J)+SIGMA(J)/2.
      GU TO(2178,2178,2179,2178,2178),NTYP
2178 CONTINUE
      SE(N)=(S2(N,1)**2+S2(N,2)**2-S2(N,1)*S2(N,2)+3.*S2(N,3)**2)**.5
      GO TO 2180
2179 SE(N)=S2(N,3)
2180 CONTINUE
      GO TO 111
      DO 80 J=1,3
      S1(N,J)=S1(N,J)+SIGMA(J)/3.
80 S2(N,J)=S3(N,J)+SIGMA(J)
      GO TO(3178,3178,3179,3178,3178),NTYP
3178 CONTINUE
      SE(N)=(S2(N,1)**2+S2(N,2)**2-S2(N,1)*S2(N,2)+3.*S2(N,3)**2)**.5
      GO TO 3180
3179 SE(N)=S2(N,3)
3180 CONTINUE
      GO TO 111
      DO 81 J=1,3
81 S1(N,J)=S1(N,J)+SIGMA(J)/6.
111 CONTINUE
      IF(MODE) 112,112,113
112 IF(JRK.NE.1.0) GO TO 150
      IF(IRK.NE.1.0) GO TO 150
130 WRITE(6,616)
      WRITE(6,617)
      DO 8202 N=1,NODES
8202 P(N) = P(N)*TLC
      WRITE(6,618) (N,P(N),N=1,NODES)
      DO 8203 N=1,NODES
8203 P(N) = P(N)/TLC
150 IRK = IRK+1
      IF(IRK-5)100,120,120
120 IRK=1
      DO 183 N=1,NUMEL
      NTYP=NTYPE(N)
      GO TO(4178,4178,4179,4178,4178),NTYP
4178 CONTINUE
      SE(N)=(S1(N,1)**2+S1(N,2)**2-S1(N,1)*S1(N,2)+3.*S1(N,3)**2)**.5
      GO TO 183
4179 SE(N)=S1(N,3)
183 CONTINUE
113 DO 180 II=1,NUMEL
      DO 180 JJ=1,3
180 S2(II,JJ)=S1(II,JJ)
C***** COMPUTE END OF INTERVAL STRESSES AND STRAINS
      DO 283 N = 1, NODES
283 P(N) = P1(N)
      DO 184 N=1,NUMEL
      NN=N
      MATYP = MATYPE(N)
      NTYP=NTYPE(N)
      GO TO(1283,1283,1284,1283,1283),NTYP

```

```

RQ1$393
RQ1$394
RQ1$395
RQ1$396
RQ1$397
RQ1$398
RQ1$399
RQ1$400
RQ1$401
RQ1$402
RQ1$403
RQ1$404
RQ1$405
RQ1$406
RQ1$407
RQ1$408
RQ1$409
RQ1$410
RQ1$411
RQ1$412
RQ1$413
RQ1$414
RQ1$415
RQ1$416
RQ1$417
RQ1$418
RQ1$419
RQ1$420
RQ1$421
RQ1$422
RQ1$423
RQ1$424
RQ1$425
RQ1$426
RQ1$427
RQ1$428
RQ1$429
RQ1$430
RQ1$431
RQ1$432
RQ1$433
RQ1$434
RQ1$435
RQ1$436
RQ1$437
RQ1$438
RQ1$439
RQ1$440
*****RQ1$441
RQ1$442
RQ1$443
RQ1$444
RQ1$445
RQ1$446
RQ1$447
RQ1$448

```

```

1283 SYE = SY(MATYP)
      PN =PNL(MATYP)
      EME = EM(MATYP)
      RR = PR(MATYP)
      AE=A(N)
      NLP=PN
      BM=1.+(ABS(SE(N)/SYE)**NLP
      EME=EME/BM**(1./PN)
      RR = .5-(.5-RR)*(EME/EM(MATYP))
      GO TO 1285
1284 SYE = SY(MATYP)
      PN =PNL(MATYP)
      E1 = EM(MATYP)
      E2 =EMM(MATYP)
      PR1 = PR(MATYP)
      PR2=PR1*E2/E1
      NLP=PN
      BM = 1.+(ABS(SE(N)/SYE)**NLP
      GT = G(MATYP)/BM**(1./PN)
      AE=A(N)
      BETA = THE TA(MATYP)
1285 CONTINUE
      CALL ELEMS
      CALL STRES
      DO 185 M=1,3
185 S1(N,M)=SIGMA(M)
      NTP=NTYPE(N)
      GO TO(285,286,286,1286,1286),NTP
285 S3(N,1)=(UU(2)-UU(1))/D1
      S3(N,2)=0.
      S3(N,3)=0.
      GO TO 184
286 S3(N,1)=( Y32*UU(1)-Y31*UU(3)+Y21*UU(5))/(2.*A123)
      S3(N,2)=(-X32*UU(2)+X31*UU(4)-X21*UU(6))/(2.*A123)
      S3(N,3)=(-X32*UU(1)+Y32*UU(2)+X31*UU(3)-
1Y31*UU(4)-X21*UU(5)+Y21*UU(6))/(2.*A123)
      GO TO(184,184,287,1286,1286),NTP
287 R(1)=S3(N,1)
      R(2)=S3(N,2)
      R(3)=S3(N,3)
      S3(N,1)=R(1)*CB+R(2)*SB+R(3)*S*C
      S3(N,2)=R(1)*SB+R(2)*CB-R(3)*S*C
      S3(N,3)=-2.*R(1)*S*C+2.*R(2)*S*C+R(3)*(CB-SB)
      GO TO 184
1286 S3(N,1) = (S1(N,1)-S1(N,2)*RR)/EME
      S3(N,2) = (S1(N,2)-S1(N,1)*RR)/EME
      S3(N,3) = (S1(N,3)/EME)*2.*(1.+RR)
184 CONTINUE
C*****WRITE END OF INTERVAL STRESSES AND STRAINS
      IF(MODE) 123,123,124
124 WRITE(6,612)
      GO TO 125
123 WRITE(6,602)
125 WRITE(6,604) JRK
      WRITE(6,619)
      WRITE(6,630)(II, S1(II,1),S1(II,2),S1(II,3),S3(II,1),
RQ1$449
RQ1$450
RQ1$451
RQ1$452
RQ1$453
RQ1$454
RQ1$455
RQ1$456
RQ1$457
RQ1$458
RQ1$459
RQ1$460
RQ1$461
RQ1$462
RQ1$463
RQ1$464
RQ1$465
RQ1$466
RQ1$467
RQ1$468
RQ1$469
RQ1$470
RQ1$471
RQ1$472
RQ1$473
RQ1$474
RQ1$475
RQ1$476
RQ1$477
RQ1$478
RQ1$479
RQ1$480
RQ1$481
RQ1$482
RQ1$483
RQ1$484
RQ1$485
RQ1$486
RQ1$487
RQ1$488
RQ1$489
RQ1$490
RQ1$491
RQ1$492
RQ1$493
RQ1$494
RQ1$495
RQ1$496
*****RQ1$497
RQ1$498
RQ1$499
RQ1$500
RQ1$501
RQ1$502
RQ1$503
RQ1$504

```

```

1          S3(II,2),S3(II,3), II = 1, NUMEL)
IF(MODE)1123,1123,1124
1124 WRITE(6,653)
GO TO 1125
1123 WRITE(6,654)
1125 WRITE(6,604) JRK
WRITE(6,617)
WRITE(6,618) (N,P1(N), N=1, NODES)
C*****CALCULATE PRINCIPAL STRESSES AND MAXIMUM SHEAR
DO 900 N=1, NUMEL
VE(N) = 0.0
SAFTY(N) = 0.0
STP1 = S1(N,1)
STP2 = S1(N,2)
STP3 = S1(N,3)
C**** ORIENT ORTHOTROPIC ELEMENT STRESSES AND STORE IN S7 *****
IF(NTYPE(N).NE.3) GO TO 1488
BETA = -THETA(MATYPE(N))
C = COS(BETA)
S = SIN(BETA)
CB= C*C
SB= S*S
S7(N,1)= STP1*CB +STP2*SB +STP3*S*C*2.
S7(N,2)= STP1*SB +STP2*CB -STP3*S*C*2.
S7(N,3)=-STP1*S*C+STP2*S*C+STP3*(CB-SB)
GO TO 900
1488 CONTINUE
S7(N,3) = (((STP1-STP2)/2.)**2 +STP3**2)**.5
S7(N,1) = (STP1+STP2)/2. +S7(N,3)
S7(N,2) = (STP1+STP2)/2. -S7(N,3)
C*****CALCULATE EFFECTIVE STRESS AND MARGIN OF SAFETY
VE(N) = (S7(N,1)**2 +S7(N,2)**2 -S7(N,1)*S7(N,2))**.5
IF(VE(N).LT.100.0) GO TO 900
903 SAFTY(N) = (SY(MATYPE(N))/VE(N)-1.0)*100.0
900 CONTINUE
WRITE (6,639)
WRITE(6,604) JRK
WRITE (6,640)
NN8=0
DO 901 N=1, NUMEL
WRITE(6,630) N, S7(N,1), S7(N,2), S7(N,3), VE(N),
1 SY(MATYPE(N)), SAFTY(N)
NN8=NN8+1
IF(NN8.NE.45) GO TO 901
NN8=0
WRITE(6,657)
WRITE(6,640)
901 CONTINUE
IF(MODE)114,114,215
215 IF(JRK -1)115,216,115
216 DO 1287 N=1, NUMEL
DO 1287 J=1,3
1287 S4(N,J) = S2(N,J)
115 DO 187 N=1, NUMEL
C*****CALCULATE ELASTIC EFFECTIVE STRESS
NTYP=NTYPE(N)

```

```

RQ1$505
RQ1$506
RQ1$507
RQ1$508
RQ1$509
RQ1$510
RQ1$511
RQ1$512
RQ1$513
RQ1$514
RQ1$515
RQ1$516
RQ1$517
RQ1$518
RQ1$519
RQ1$520
RQ1$521
RQ1$522
RQ1$523
RQ1$524
RQ1$525
RQ1$526
RQ1$527
RQ1$528
RQ1$529
RQ1$530
RQ1$531
RQ1$532
RQ1$533
RQ1$534
RQ1$535
RQ1$536
RQ1$537
RQ1$538
RQ1$539
RQ1$540
RQ1$541
RQ1$542
RQ1$543
RQ1$544
RQ1$545
RQ1$546
RQ1$547
RQ1$548
RQ1$549
RQ1$550
RQ1$551
RQ1$552
RQ1$553
RQ1$554
RQ1$555
RQ1$556
RQ1$557
RQ1$558
RQ1$559
RQ1$560

```

```

GO TO(1115,1115,1116,1115,1115),NTYP
1115 SE(N)=(S2(N,1)**2+S2(N,2)**2-S2(N,1)*S2(N,2)+3.*S2(N,3)**2)**.5
GO TO 187
1116 SE(N)=S2(N,3)
187 CONTINUE
C*****NOW LETS CALCULATE EXTERNAL FORCES AT EACH NODE
114 NPASS=1
IF(MODE-NRKI)516,517,516
517 DO 518 N=1,NUMEL
518 SE(N)=0.
516 CONTINUE
DO 510 II = 1,NODES
DO 510 JJ = 1,NBSYM
510 SS(JJ, II) = 0.0
DO 484 N=1,NUMEL
NN=N
MATYP = MATYPE(N)
NTYP=NTYPE(N)
GO TO(4484,4484,4485,4484,4484),NTYP
4484 SYE = SY(MATYP)
PN =PNL(MATYP)
EME = EM(MATYP)
RR = PR(MATYP)
AE=A(N)
NLP=PN
BM=1.+(ABS(SE(N)/SYE)**NLP
CME=EME/BM**(1./PN)
RR = .5-(.5-RR)*(EME/EM(MATYP))
GO TO 4486
4485 SYE = SY(MATYP)
PN =PNL(MATYP)
E1 = EM(MATYP)
E2 =EMM(MATYP)
PR1 = PR(MATYP)
PR2=PR1*E2/E1
NLP=PN
AE=A(N)
BM = 1. +(ABS(SE(N)/SYE)**NLP
GT = G(MATYP)/BM**(1./PN)
HETA = THETA(MATYP)
4486 CALL ELEMS
CALL STORE
WEIGHT = WEIGHT+A123*AE*DENSE(MATYP)
484 CONTINUE
DO 485 II=1,NODES
P(II)=0.
KI=IX(II)
JLT=JL(II)
JRT=JR(II)
DO 487 J=II,JRT
487 P(II)=P(II)+SS(KI,J)*P1(J)
DO 488 J=JLT,II
KJ=IX(J)
488 P(II)=P(II)+SS(KJ,II)*P1(J)
485 P(II)=P(II)-SS(KI,II)*P1(II)
N003 = NO0ES/3

```

```

RQ1$561
RQ1$562
RQ1$563
RQ1$564
RQ1$565
RQ1$566
RQ1$567
RQ1$568
RQ1$569
RQ1$570
RQ1$571
RQ1$572
RQ1$573
RQ1$574
RQ1$575
RQ1$576
RQ1$577
RQ1$578
RQ1$579
RQ1$580
RQ1$581
RQ1$582
RQ1$583
RQ1$584
RQ1$585
RQ1$586
RQ1$587
RQ1$588
RQ1$589
RQ1$590
RQ1$591
RQ1$592
RQ1$593
RQ1$594
RQ1$595
RQ1$596
RQ1$597
RQ1$598
RQ1$599
RQ1$600
RQ1$601
RQ1$602
RQ1$603
RQ1$604
RQ1$605
RQ1$606
RQ1$607
RQ1$608
RQ1$609
RQ1$610
RQ1$611
RQ1$612
RQ1$613
RQ1$614
RQ1$615
RQ1$616

```

```

SUMFX = 0.0
SUMFY=0.
SUMFZ=0.
SUMMX = 0.0
SUMMY = 0.0
SUMMZ = 0.0
DO 486 II=1,NOI3
JJ=II*3
SUMFX=SUMFX+P(JJ-2)
SUMFY=SUMFY+P(JJ-1)
SUMFZ=SUMFZ+P(JJ )
SUMMX = SUMMX + P(JJ) * Y(II) -P(JJ-1)* Z(II)
SUMMY = SUMMY + P(JJ-2)* Z(II) -P(JJ) * X(II)
SUMMZ = SUMMZ + P(JJ-1)* X(II) -P(JJ-2)* Y(II)
486 CONTINUE
WRITE(6,635)
WRITE(6,604) JRK
WRITE(6,636)
WRITE(6,637) (SUMFX, SUMFY, SUMFZ)
WRITE(6,662)
WRITE(6,637) (SUMMX, SUMMY, SUMMZ)
WRITE(6,634)
WRITE(6,618) (N,P(N),N=1,NOIES)
300 CONTINUE
WEIGHT = WEIGHT/NRKI
WRITE(6,661)
WRITE(6,606) WEIGHT
IF(MODE)1590,1590,1500
1500 IF(ITERAT.EQ.0) GO TO 1600
ITEPAT = ITERAT-1
ITEST= 0
DO 1510 N=1,NUMEL
IF(DENSE(MATYP(N)).EQ.0.) GO TO 1510
IF(SAFY(N).LT.5. .AND.SAFY(N).GT.-5.)GO TO 1510
ITEST= 1
A(N) = A(N) + A(N)*(VE(N)-SY(MATYP(N)))/SY(MATYP(N))
1510 CONTINUE
NOIES = NOIES/3.0
IF(ITEST.EQ.0) GO TO 1600
GO TO 1830
C*****COMPUTE RESIDUAL STRESSES STRAINS AND DISPLACEMENTS
1590 DO 505 N=1,NOIES
505 PE(N)=P1(N)-PE(N)*TLC
DO 506 N=1,NUMEL
NTYP=NTYP(N)
MATYP= MATYP(N)
EME = EM(MATYP)
S1(N,1) = S1(N,1) -S4(N,1)*TLC
S1(N,2) = S1(N,2) -S4(N,2)*TLC
S1(N,3) = S1(N,3) -S4(N,3)*TLC
GO TO(5505,5506,5506,5506,5506),NTYP
5505 S3(N,1)=(S3(N,1)-TLC*S4(N,1))/EME
GO TO 506
5506 S3(N,1)=S3(N,1)-TLC*(S4(N,1)-PR(MATYP)*S4(N,2))/EME
S3(N,2) = S3(N,2) - TLC*(S4(N,2)-PR(MATYP)*S4(N,1))/EME
S3(N,3)=S3(N,3)-TLC*(S4(N,3)*(2.*(1.+PR(MATYP))))/EME
RQ1$617
RQ1$618
RQ1$619
RQ1$620
RQ1$621
RQ1$622
RQ1$623
RQ1$624
RQ1$625
RQ1$626
RQ1$627
RQ1$628
RQ1$629
RQ1$630
RQ1$631
RQ1$632
RQ1$633
RQ1$634
RQ1$635
RQ1$636
RQ1$637
RQ1$638
RQ1$639
RQ1$640
RQ1$641
RQ1$642
RQ1$643
RQ1$644
RQ1$645
RQ1$646
RQ1$647
RQ1$648
RQ1$649
RQ1$650
RQ1$651
RQ1$652
RQ1$653
RQ1$654
RQ1$655
RQ1$656
RQ1$657
RQ1$658
RQ1$659
RQ1$660
RQ1$661
RQ1$662
RQ1$663
RQ1$664
RQ1$665
RQ1$666
RQ1$667
RQ1$668
RQ1$669
RQ1$670
RQ1$671
RQ1$672

```

```

506 CONTINUE
WRITE(6,638)
WRITE(6,619)
WRITE(6,630)(II,S1(II,1),S1(II,2),S1(II,3),S3(II,1),
1          S3(II,2),S3(II,3),II=1,NUMEL)
WRITE(6,655)
WRITE(6,617)
WRITE(6,618)(N,PE(N),N=1,NODES)
1600 CONTINUE
GO TO 800
END
SUBROUTINE ELEMS
C*****PRZEMIENIECKI-BERKE 3D ELEMENT STIFFNESS ROUTINE *****
DIMENSION ALAM(15,15),ALAMT(15,15),R(12),U(12),UU(10),AL(3),
1SIGMA(3),LP(333),NS(666),AL2(3),OSK(8,8),PMODE(10),QXY(333),
2PXY(750),P(750),P1(750),PE(750),IX(750),JL(750),JR(750),
3NSP(750),SS(87,750),NPT(250),X(250),Y(250),Z(250),IS(1000),
4SE(1000),S1(1000,3),S2(1000,3),S3(1000,3),IE(1000),IP(1000),
5IQ(1000),IR(1000),NTYPE(1000),EM(20),PR(20),SY(20),PNL(20),
6MATYPE(1000),A(1000),SAFETY(1000),VE(1000),S4(1000,3),S7(1000,3),
7EMM(20),G(20),THETA(20),ZZ(15,15),
8TT(15,15),T11(8,8),T22(2,2),T12(8,2),T21(2,8),T22INV(2,2)
9,SIG(3),ZIGMA(3),TMATRIX(3,3),DENSE(20)
COMMON SS,IX,JL,JR,AEI,NBAND,ALAM,ALAMT,R,RR,D1,AL,X21,X31,X32,Y21
1,Y31,Y32,A123,U,UU,SIGMA,SYE,PN,EME,A,NLP,BM,SE,S1,S2,S3,P1,
2NTYPE,N,IM,NPASS,NN,NPT,X,Y,Z,IE,IP,IQ,IR,AE,NODES,II,JJ,AL2,OSK,
3P,SAFETY,VE,S4,S7,PE,MID,NSP,IS,D2,
4EMM,G,THETA,BETA,S,C,SB,CB,GT,PR1,PR2,E1,E2
5,LP,PK,NS,SY,PMODE,PNL,PXY,EM,MATYPE,
6TT,T11,T22,T12,T21,T22INV,ZZ,NPASS],NTRI,XIT,YIT,ZIT,ILAM,JLAM
7,DIR1,DIR2,DIR3,THETA1,QXY
GO TO(888,400),NPASS1
888 XQP=X(IQ(NN))-X(IP(NN))
YQP=Y(IQ(NN))-Y(IP(NN))
ZQP=Z(IQ(NN))-Z(IP(NN))
D1=SQRT(XQP**2+YQP**2+ZQP**2)
IF(D1.NE.0.0) GO TO 1400
1401 FORMAT(52H * * * THERE IS A GEOMETRY ERROR IN ELEMENT NUMBER /)
WRITE(6,1401)
1402 FORMAT(17)
WRITE(6,1402) NN
CALL ERROR(103)
1400 CONTINUE
CALCULATE THE PQ DIRECTION COSINES
AL(1)=XQP/D1
AL(2)=YQP/D1
AL(3)=ZQP/D1
AE1=AE*EME
NTYP=NTYPE(NN)
GO TO(1,2,2,3,4),NTYP
CALCULATIONS FOR THE BAR
1 ILAM=2
JLAM=6
DO 239 I=1,3
ALAM(1,I)=AL(I)
ALAM(1,I+3)=0.
RQ1$673
RQ1$674
RQ1$675
RQ1$676
RQ1$677
RQ1$678
RQ1$679
RQ1$680
RQ1$681
RQ1$682
RQ1$683
RQ1A001
RQ1A002
RQ1A003
RQ1A004
RQ1A005
RQ1A006
RQ1A007
RQ1A008
RQ1A009
RQ1A010
RQ1A011
RQ1A012
RQ1A013
RQ1A014
RQ1A015
RQ1A016
RQ1A017
RQ1A018
RQ1A019
RQ1A020
RQ1A021
RQ1A022
RQ1A023
RQ1A024
RQ1A025
RQ1A026
RQ1A027
RQ1A028
RQ1A029
RQ1A030
RQ1A031
RQ1A032
RQ1A033
RQ1A034
RQ1A035
RQ1A036
RQ1A037
RQ1A038
RQ1A039
RQ1A040
RQ1A041
RQ1A042
RQ1A043
RQ1A044
RQ1A045

```

```

ALAM(2,I+3)=AL(I)
ALAM(2,I)=0.
GO TO (231,239),NPASS
231 DO 240 J=1,3
ALAMT(I,J)=AL(I)*AL(J)*AE1/D1
ALAMT(I+3,J)=-ALAMT(I,J)
ALAMT(I,J+3)=-ALAMT(I,J)
ALAMT(I+3,J+3)=ALAMT(I,J)
240 CONTINUE
239 A123 = D1
GO TO 40
CALCULATIONS FOR THE TRIANGLE
2 ILAM=6
JLAM=9
XRP=X(IR(NN))-X(IP(NN))
YRP=Y(IR(NN))-Y(IP(NN))
ZRP=Z(IR(NN))-Z(IP(NN))
XRQ=X(IR(NN))-X(IQ(NN))
YRQ=Y(IR(NN))-Y(IQ(NN))
ZRQ=Z(IR(NN))-Z(IQ(NN))
RP=AL(1)*XRP+AL(2)*YRP+AL(3)*ZRP
X2=XRP-AL(1)*RP
Y2=YRP-AL(2)*RP
Z2=ZRP-AL(3)*RP
D2=SQRT(X2**2+Y2**2+Z2**2)
IF(D2.NE.0.0) GO TO 1500
1501 FORMAT (52H * * * THERE IS A GEOMETRY ERROR IN TRI PLATE NO. /)
WRITE (6,1501)
1502 FORMAT (17)
WRITE (6,1502) NN
CALL ERROR (104)
1500 CONTINUE
CALCULATE THE TRIANGLE DIRECTION COSINES
AL2(1)=X2/D2
AL2(2)=Y2/D2
AL2(3)=Z2/D2
CHANGE FROM DATUM TO LOCAL COORDINATES
X21=XQP*AL2(1)+YQP*AL2(2)+ZQP*AL2(3)
Y21=XQP*AL(1)+YQP*AL(2)+ZQP*AL(3)
X31=XRP*AL2(1)+YRP*AL2(2)+ZRP*AL2(3)
Y31=XRP*AL(1)+YRP*AL(2)+ZRP*AL(3)
X32=XRQ*AL2(1)+YRQ*AL2(2)+ZRQ*AL2(3)
Y32=XRQ*AL(1)+YRQ*AL(2)+ZRQ*AL(3)
A123=(X32*Y21-X21*Y32)/2.
IF(A123.NE.0.0) GO TO 1600
1601 FORMAT (52H * * * THERE IS A GEOMETRY ERROR IN TRI PLATE NO. /)
WRITE (6,1601)
1602 FORMAT (17)
WRITE (6,1602) NN
CALL ERKOR (105)
1600 CONTINUE
GO TO (232, 61),NPASS
232 GO TO(233,233,234),NTYP
233 ET1=AE1/(4.*A123*(1.-RR**2))
ET2=AE1/(8.*A123*(1.+RR))
CALCULATE THE STIFFNESS MATRIX FOR THE TRIANGLE IN LOCAL COORD

```

RQ1A046
RQ1A047
RQ1A048
RQ1A049
RQ1A050
RQ1A051
RQ1A052
RQ1A053
RQ1A054
RQ1A055
RQ1A056
RQ1A057
RQ1A058
RQ1A059
RQ1A060
RQ1A061
RQ1A062
RQ1A063
RQ1A064
RQ1A065
RQ1A066
RQ1A067
RQ1A068
RQ1A069
RQ1A070
RQ1A071
RQ1A072
RQ1A073
RQ1A074
RQ1A075
RQ1A076
RQ1A077
RQ1A078
RQ1A079
RQ1A080
RQ1A081
RQ1A082
RQ1A083
RQ1A084
RQ1A085
RQ1A086
RQ1A087
RQ1A088
RQ1A089
RQ1A090
RQ1A091
RQ1A092
RQ1A093
RQ1A094
RQ1A095
RQ1A096
RQ1A097
RQ1A098
RQ1A099
RQ1A100
RQ1A101

```

DSK(1,1)= ET1*Y32**2 +E T2*X32**2
DSK(2,1)=-ET1*RR*Y32*X32-E T2*X32*Y32
DSK(2,2)= ET1*X32**2 +E T2*Y32**2
DSK(3,1)=-ET1*Y32*Y31 -E T2*X32*X31
DSK(3,2)= ET1*RR*X32*Y31+E T2*Y32*X31
DSK(3,3)= ET1*Y31**2 +E T2*X31**2
DSK(4,1)= ET1*RR*Y32*X31+E T2*X32*Y31
DSK(4,2)=-ET1*X32*X31 -E T2*Y32*Y31
DSK(4,3)=-ET1*RR*Y31*X31-E T2*X31*Y31
DSK(4,4)= ET1*X31**2 +E T2*Y31**2
DSK(5,1)= ET1*Y32*Y21 +E T2*X32*X21
DSK(5,2)=-ET1*RR*X32*Y21-E T2*Y32*X21
DSK(5,3)=-ET1*Y31*Y21 -E T2*X31*X21
DSK(5,4)= ET1*RR*X31*Y21+E T2*Y31*X21
DSK(5,5)= ET1*Y21**2 +E T2*X21**2
DSK(6,1)=-ET1*RR*Y32*X21-E T2*X32*Y21
DSK(6,2)= ET1*X32*X21 +E T2*Y32*Y21
DSK(6,3)= ET1*RR*Y31*X21+E T2*X31*Y21
DSK(6,4)=-ET1*X31*X21 -E T2*Y31*Y21
DSK(6,5)=-ET1*RR*Y21*X21-E T2*X21*Y21
DSK(6,6)= ET1*X21**2 +E T2*Y21**2
GO TO 61
234 C11=F1*AE/(4.*A123*(1.-PR1*PR2))
C12=C11*PR2
C21=C12
C22=C11*E2/E1
C66=GT*AE/(4.*A123)
C=COS(BETA)
CB=C**2
S=SIN(BETA)
SH=S**2
ALAMT(1,1)=C11*CB**2+2.*(C12+2.*C66)*CB*SB+C22*SB**2
ALAMT(1,2)=(C11+C22-4.*C66)*SB*CB+C12*(CB**2+SB**2)
ALAMT(2,2)=C11*SB**2+2.*(C12+2.*C66)*SB*CB+C22 *CB**2
ALAMT(1,3)=(C11-C12-2.*C66)*S*CB*C+(C12-C22+2.*C66)*S*SB*C
ALAMT(2,3)=(C11-C12-2.*C66)*S*SB*C+(C12-C22+2.*C66)*S*CB*C
ALAMT(3,3)=(C11+C22-C12-2.*C66)*SB*CB+C66*(SB**2+CB**2)
ALAMT(2,1)=ALAMT(1,2)
ALAMT(3,1)=ALAMT(1,3)
ALAMT(3,2)=ALAMT(2,3)
ALAM(1,1)= Y32
ALAM(1,2)=0.
ALAM(1,3)=-Y31
ALAM(1,4)=0.
ALAM(1,5)= Y21
ALAM(1,6)=0.
ALAM(2,1)=0.
ALAM(2,2)=-X32
ALAM(2,3)=0.
ALAM(2,4)= X31
ALAM(2,5)=0.
ALAM(2,6)=-X21
ALAM(3,1)=-X32
ALAM(3,2)= Y32
ALAM(3,3)= X31
ALAM(3,4)=-Y31
RQ1A102
RQ1A103
RQ1A104
RQ1A105
RQ1A106
RQ1A107
RQ1A108
RQ1A109
RQ1A110
RQ1A111
RQ1A112
RQ1A113
RQ1A114
RQ1A115
RQ1A116
RQ1A117
RQ1A118
RQ1A119
RQ1A120
RQ1A121
RQ1A122
RQ1A123
RQ1A124
RQ1A125
RQ1A126
RQ1A127
RQ1A128
RQ1A129
RQ1A130
RQ1A131
RQ1A132
RQ1A133
RQ1A134
RQ1A135
RQ1A136
RQ1A137
RQ1A138
RQ1A139
RQ1A140
RQ1A141
RQ1A142
RQ1A143
RQ1A144
RQ1A145
RQ1A146
RQ1A147
RQ1A148
RQ1A149
RQ1A150
RQ1A151
RQ1A152
RQ1A153
RQ1A154
RQ1A155
RQ1A156
RQ1A157

```

```

      ALAM(3,5)=-X2I
      ALAM(3,6)= Y2I
      DO 235 I=1,3
      DO 235 J=1,6
      ALAMT(I+3,J)=0.
      DO 235 K=1,3
235  ALAMT(I+3,J)=ALAMT(I+3,J)+ALAMT(I,K)*ALAM(K,J)
      DO 236 I=1,6
      DO 236 J=1,I
      USK(I,J)=0.
      DO 236 K=1,3
236  DSK(I,J)=DSK(I,J)+ALAM(K,I)*ALAMT(K+3,J)
      GO TO 61
C  CALCULATIONS FOR THE RECTANGULAR PLATE *****
C
      3  ILAM=8
      JLAM=12
      X2=X(IR(NN))-X(IQ(NN))
      Y2=Y(IR(NN))-Y(IQ(NN))
      Z2=Z(IR(NN))-Z(IQ(NN))
      D2=SQRT(X2**2+Y2**2+Z2**2)
      IF(D2.NE.0.0) GO TO 1700
1701  FORMAT (52H * * * THERE IS A GEOMETRY ERROR IN RECT PLATE NO. //)
      WRITE (6,1701)
1702  FURMAT (17)
      WRITE (6,1702) NN
      CALL ERROR (106)
1700  CONTINUE
      AL2(1)=X2/D2
      AL2(2)=Y2/D2
      AL2(3)=Z2/D2
      A123 = D1*D2
      GO TO(261,61),NPASS
261  BETA = D1/D2
      ET1 =AE1/(1.-RR**2)
      ET2 =AE1/(2.+2.*RR)
      ET3 =AE1*D2/(2.-2.*RR)
C  CALCULATE THE KU+KS MATRIX
      RR2 = RR**2
      USK(1,1)=ET1*BETA/3.+ET2/(3.*BETA)
      DSK(2,1)=(ET1*RR+ET2)/4.
      DSK(3,1)=ET1*BETA/6.-ET2/(3.*BETA)
      USK(4,1)=(-ET1*RR+ET2)/4.
      DSK(5,1)=-ET1*BETA/6.-ET2/(6.*BETA)
      DSK(7,1)=-ET1*BETA/3.+ET2/(6.*BETA)
      USK(2,2)=ET1/(3.*BETA)+ET2*BETA/3.
      DSK(4,2)=-ET1/(3.*BETA)+ET2*BETA/6.
      DSK(6,2)=-ET1/(6.*BETA)-ET2*BETA/6.
      DSK(8,2)=ET1/(6.*BETA)-ET2*BETA/3.
      DSK(3,3)=ET1*BETA/3.+ET2/(3.*BETA)
      USK(5,3)=-ET1*BETA/3.+ET2/(6.*BETA)
      DSK(6,1)=-DSK(2,1)
      DSK(8,1)=-DSK(4,1)
      DSK(3,2)=-DSK(4,1)
      DSK(5,2)=-DSK(2,1)
      DSK(7,2)= DSK(4,1)
      RQ1A158
      #Q1A159
      RQ1A160
      RQ1A161
      RQ1A162
      RQ1A163
      RQ1A164
      RQ1A165
      RQ1A166
      RQ1A167
      RQ1A168
      RQ1A169
      RQ1A170
      RQ1A171
      RQ1A172
      RQ1A173
      RQ1A174
      RQ1A175
      RQ1A176
      RQ1A177
      RQ1A178
      RQ1A179
      RQ1A180
      RQ1A181
      RQ1A182
      RQ1A183
      RQ1A184
      RQ1A185
      RQ1A186
      RQ1A187
      RQ1A188
      RQ1A189
      RQ1A190
      RQ1A191
      RQ1A192
      RQ1A193
      RQ1A194
      RQ1A195
      RQ1A196
      RQ1A197
      RQ1A198
      RQ1A199
      RQ1A200
      RQ1A201
      RQ1A202
      RQ1A203
      RQ1A204
      RQ1A205
      RQ1A206
      RQ1A207
      RQ1A208
      RQ1A209
      RQ1A210
      RQ1A211
      RQ1A212
      RQ1A213

```

```

DSK(4,3) = -DSK(2,1)
DSK(6,3) = DSK(4,1)
DSK(7,3) = DSK(5,1)
DSK(8,3) = DSK(2,1)
DSK(4,4) = DSK(2,2)
DSK(5,4) = DSK(3,2)
DSK(6,4) = DSK(8,2)
DSK(7,4) = DSK(2,1)
DSK(8,4) = DSK(6,2)
DSK(5,5) = DSK(1,1)
DD 8620 I=2,4
DSK (I+4,5)=DSK(I,1)
3620 DSK (I+4,6)=DSK(I,2)
DSK(7,7) = DSK(1,1)
DSK(8,7) = -DSK(2,1)
DSK(8,8) = DSK(2,2)
GO TO 61
C CALCULATIONS FOR THE QUAD PLATE *****
4 NTRI = 1
A1234 = 0.0
DD 379 I=1,15
DD 379 J=1,15
379 TT(I,J)=0.0
XIT = (X(IP(NN))+X(IQ(NN))+X(IR(NN))+X(IS(NN)))/4.0
YIT = (Y(IP(NN))+Y(IQ(NN))+Y(IR(NN))+Y(IS(NN)))/4.0
ZIT = (Z(IP(NN))+Z(IQ(NN))+Z(IR(NN))+Z(IS(NN)))/4.0
400 GO TO (401,402,403,404,405),NTRI
C
C
401 XRP = XIT-X(IP(NN))
YRP = YIT-Y(IP(NN))
ZRP = ZIT-Z(IP(NN))
XRQ = XIT-X(IQ(NN))
YRQ = YIT-Y(IQ(NN))
ZRQ = ZIT-Z(IQ(NN))
ILAM = 8
JLAM = 12
IP3=3
IQ3=6
GO TO 500
402 XQP = X(IR(NN))-X(IQ(NN))
YQP = Y(IR(NN))-Y(IQ(NN))
ZQP = Z(IR(NN))-Z(IQ(NN))
XRP = XIT-X(IQ(NN))
YRP = YIT-Y(IQ(NN))
ZRP = ZIT-Z(IQ(NN))
XRQ = XIT-X(IR(NN))
YRQ = YIT-Y(IR(NN))
ZRQ = ZIT-Z(IR(NN))
IP3=6
IQ3=9
GO TO 500
403 XQP = X(IS(NN))-X(IR(NN))
YQP = Y(IS(NN))-Y(IR(NN))
ZQP = Z(IS(NN))-Z(IR(NN))
XRP = XIT-X(IR(NN))

```

```

RQ1A214
RQ1A215
RQ1A216
RQ1A217
RQ1A218
RQ1A219
RQ1A220
RQ1A221
RQ1A222
RQ1A223
RQ1A224
RQ1A225
RQ1A226
RQ1A227
RQ1A228
RQ1A229
RQ1A230
RQ1A231
RQ1A232
RQ1A233
RQ1A234
RQ1A235
RQ1A236
RQ1A237
RQ1A238
RQ1A239
RQ1A240
RQ1A241
RQ1A242
RQ1A243
RQ1A244
RQ1A245
RQ1A246
RQ1A247
RQ1A248
RQ1A249
RQ1A250
RQ1A251
RQ1A252
RQ1A253
RQ1A254
RQ1A255
RQ1A256
RQ1A257
RQ1A258
RQ1A259
RQ1A260
RQ1A261
RQ1A262
RQ1A263
RQ1A264
RQ1A265
RQ1A266
RQ1A267
RQ1A268
RQ1A269

```

```

YRP = YIT-Y(IR(NN))
ZRP = ZIT-Z(IR(NN))
XRQ = XIT-X(IS(NN))
YRQ = YIT-Y(IS(NN))
ZRQ = ZIT-Z(IS(NN))
IP3=9
IQ3=12
C
GO TO 500
404 XQP = X(IP(NN))-X(IS(NN))
YQP = Y(IP(NN))-Y(IS(NN))
ZQP = Z(IP(NN))-Z(IS(NN))
XRP = XIT-X(IS(NN))
YRP = YIT-Y(IS(NN))
ZRP = ZIT-Z(IS(NN))
XRQ = XIT-X(IP(NN))
YRQ = YIT-Y(IP(NN))
ZRQ = ZIT-Z(IP(NN))
IP3 = 12
IQ3 = 3
--C
500 D1=SQRT(XQP**2+YQP**2+ZQP**2)
IF(D1.NE.0.0) GO TO 1450
1451 FORMAT (52H * * * THERE IS A GEOMETRY ERROR IN QUAD PLATE NO. /)
WRITE (6,1451)
1452 FORMAT (I7)
WRITE (6,1452) NN
CALL ERROR(103)
1450 CONTINUE
C CALCULATE THE PQ DIRECTION COSINES
AL(1)=XQP/D1
AL(2)=YQP/D1
AL(3)=ZQP/D1
RP=AL(1)*XRP+AL(2)*YRP+AL(3)*ZRP
X2=XRP-AL(1)*RP
Y2=YRP-AL(2)*RP
Z2=ZRP-AL(3)*RP
D2=SQRT(X2**2+Y2**2+Z2**2)
IF(D2.NE.0.0) GO TO 1550
1551 FORMAT (52H * * * THERE IS A GEOMETRY ERROR IN QUAD PLATE NO. /)
WRITE (6,1551)
1552 FORMAT (I7)
WRITE (6,1552) NN
CALL ERROR(104)
1550 CONTINUE
CALCULATE THE TRIANGLE DIRECTION COSINES
AL2(1)=X2/D2
AL2(2)=Y2/D2
AL2(3)=Z2/D2
IF(NTRI.NE.1) GO TO 870
DIR1 = AL(1)
DIR2 = AL(2)
DIR3 = AL(3)
DIR4 = AL2(1)
DIR5 = AL2(2)
DIR6 = AL2(3)
RQ1A270
RQ1A271
RQ1A272
RQ1A273
RQ1A274
RQ1A275
RQ1A276
RQ1A277
RQ1A278
RQ1A279
RQ1A280
RQ1A281
RQ1A282
RQ1A283
RQ1A284
RQ1A285
RQ1A286
RQ1A287
RQ1A288
RQ1A289
RQ1A290
RQ1A291
RQ1A292
RQ1A293
RQ1A294
RQ1A295
RQ1A296
RQ1A297
RQ1A298
RQ1A299
RQ1A300
RQ1A301
RQ1A302
RQ1A303
RQ1A304
RQ1A305
RQ1A306
RQ1A307
RQ1A308
RQ1A309
RQ1A310
RQ1A311
RQ1A312
RQ1A313
RQ1A314
RQ1A315
RQ1A316
RQ1A317
RQ1A318
RQ1A319
RQ1A320
RQ1A321
RQ1A322
RQ1A323
RQ1A324
RQ1A325

```

```

CHANGE FROM DATUM TO LOCAL COORDINATES
870 X21=XQP*AL2(1)+YQP*AL2(2)+ZQP*AL2(3)
    Y21=XQP*AL (1)+YQP*AL (2)+ZQP*AL (3)
    X31=XRP*AL2(1)+YRP*AL2(2)+ZRP*AL2(3)
    Y31=XRP*AL (1)+YRP*AL (2)+ZRP*AL (3)
    X32=XRQ*AL2(1)+YRQ*AL2(2)+ZRQ*AL2(3)
    Y32=XRQ*AL (1)+YRQ*AL (2)+ZRQ*AL (3)
    A123=(X32*Y21-X21*Y32)/2.
    IF(A123.NE.0.0) GO TO 1650
1651 FORMAT (52H * * * THERE IS A GEOMETRY ERROR IN QUAD PLATE NO. /)
    WRITE (6,1651)
1652 FORMAT (17)
    WRITE (6,1652) NN
    CALL ERROR (105)
1650 CONTINUE
    A1234 = A1234+A123
    GO TO(1232,161),NPASS
1232 ILAM =6
    JLAM =9
    ET1=AE1/(4.*A123*(1.-RR**2))
    ET2=AE1/(8.*A123*(1.+RR))
CALCULATE THE STIFFNESS MATRIX FOR THE TRIANGLE IN LOCAL COORD
DSK(1,1)= ET1*Y32**2 +ET2*X32**2
DSK(2,1)=-ET1*RR*Y32*X32-ET2*X32*Y32
DSK(2,2)= ET1*X32**2 +ET2*Y32**2
DSK(3,1)=-ET1*Y32*Y31 -ET2*X32*X31
DSK(3,2)= ET1*RR*X32*Y31+ET2*Y32*X31
DSK(3,3)= ET1*Y31**2 +ET2*X31**2
DSK(4,1)= ET1*RR*Y32*X31+ET2*X32*Y31
DSK(4,2)=-ET1*X32*X31 -ET2*Y32*Y31
DSK(4,3)=-ET1*RR*Y31*X31-ET2*X31*Y21
DSK(4,4)= ET1*X31**2 +ET2*Y31**2
DSK(5,1)= ET1*Y32*Y21 +ET2*X32*X21
DSK(5,2)=-ET1*RR*X32*Y21-ET2*Y32*X21
DSK(5,3)=-ET1*Y31*Y21 -ET2*X31*X21
DSK(5,4)= ET1*RR*X31*Y21+ET2*Y31*X21
DSK(5,5)= ET1*Y21**2 +ET2*X21**2
DSK(6,1)=-ET1*RR*Y32*X21-ET2*X32*Y21
DSK(6,2)= ET1*X32*X21 +ET2*Y32*Y21
DSK(6,3)= ET1*RR*Y31*X21+ET2*X31*Y21
DSK(6,4)=-ET1*X31*X21 -ET2*Y31*Y21
DSK(6,5)=-ET1*RR*Y21*X21-ET2*X21*Y21
DSK(6,6)= ET1*X21**2 +ET2*Y21**2
CALCULATE LAMBDA AND ITS TRANSPOSE
161 DO160 I=1,ILAM
    DO160 J=1,JLAM
    ALAM(I,J)=0.
160 ALAMT(J,I)=0.
    K=0
    DO170 J=1,ILAM,2
    DO170 I=1,3
    K=K+1
    ALAMT(K,J )=AL2(I)
    ALAMT(K,J+1)=AL(I)
    ALAM (J ,K)=ALAMT(K,J )
170 ALAM (J+1,K)=ALAMT(K,J+1)
RQ1A326
RQ1A327
RQ1A328
RQ1A329
RQ1A330
RQ1A331
RQ1A332
RQ1A333
RQ1A334
RQ1A335
RQ1A336
RQ1A337
RQ1A338
RQ1A339
RQ1A340
RQ1A341
RQ1A342
RQ1A343
RQ1A344
RQ1A345
RQ1A346
RQ1A347
RQ1A348
RQ1A349
RQ1A350
RQ1A351
RQ1A352
RQ1A353
RQ1A354
RQ1A355
RQ1A356
RQ1A357
RQ1A358
RQ1A359
RQ1A360
RQ1A361
RQ1A362
RQ1A363
RQ1A364
RQ1A365
RQ1A366
RQ1A367
RQ1A368
RQ1A369
RQ1A370
RQ1A371
RQ1A372
RQ1A373
RQ1A374
RQ1A375
RQ1A376
RQ1A377
RQ1A378
RQ1A379
RQ1A380
RQ1A381

```

```

      GO TO(171,40),NPASS
CALCULATE THE STIFFNESS MATRIX IN DATUM COORD
171 DO190 I=1,ILAM
      DO190 J=1,ILAM
190 DSK(I,J)=DSK(J,I)
      DO1110 I=1,JLAM
      DO1100 J=1,ILAM
      R(J)=0.
      DO11100 K1=1,ILAM
1100 R(J)=R(J)+ALAMT(I,K1)*DSK(K1,J)
      DO1110 J=1,ILAM
1110 ALAMT(I,J)=R(J)
      DO1210 I=1,JLAM
      DO1200 J=1,JLAM
      R(J)=0.
      DO1200 K1=1,ILAM
1200 R(J)=R(J)+ALAMT(I,K1)*ALAM(K1,J)
      DO1210 J=1,JLAM
1210 ALAMT(I,J)=R(J)
      DO 380 IROW=1,3
      JROW=3-IROW
      KROW=IP3-JROW
      LROW=IQ3-JROW
      MROW= 15-JROW
      DO 380 ICOL=1,3
      JCOL=3-ICOL
      KCOL=IP3-JCOL
      LCOL=IQ3-JCOL
      MCOL= 15-JCOL
      TT(KROW,KCOL)=TT(KROW,KCOL)+ALAMT(IROW,ICOL)
      TT(KROW,LCOL)=TT(KROW,LCOL)+ALAMT(IROW,ICOL+3)
      TT(LROW,KCOL)=TT(LROW,KCOL)+ALAMT(IROW+3,ICOL)
      TT(KROW,MCOL)=TT(KROW,MCOL)+ALAMT(IROW,ICOL+6)
      TT(LROW,LCOL)=TT(LROW,LCOL)+ALAMT(IROW+3,ICOL+3)
      TT(LROW,MCOL)=TT(LROW,MCOL)+ALAMT(IROW+3,ICOL+6)
      TT(MROW,KCOL)=TT(MROW,KCOL)+ALAMT(IROW+6,ICOL)
      TT(MROW,LCOL)=TT(MROW,LCOL)+ALAMT(IROW+6,ICOL+3)
      TT(MROW,MCOL)=TT(MROW,MCOL)+ALAMT(IROW+6,ICOL+6)
380 CONTINUE
      NTRI = NTRI +1
      GO TO 400
405 A123=A1234
      AL(1) = DIR1
      AL(2) = DIR2
      AL(3) = DIR3
      AL2(1) = DIR4
      AL2(2) = DIR5
      AL2(3) = DIR6
CALCULATE LAMBDA AND ITS TRANSPOSE
      ILAM=10
      JLAM=15
      DO260 I=1,ILAM
      DO260 J=1,JLAM
      ALAM(I,J)=0.
260 ALAMT(J,I)=0.
      K=0

```

```

RQ1A382
RQ1A383
RQ1A384
RQ1A385
RQ1A386
RQ1A387
RQ1A388
RQ1A389
RQ1A390
RQ1A391
RQ1A392
RQ1A393
RQ1A394
RQ1A395
RQ1A396
RQ1A397
RQ1A398
RQ1A399
RQ1A400
RQ1A401
RQ1A402
RQ1A403
RQ1A404
RQ1A405
RQ1A406
RQ1A407
RQ1A408
RQ1A409
RQ1A410
RQ1A411
RQ1A412
RQ1A413
RQ1A414
RQ1A415
RQ1A416
RQ1A417
RQ1A418
RQ1A419
RQ1A420
RQ1A421
RQ1A422
RQ1A423
RQ1A424
RQ1A425
RQ1A426
RQ1A427
RQ1A428
RQ1A429
RQ1A430
RQ1A431
RQ1A432
RQ1A433
RQ1A434
RQ1A435
RQ1A436
RQ1A437

```

```

      DD270 J=1,ILAM,2
      DD270 I=1,3
      K=K+1
      ALAMT(K,J)=AL2(I)
      ALAMT(K,J+1)=AL(I)
      ALAM(J,K)=ALAMT(K,J)
270 ALAM(J+1,K)=ALAMT(K,J+1)
C***** MULTIPLY LAMBDA*TT*LAMBDA TRANSPOSE
      DD 800 I=1,15
      DD 800 J=1,10
      ZZ(I,J)=0.
      DD 800 K=1,15
      800 ZZ(I,J)= ZZ(I,J) +TT(I,K)*ALAMT(K,J)
      DD 810 I=1,10
      DD 810 J=1,10
      TT(I,J) =0.
      DD 810 K=1,15
      810 TT(I,J) = TT(I,J) +ALAM(I,K)*ZZ(K,J)
      DD 998 II=1,2
      DD 998 JJ=1,2
      998 T22(II,JJ)=TT(II+8,JJ+8)
      DD 101 II=1,8
      DD 101 JJ=1,8
      101 T11(II,JJ)=TT(II,JJ)
      DD 102 II=1,8
      DD 102 JJ=1,2
      102 T12(II,JJ)=TT(II,JJ+8)
      DD 103 II=1,2
      DD 103 JJ=1,8
      103 T21(II,JJ)=TT(II+8,JJ)
C*****CALCULATIONS TO INVERT THE T22 MATRIX
      DD203I=1,2
      DD203J=1,2
      IF(I-J)201,202,201
      201 T22INV(I,J)=0.
      GO TO 203
      202 T22INV(I,J)=1.0
      203 CONTINUE
      DD207I=1,2
      IF(T22(I,I).NE.0.0) GO TO 1750
      1751 FORMAT (52H * * * THERE IS A GEOMETRY ERROR IN QUAD PLATE NO. /)
      WRITE (6,1751)
      1752 FORMAT (17)
      WRITE (6,1752) NN
      CALL ERROR (106)
      1750 CONTINUE
      C=1./T22(I,I)
      DD204J=1,2
      T22(I,J)= T22(I,J)*C
      204 T22INV(I,J)=T22INV(I,J)*C
      DD207J=1,2
      IF(J-1)205,207,205
      205 D=T22(J,I)
      DD206JJ=1,2
      T22(J,JJ)=T22(J,JJ)-T22(I,JJ)*D
      206 T22INV(J,JJ)=T22INV(J,JJ)-T22INV(I,JJ)*D
      RQ1A438
      RQ1A439
      RQ1A440
      RQ1A441
      RQ1A442
      RQ1A443
      RQ1A444
      RQ1A445
      RQ1A446
      RQ1A447
      RQ1A448
      RQ1A449
      RQ1A450
      RQ1A451
      RQ1A452
      RQ1A453
      RQ1A454
      RQ1A455
      RQ1A456
      RQ1A457
      RQ1A458
      RQ1A459
      RQ1A460
      RQ1A461
      RQ1A462
      RQ1A463
      RQ1A464
      RQ1A465
      RQ1A466
      RQ1A467
      RQ1A468
      RQ1A469
      RQ1A470
      RQ1A471
      RQ1A472
      RQ1A473
      RQ1A474
      RQ1A475
      RQ1A476
      RQ1A477
      RQ1A478
      RQ1A479
      RQ1A480
      RQ1A481
      RQ1A482
      RQ1A483
      RQ1A484
      RQ1A485
      RQ1A486
      RQ1A487
      RQ1A488
      RQ1A489
      RQ1A490
      RQ1A491
      RQ1A492
      RQ1A493

```

```

207 CONTINUE
C*** OBTAIN THE REDUCED STIFFNESS MATRIX AND STORE IN ALAMT
  DO 710 I=1,2
    DO 710 J=1,8
      ALAM(I,J)=0.0
    DO 710 K=1,2
      710 ALAM(I,J) = T22INV(I,K)*T21(K,J) +ALAM(I,J)
    DO 711 I=1,8
      DO 711 J=1,8
        ALAMT(I,J)=0.0
      DO 711 K=1,2
        711 ALAMT(I,J) = T12(I,K)*ALAM(K,J) + ALAMT(I,J)
      DO 712 I=1,8
        DO 712 J=1,8
          712 DSK(I,J) = T11(I,J)-ALAMT(I,J)
        ILAM = 8
        JLAM = 12
CALCULATE LAMBDA AND ITS TRANSPOSE
  61 DO 60 I=1, ILAM
    DO 60 J=1, JLAM
      ALAM(I,J)=0.
  60 ALAMT(J, I)=0.
    K=0
    DO 70 J=1, ILAM,2
      DO 70 I=1,3
        K=K+1
        ALAMT(K, J )=AL2(I)
        ALAMT(K, J+1)=AL(I)
        ALAM ( J , K)=ALAMT(K, J )
  70 ALAM (J+1, K)=ALAMT(K, J+1)
    GO TO (71,40),NPASS
CALCULATE THE STIFFNESS MATRIX IN DATUM COORD
  71 DO 90 I=1, ILAM
    DO 90 J=1, JLAM
      90 DSK(I,J)=DSK(J,I)
  95 DO 110 I=1, JLAM
    DO 100 J=1, ILAM
      R(J)=0.
    DO 100 K1=1, ILAM
  100 R(J)=R(J)+ALAMT(I,K1)*DSK(K1,J)
    DO 110 J=1, JLAM
  110 ALAMT(I,J)=R(J)
    DO 210 I=1, JLAM
      DO 200 J=1, JLAM
        P(J)=0.
      DO 200 K1=1, ILAM
  200 R(J)=R(J)+ALAMT(I,K1)*ALAM(K1,J)
      DO 210 J=1, JLAM
  210 ALAMT(I,J)=R(J)
  40 RETURN
    END
SUBROUTINE STRES
C
ELEMENT STRESSES AND DISPLACEMENTS
DIMENSION ALAM(15,15),ALAMT(15,15),R(12),U(12),UU(10),AL(3),
1SIGMA(3),LPI(333),NS(666),AL2(3),DSK(8,8),PMUDE(10),QXY(333),
2PXY(750),P(750),PI(750),PE(750),IX(750),JL(750),JR(750),
RQ1A494
RQ1A495
RQ1A496
RQ1A497
RQ1A498
RQ1A499
RQ1A500
RQ1A501
RQ1A502
RQ1A503
RQ1A504
RQ1A505
RQ1A506
RQ1A507
RQ1A508
RQ1A509
RQ1A510
RQ1A511
RQ1A512
RQ1A513
RQ1A514
RQ1A515
RQ1A516
RQ1A517
RQ1A518
RQ1A519
RQ1A520
RQ1A521
RQ1A522
RQ1A523
RQ1A524
RQ1A525
RQ1A526
RQ1A527
RQ1A528
RQ1A529
RQ1A530
RQ1A531
RQ1A532
RQ1A533
RQ1A534
RQ1A535
RQ1A536
RQ1A537
RQ1A538
RQ1A539
RQ1A540
RQ1A541
RQ1A542
RQ1A543
RQ1A544
RQ1B001
RQ1B002
RQ1B003
RQ1B004
RQ1B005

```



```

7 EXX=(Y32*UU(1)-Y31*UU(3)+Y21*UU(5))
EYY=(-X32*UU(2)+X31*UU(4)-X21*UU(6))
EXY=(-X32*UU(1)+Y32*UU(2)+X31*UU(3)-Y31*UU(4)-X21*UU(5)+Y21*UU(6))
S=SIN(BETA)
C=COS(BETA)
SH=S**2
CB=C**2
E11=EXX*CB+EYY*SH+EXY*S*C
E22=EXX*SB+EYY*CB-EXY*S*C
E12=-EXX*2.*S*C+EYY*2.*S*C+EXY*(CB-SB)
C11=E1/(2.*A123*(1.-PR1*PR2))
C22=C11*E2/E1
C12=C11*PR2
C21=C12
C66=GT/(2.*A123)
SIGMA(1)=C11*E11+C12*E22
SIGMA(2)=C21*E11+C22*E22
SIGMA(3)=C66*E12
GO TO 4
300 U(1)=P(IP(N)*3-2)
U(2)=P(IP(N)*3-1)
U(3)=P(IP(N)*3)
U(4)=P(IQ(N)*3-2)
U(5)=P(IQ(N)*3-1)
U(6)=P(IQ(N)*3)
U(7)=P(IR(N)*3-2)
U(8)=P(IR(N)*3-1)
U(9)=P(IR(N)*3)
U(10)=P(IS(N)*3-2)
U(11)=P(IS(N)*3-1)
U(12)=P(IS(N)*3)
DO 310 I=1,8
UU(I)=0.
DO 310 J=1,12
310 UU(I)=UU(I)+ALAM(I,J)*U(J)
C****X CALCULATE THE RECTANGULAR PLATE STRESSES
DA=1./(2.*D2)
DB=1./(2.*D1)
F4=E*ME/(1.-RR*RR)
EXX=DA*(-UU(1)-UU(3)+UU(5)+UU(7))
EYY=DB*(-UU(2)+UU(4)+UU(6)-UU(8))
EXY=DA*(-UU(2)-UU(4)+UU(6)+UU(8))+
1 DB*(-UU(1)+UU(3)+UU(5)-UU(7))
SIGMA(1)= F4*(EXX+RR*EYY)
SIGMA(2)= E4*(RR*EXX+EYY)
SIGMA(3)= E4* EXY*(1.-RR)/2.
GO TO 4
400 U(1) =P(IP(N)*3-2)
U(2) =P(IP(N)*3-1)
U(3) =P(IP(N)*3 )
U(4) =P(IQ(N)*3-2)
U(5) =P(IQ(N)*3-1)
U(6) =P(IQ(N)*3 )
U(7) =P(IR(N)*3-2)
U(8) =P(IR(N)*3-1)
U(9) =P(IR(N)*3 )

```

RQ1B062
RQ1B063
RQ1B064
RQ1B065
RQ1B066
RQ1B067
RQ1B068
RQ1B069
RQ1B070
RQ1B071
RQ1B072
RQ1B073
RQ1B074
RQ1B075
RQ1B076
RQ1B077
RQ1B078
RQ1B079
RQ1B080
RQ1B081
RQ1B082
RQ1B083
RQ1B084
RQ1B085
RQ1B086
RQ1B087
RQ1B088
RQ1B089
RQ1B090
RQ1B091
RQ1B092
RQ1B093
RQ1B094
RQ1B095
RQ1B096
RQ1B097
RQ1B098
RQ1B099
RQ1B100
RQ1B101
RQ1B102
RQ1B103
RQ1B104
RQ1B105
RQ1B106
RQ1B107
RQ1B108
RQ1B109
RQ1B110
RQ1B111
RQ1B112
RQ1B113
RQ1B114
RQ1B115
RQ1B116
RQ1B117

```

U(10)=P(1S(N)*3-2)
U(11)=P(1S(N)*3-1)
U(12)=P(1S(N)*3 )
DO 410 I=1,8
UU(I)=0.
DO 410 J=1,12
410 UU(I)=UU(I)+ALAM(I,J)*U(J)
UU(9) = (UU(1)+UU(3)+UU(5)+UU(7))/4.
UU(10)= (UU(2)+UU(4)+UU(6)+UU(8))/4.
GO TO(401,402,403,404),NTRI
401 SIGMA(1)=0.0
SIGMA(2)= 0.0
SIGMA(3)= 0.0
THETA1 = 0.0
U(1)= UU(1)
U(2)= UU(2)
U(3)= UU(3)
U(4)= UU(4)
U(5)= UU(9)
U(6)= UU(10)
NPASS1= 2
GO TO 500
402 U(1)=UU(3)
U(2)=UU(4)
U(3)=UU(5)
U(4)=UU(6)
U(5)=UU(9)
U(6)=UU(10)
C
GO TO 500
C
403 U(1)=UU(5)
U(2)=UU(6)
U(3)=UU(7)
U(4)=UU(8)
U(5)=UU(9)
U(6)=UU(10)
C
GO TO 500
404 U(1)=UU(7)
U(2)=UU(8)
U(3)=UU(1)
U(4)=UU(2)
U(5)=UU(9)
U(6)=UU(10)
NPASS1 = 1
500 NTRI = NTRI+1
AKK=2.*A123*(1.-RR**2)
ZIGMA(1) = +(Y32*U(1)-RR*X32*U(2)-Y31*U(3)+RR*X31*U(4)
1 +Y21*U(5)-RR*X21*U(6))*EME/(4.*AKK)
ZIGMA(2) = +(RR*Y32*U(1)-X32*U(2)-RR*Y31*U(3)+X31*U(4)
1 +RR*Y21*U(5)-X21*U(6))*EME/(4.*AKK)
ZIGMA(3) = +(-X32*U(1)+Y32*U(2)+X31*U(3)-Y31*U(4)
2 -X21*U(5)+Y21*U(6))*EME*(1.-RR)/(8.*AKK)
AR=DIR1*AL(1)+DIR2*AL(2)+DIR3*AL(3)
IF(AR.GE.1.0) GOTO 600
RQ18118
RQ18119
RQ18120
RQ18121
RQ18122
RQ18123
RQ18124
RQ18125
RQ18126
RQ18127
RQ18128
RQ18129
RQ18130
RQ18131
RQ18132
RQ18133
RQ18134
RQ18135
RQ18136
RQ18137
RQ18138
RQ18139
RQ18140
RQ18141
RQ18142
RQ18143
RQ18144
RQ18145
RQ18146
RQ18147
RQ18148
RQ18149
RQ18150
RQ18151
RQ18152
RQ18153
RQ18154
RQ18155
RQ18156
RQ18157
RQ18158
RQ18159
RQ18160
RQ18161
RQ18162
RQ18163
RQ18164
RQ18165
RQ18166
RQ18167
RQ18168
RQ18169
RQ18170
RQ18171
RQ18172
RQ18173

```

```

        THETA1 = THETA1 +ARCCS(AR)
600 CONTINUE
        DIR1 = AL(1)
        DIR2 = AL(2)
        DIR3 = AL(3)
        S = SIN(THETA1)
        C = COS(THETA1)
        SB= S*S
        CB= C*C
        SC= C*S
        TMATRX(1,1) = CB
        TMATRX(1,2) = SB
        TMATRX(1,3) = 2.*SC
        TMATRX(2,1) = SB
        TMATRX(2,2) = CB
        TMATRX(2,3) = -2.*SC
        TMATRX(3,1) = -SC
        TMATRX(3,2) = SC
        TMATRX(3,3) = CB-SB
        DO 890 I= 1,3
        SIG(I) = 0.0
        DO 890 K= 1,3
890 SIG(I) = SIG(I)+TMATRX(I,K)*ZIGMA(K)
        SIGMA(1) = SIGMA(1)+ SIG(I)
        SIGMA(2) = SIGMA(2)+ SIG(I)
        SIGMA(3) = SIGMA(3)+ SIG(I)
        IF(NTRI.EQ.5)GO TO 4
        CALL ELEMS
        GO TO 400
4 RETURN
END
SUBROUTINE STORKE
C STORE ELEMENT STIFFNESS COEFFICIENTS IN SYSTEM ARRAY
DIMENSION ALAM(15,15),ALAMT(15,15),R(12),U(12),UU(10),AL(3),
1SIGMA(3),LP(333),NS(666),AL2(3),DSK(8,8),PMODE(10),QXY(333),
2PXY(750),P(750),PI(750),PE(750),IX(750),JL(750),JR(750),
3NSP(750),SS(87,750),NPT(250),X(250),Y(250),Z(250),IS(1000),
4SE(1000),S1(1000,3),S2(1000,3),S3(1000,3),IE(1000),IP(1000),
5IQ(1000),IR(1000),NTYPE(1000),EM(20),PR(20),SY(20),PNL(20),
6MATYPE(1000),A(1000),SAFTY(1000),VE(1000),S4(1000,3),S7(1000,3),
7FMM(20),G(20),THETA(20),ZZ(15,15),
8TT(15,15),T11(8,8),T22(2,2),T12(8,2),T21(2,3),T22INV(2,2)
9,SIG(3),ZIGMA(3),TMATRX(3,3),DENSE(20)
COMMON SS,IX,JL,JR,AE1,NHAND,ALAM,ALAMT,R,RR,D1,AL,X21,X31,X32,Y21
1,Y31,Y32,A123,U,UU,SIGMA,SYE,PN,EME,A,NLP,BM,SE,S1,S2,S3,PI,
2NTYPE,N,IM,NPASS,NN,NPT,X,Y,Z,IE,IP,IQ,IR,AE,NODES,II,JJ,AL2,DSK,
3P,SAFTY,VE,S4,S7,PE,MID,NSP,IS,D2,
4EMM,G,THETA,BETA,S,C,SH,CB,GT,PR1,PR2,E1,E2
5,LP,PR,NS,SY,PMODE,PNL,PXY,EM,MATYPE,
6TT,T11,T22,T12,T21,T22INV,ZZ,NPASS1,NTRI,XIT,YIT,ZIT,ILAM,JLAM
7,DIR1,DIR2,DIR3,THETA1,QXY
NTYP=NTYPE(NN)
IP3=IP(NN)*3
IQ3=IQ(NN)*3
IR3= IR(NN)*3
IS3= IS(NN)*3
RQ1B174
RQ1B175
RQ1B176
RQ1B177
RQ1B178
RQ1B179
RQ1B180
RQ1B181
RQ1B182
RQ1B183
RQ1B184
RQ1B185
RQ1B186
RQ1B187
RQ1B188
RQ1B189
RQ1B190
RQ1B191
RQ1B192
RQ1B193
RQ1B194
RQ1B195
RQ1B196
RQ1B197
RQ1B198
RQ1B199
RQ1B200
RQ1B201
RQ1B202
RQ1B203
RQ1B204
RQ1C001
RQ1C002
RQ1C003
RQ1C004
RQ1C005
RQ1C006
RQ1C007
RQ1C008
RQ1C009
RQ1C010
RQ1C011
RQ1C012
RQ1C013
RQ1C014
RQ1C015
RQ1C016
RQ1C017
RQ1C018
RQ1C019
RQ1C020
RQ1C021
RQ1C022
RQ1C023
RQ1C024
RQ1C025

```

```

DO 380 IROW=1,3
  JROW=3-IROW
  KROW =IX(IP3-JROW)
  LROW =IX(IQ3-JROW)
  MROW =IX(IR3-JROW)
  NROW =IX(IS3-JROW)
  DO 381 ICOL = 1,3
    JCOL = 3-ICOL
    KCOL = IP3-JCOL
    LCOL = IQ3-JCOL
    MCOL = IR3-JCOL
    NCOL = IS3-JCOL
    IF(IP3-IQ3)315,314,314
315 SS(KROW,LCOL)=SS(KROW,LCOL) + ALAMT(IROW,ICOL+3)
314 GO TO(320,308,308,308,308),NTYP
308 IF(IP3-IR3)317,316,316
317 SS(KROW,MCOL) = SS(KROW,MCOL) +ALAMT(IROW,ICOL+6)
316 IF(IQ3-IR3) 318,358,398
318 SS(LROW,MCOL) = SS(LROW,MCOL) +ALAMT(IROW+3,ICOL+6)
398 GO TO(320,320,320,320,330),NTYP
330 IF(IP3-IS3)331,332,332
331 SS(KROW,NCOL) = SS(KROW,NCOL)+ALAMT(IROW,ICOL+9)
332 IF(IQ3-IS3)333,334,334
333 SS(LROW,NCOL) = SS(LROW,NCOL)+ALAMT(IROW+3,ICOL+9)
334 IF(IR3-IS3)335,320,320
335 SS(MROW,NCOL) = SS(MROW,NCOL)+ALAMT(IROW+6,ICOL+9)
C
320 IF(IP3-IQ3)319,319,307
307 SS(LROW,KCOL) = SS(LROW,KCOL)+ALAMT(IROW+3,ICOL)
319 GO TO(381,321,321,321,321),NTYP
321 IF(IP3-IR3)324,324,322
322 SS(MROW,KCOL) = SS(MROW,KCOL)+ALAMT(IROW+6,ICOL)
324 IF(IQ3-IR3)399,399,323
323 SS(MROW,LCOL) = SS(MROW,LCOL)+ALAMT(IROW+6,ICOL+3)
399 GO TO(381,381,381,340,340),NTYP
340 IF(IP3-IS3) 342,342,341
341 SS(NROW,KCOL) = SS(NROW,KCOL)+ALAMT(IROW+9,ICOL)
342 IF(IQ3-IS3) 344,344,343
343 SS(NROW,LCOL) = SS(NROW,LCOL)+ALAMT(IROW+9,ICOL+3)
344 IF(IR3-IS3) 381,381,345
345 SS(NROW,MCOL) = SS(NROW,MCOL)+ALAMT(IROW+9,ICOL+6)
381 CONTINUE
  DO 382 ICOL=IROW,3
    JCOL = 3-ICOL
    KCOL = IP3-JCOL
    LCOL = IQ3-JCOL
    MCOL = IR3-JCOL
    NCOL = IS3-JCOL
    SS(KROW,KCOL) = SS(KROW,KCOL)+ALAMT(IROW,ICOL)
    SS(LROW,LCOL) = SS(LROW,LCOL)+ALAMT(IROW+3,ICOL+3)
    GO TO(382,313,313,313,313),NTYP
313 SS(MROW,MCOL) = SS(MROW,MCOL)+ALAMT(IROW+6,ICOL+6)
    GO TO(382,382,382,350,350),NTYP
350 SS(NROW,NCOL) = SS(NROW,NCOL)+ALAMT(IROW+9,ICOL+9)
382 CONTINUE
380 CONTINUE
  RETURN
  END
RQ1C026
RQ1C027
RQ1C028
RQ1C029
RQ1C030
RQ1C031
RQ1C032
RQ1C033
RQ1C034
RQ1C035
RQ1C036
RQ1C037
RQ1C038
RQ1C039
RQ1C040
RQ1C041
RQ1C042
RQ1C043
RQ1C044
RQ1C045
RQ1C046
RQ1C047
RQ1C048
RQ1C049
RQ1C050
RQ1C051
RQ1C052
RQ1C053
RQ1C054
RQ1C055
RQ1C056
RQ1C057
RQ1C058
RQ1C059
RQ1C060
RQ1C061
RQ1C062
RQ1C063
RQ1C064
RQ1C065
RQ1C066
RQ1C067
RQ1C068
RQ1C069
RQ1C070
RQ1C071
RQ1C072
RQ1C073
RQ1C074
RQ1C075
RQ1C076
RQ1C077
RQ1C078
RQ1C079
RQ1C080
RQ1C081
RQ1C082
RQ1C083

```

LIST OF REFERENCES

- Argyris, J. H., Kelsey, S., and Kamel, H. "A Precis of Recent Developments," Matrix Methods of Structural Analysis (F. de Veubeke, ed.), AGARDograph 72. The MacMillan Company, 1964.
- Denke, P. H. "The Matric Solution of Certain Nonlinear Problems in Structural Analysis," J. Aero. Sci., Vol. 23, 1956, pp. 231-236.
- Galagher, R. H., Padlog, J., and Bijlaard, P. P. "Stress Analysis of Heated Complex Shapes," ARS Journal, Vol. 32, No. 5, May, 1962, pp. 700-707.
- Goldberg, J. E., and Richard, R. M. "Analysis of Nonlinear Structures," J. of the Str. Div., ASCE, Aug. 1963.
- Lansing, W., Jensen, W. R., and Falby, W. E. "Matrix Analysis Methods for Inelastic Structures, Grumman Advanced Development Report No. ADR 02-11-65.4. Presented at conference on "Matrix Methods in Structural Mechanics," October 26-28, 1965, at the Air Force Institute of Technology, Wright-Patterson Air Force Base, Dayton, Ohio, November 1965.
- Padlog, J., Huff, R. D., and Holloway, F. C. "Unelastic Behavior of Structures Subjected to Cyclic Thermal and Mechanical Stressing Conditions." WADD Technical Report 60-271. December, 1960.
- Percy, J. H., Loden, W. A., and Navaratna, D. "A Study of Matrix Analysis Methods for Inelastic Structures." Air Force Systems Command, Technical Document Report No. RDT-TDR-63-4032. October, 1963.
- Pope, G. G. "The Application Method in Plane Elasto-Plastic Problems." Presented at conference on "Matrix

Methods in Structural Mechanics," October 26-28, 1965 at the Air Force Institute of Technology, Wright-Patterson Air Force Base, Dayton, Ohio.

- Przemieniecki, J. S., and Berke, Laszlo. "Digital Computer Program for the Analysis of Aerospace Structures by the Matrix Displacement Method." Technical Documentary Report No. FDL TDR 64-18, April, 1964.
- Richard, R. M., and Blacklock, J. R. "Finite Element Analysis of Inelastic Structures." Presented at AIAA/ASME 9th Structures, Structural Dynamics and Materials Conference, Palm Springs, California April 1-3, 1968.
- Richard, R. M., and Callabresi, M. L. "Nonlinear Finite Element Analysis." Engineering Experiment Station Rpt. 13. The University of Arizona, Tucson, Arizona, 1967.
- Turner, M. J., Clough, R. W., Martin, H. C., and Topp, L. J. "Stiffness and Deflection Analysis of Complex Structures," J. of the Aero. Sci., Vol. 23, September, 1956.
- Wilson, E. L. "Finite Element Analysis of Two-Dimensional Structures." Structures and Materials Research, Dept. of Civil Engr., Report No. 63-2, June, 1963.